

Supporting Information for

**Ruthenium-catalyzed Hydrogenation of CO₂ as a Route to Methyl Esters for use as
Biofuels or fine Chemicals**

Zheng Wang,^{a,b,c} Ziwei, Zhao,^a Yong Li,^a Yanxia Zhong,^d Qiuyue Zhang,^b Qingbin Liu,^{*,a} Gregory A. Solan,^{*,b,e} Yanping Ma^b and Wen-Hua Sun^{*,b}

^aCollege of Chemistry and Material Science, Hebei Normal University, Shijiazhuang 050024, China

^bKey Laboratory of Engineering Plastics and Beijing National Laboratory for Molecular Science, Institute of Chemistry, Chinese Academy of Sciences, Beijing 100190, China

^cCollege of Science, Agricultural University of Hebei, Baoding 071001, China

^dDepartment of Nursing Shijiazhuang Medical College, Shijiazhuang 050000, China

^eDepartment of Chemistry, University of Leicester, University Road, Leicester LE1 7RH, UK.

Corresponding Author

*E-mail: whsun@iccas.ac.cn; Tel: +86-10-62557955; Fax: +86-10-62618239 (W.-H.S.)

*E-mail: gas8@leicester.ac.uk; Tel: +44-116-2522096 (G.A.S.)

*E-mail: qbinliu@sina.com; Tel: +86-0311-80787432 (Q. L.)

Table of contents

1.	General information	S2
2.	Syntheses and characterization of the complexes Ru1 - Ru4	S3
3.	¹ H, ¹³ C and ³¹ P NMR spectra of Ru1 - Ru4	S8
4.	Identification of Ru1 - Ru4 and their fragments by using ESI-MS	S17
5.	Catalytic study, GC-MS spectra for the products and various data	S19
6.	GC-MS and NMR spectra used in the mechanistic study	S52
7.	X-ray structure determination	S58
8.	References	S59

1. General information

All manipulations involving organophosphines and their ruthenium complexes were carried out under a nitrogen atmosphere using standard Schlenk techniques. All solvents were dried and distilled under nitrogen prior to use. ^1H , ^{13}C and ^{31}P NMR spectra were recorded on a Bruker AVIII –500 NMR spectrometer. Elemental analysis was carried out with a Vario ELIII CHN microanalyzer. GC–MS was carried out on DSQII instrument using an HP-5MS column: injector temp. 300 °C, detector temp. 30 °C, column temp. 40 °C, withdraw time 2 min, then 20 °C /min to 230 °C for 5 min, then 20 °C/min to 300 °C, withdraw time for 5 min. GC was performed using Agilent 6820 instrument using an Agilent 19091J-113 HP-5 column: injector temp. 300 °C, detector temp. 300 °C, column temp. 40 °C, withdraw time 2 min, then 20 °C /min to 230 °C keeping for 5 min, then 20 °C /min to 300 °C, withdraw time for 5 min. ESI-MS was performed on a 3200 QTRAP 1200 infinity series instrument using an Agilent ZORBAX SB-C18 column (dimensions in mm: 150 × 4.6): acetonitrile: water = 70:30, flow rate = 1 mL/min, electronic energy = 70 eV, Q1MS scan range = 100 ~ 1000. All the liquid substrates and solid substrates were used directly.

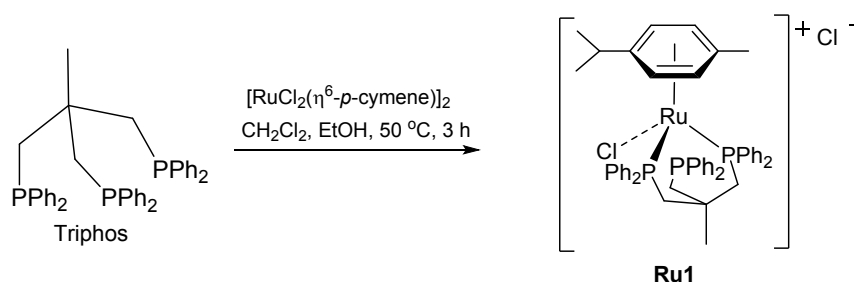
Table S1 CAS numbers for substrates and products

Products	CAS number	Substrates	CAS number
methyl benzoate	93-58-3	benzoic acid	65-85-0
benzyl alcohol	100-51-6	2-fluorobenzoic Acid	445-29-4
methyl 2-fluorobenzoate	394-35-4	2-chlorobenzoic acid	118-91-2
methyl 2-(trifluoromethyl)benzoate	344-96-7	2-bromobenzoic Acid	88-65-3
methyl 3-fluorobenzoate	455-68-5	2-(trifluoromethyl)benzoic acid	433-97-6
methyl 3-(trifluoromethyl)benzoate	2557-13-3	3-fluorobenzoic acid	455-38-9
methyl 4-fluorobenzoate	403-33-8	3-chlorobenzoic acid	535-80-8
methyl 4-trifluoromethylbenzoate	2967-66-0	3-bromobenzoic acid	585-76-2
methyl 4-methylbenzoate	99-75-2	3-(trifluoromethyl)benzoic acid	454-92-2
methyl 4-methoxybenzoate	121-98-2	4-fluorobenzoic Acid	456-22-4
ethyl 4-methoxybenzoate	94-30-4	4-chlorobenzoic acid	74-11-3
methyl 2-furoate	611-13-2	4-bromobenzoic Acid	586-76-5
methyl 3,4-difluorobenzoate	369-25-5	4-trifluoromethylbenzoic acid	455-24-3
dimethyl isophthalate	1459-93-4	methyl 4-methylbenzoic acid	99-94-5

ethyl methyl isophthalate	107731-93-1	4-methoxybenzoic acid	100-09-4
1(3 <i>H</i>)-isobenzofuranone	87-41-2	furan-2-carboxylic acid	88-14-2
diethyl terephthalate	636-09-9	furan-2-carboxylic acid	88-14-2
3,4-difluorobenzoic acid	455-86-7	isophthalic acid	121-91-5
methyl valerate	624-24-8	pathalic acid	88-99-3
methyl hexanoate	106-70-7	terephthalic acid	100-21-0
1-hexanol	111-27-3	acetic Acid	64-19-7
hexyl hexanoate	6378-65-0	valeric acid	109-52-4
methyl heptanoate	106-73-0	caproic Acid	124-62-1
methyl nonanoate	1731-84-6	heptanoic acid	111-14-8
methyl decanoate	110-42-9	nonanoic acid	112-05-0
methyl undecanoate	1731-86-8	decanoic acid	334-48-5
1-undecanol	112-42-5	undecanoic Acid	112-37-8
methyl laurate	111-82-0	dodecanoic acid	143-07-7
methyl myristate	124-10-7	myristic acid	544-63-8
methyl palmitate	112-39-0	palmitic acid	57-10-3
methyl octadecanoate	112-61-8	stearic acid	57-11-4
dimethyl adipate	627-93-0	adipic acid	124-04-9
monomethyl adipate	627-91-8	sebacic acid	111-20-6
dimethyl sebacate	106-79-6	dodecanedioic acid	693-23-2
dimethyl dodecanedioate	1731-79-9	cinnamic acid	140-10-3
benzyl propionic methyl ester	29417-83-2		

2. Syntheses and characterization of the complexes Ru1 - Ru4

2.1. Synthesis of Ru1¹

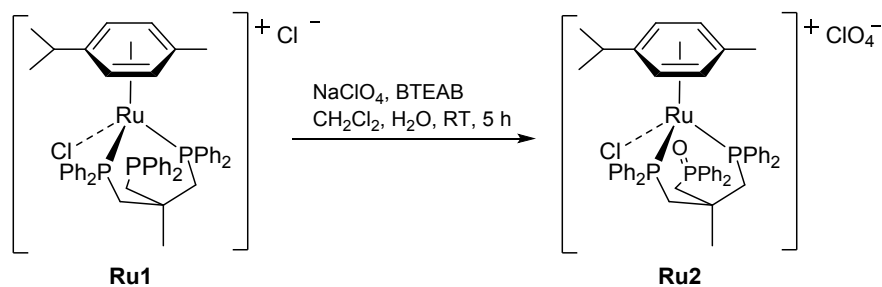


A mixture of 1,1,1-tris(diphenylphosphinomethyl)ethane(triphos) (2.50 g, 4.0 mmol) and $[\text{RuCl}_2(\eta^6\text{-}p\text{-cymene})]_2$ (1.30 g, 2.0 mmol) were loaded in a Schlenk tube followed by ethanol (120 mL) and dichloromethane (40 mL). The mixture was stirred at 50 °C for 3 h and then filtered through a celite pad. The resulting orange yellow solution was concentrated under reduced pressure to afford a yellow brown powder. The crude product was recrystallized from CH_2Cl_2 /diethyl ether (1:20) to

give **Ru1** as a yellow brown powder (3.45 g, 92%). ^1H NMR (500 MHz, CDCl_3) δ 7.72 – 7.67 (m, 3H), 7.64 – 7.56 (m, 7H), 7.48 – 7.32 (m, 15H), 7.17 (t, $J = 7.7$ Hz, 1H), 7.07 (t, $J = 7.6$ Hz, 2H), 6.70 (t, $J = 7.7$ Hz, 2H), 6.37 – 6.31 (m, 1H), 6.29 – 6.24 (m, 1H), 5.94 – 5.86 (m, 1H), 5.83 – 5.76 (m, 1H), 2.45 (dt, $J = 14.0, 6.6$ Hz, 1H), 2.22 (s, 3H), 1.96 (s, 1H), 1.65 (s, 3H), 1.43 (s, 1H), 0.94 (s, 2H), 0.73 (dd, $J = 10.6, 6.6$ Hz, 6H). ^{13}C NMR (126 MHz, CDCl_3) δ 138.71, 134.72, 134.46, 133.03, 132.87, 132.54, 132.38, 132.20, 131.92, 131.86, 131.58, 130.79, 130.51, 129.69, 128.82, 128.64, 128.58, 128.52, 128.49, 128.46, 128.40, 128.34, 98.86, 97.36, 91.36, 89.69, 39.21, 38.60, 29.62, 29.34, 22.31, 21.91, 19.04, 17.94. ^{31}P NMR (202 MHz, CDCl_3) δ 26.02 (P-Ru), 24.81 (P-Ru), -29.77 (P-C). Anal. Calcd for $\text{C}_{51}\text{H}_{53}\text{Cl}_2\text{P}_3\text{Ru}$: C, 65.80; H, 5.74. Found: C, 65.78; H, 5.88%.

2.2 Synthesis of **Ru2**²

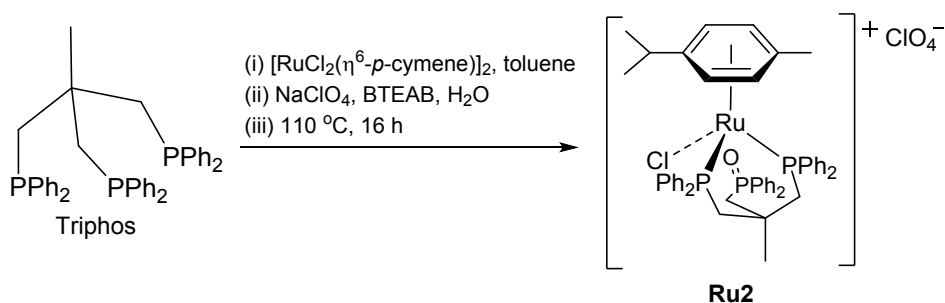
2.2.1 Route A



A mixture of **Ru1** (3.00 g, 3.2 mmol) and dichloromethane (120 mL) were loaded in a Schlenk tube followed by an aqueous solution (60 mL) of NaClO_4 (3.90 g, 32.0 mmol). An aqueous solution (10 mL) of benzyltriethylammonium bromide (BTEAB, 0.12 g, 0.48 mmol) was then added and the mixture stirred for 5 hours at ambient temperature. The dichloromethane layer was separated, washed with deionized water and then dried over anhydrous sodium sulfate. The resulting orange yellow solution was concentrated under reduced pressure to afford a yellow brown powder. The crude product was recrystallized from CH_2Cl_2 /diethyl ether (1:20) to give **Ru2** as a pale green powder (2.85 g, 90%). ^1H NMR (500 MHz, CDCl_3) δ 7.57 (t, $J = 6.4$ Hz, 4H), 7.53 – 7.40 (m, 14H), 7.36 (q, $J = 6.3$ Hz, 6H), 7.21 (d, $J = 7.3$ Hz, 1H), 7.12 (t, $J = 7.6$ Hz, 2H), 6.83 (t, $J = 7.8$ Hz, 2H), 5.84 (d, $J = 4.8$ Hz, 2H), 5.79 – 5.61 (m, 2H), 2.38 – 2.34 (m, 1H), 2.23 (s, 1H), 1.81 (s, 1H), 1.60 (s, 1H), 1.42 (s, 3H), 1.36 (s, 1H), 1.00 (s, 1H), 0.78 – 0.70 (m, 6H). ^{13}C NMR (126 MHz, CDCl_3) δ

134.23, 133.80, 133.76, 133.05, 132.89, 132.60, 132.44, 132.40, 132.36, 132.00, 131.95, 131.59, 130.99, 130.83, 130.70, 130.48, 129.81, 129.57, 129.43, 129.39, 129.35, 129.26, 128.78, 128.67, 128.62, 128.57, 128.51, 128.47, 126.83, 97.55, 96.28, 95.56, 92.71, 91.76, 90.39, 52.78 (CH₂P=O), 38.91, 38.28, 30.02, 21.99, 21.64, 21.40, 16.83, 15.29.³¹P NMR (202 MHz, CDCl₃) δ 27.05 (P=O), 26.09 (d, *J* = 12.43 Hz), 25.30 (d, *J* = 16.57 Hz). Anal. Calcd for C₅₁H₅₃Cl₂O₅P₃Ru: C, 60.59; H, 5.28. Found: C, 60.58; H, 5.38%.

2.2.2 Route B

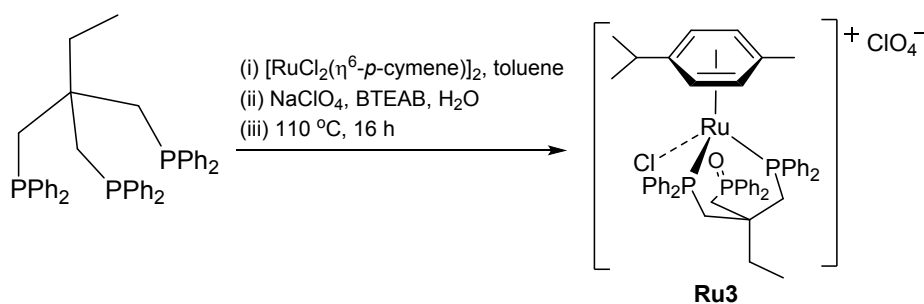


A mixture of 1,1,1-tris(diphenylphosphinomethyl)ethane (triphos) (1.25 g, 2.0 mmol) and [RuCl₂(η⁶-*p*-cymene)]₂ (0.65 g, 1.0 mmol) was loaded in a Schlenk tube and then toluene (50 mL) introduced. The reaction mixture was stirred for 10 min at room temperature and then NaClO₄ (3.00 g, 24.0 mmol) and benzyltriethylammonium bromide (BTEAB, 80 mg, 0.3 mmol) in 40 mL of deionized water were added dropwise to the reaction. After stirring the reaction mixture at 110 °C for 16 h a dark-green suspension was afforded. After cooling to room temperature, the mixture was filtered, washed with distilled water (30 mL) and diethyl ether (10 mL). The crude product was recrystallized from CH₂Cl₂/diethyl ether (1:10) to give **Ru2** as a light green solid which was dried under reduced pressure for 2 h (1.68 g, 80%). ¹H NMR (500 MHz, DMSO): δ 7.25-7.65 (m, 30H, C_{Ar}-H), 6.05 (d, *J* = 38.8 Hz, 2H, C_{Ar}-H), 5.90 – 5.55 (m, 2H, C_{Ar}-H), 3.12 (s, 3H, C_{Ar}-CH₃), 2.45 (s, 3H, -CH₃), 2.22 – 2.04 (m, 2H, CH₂-P=O), 1.67-1.56 (m, 1H, CH(CH₃)₂), 1.02 (s, 2H, P-CH₂), 0.82 (s, 2H, P-CH₂), 0.62 (brs, *J* = 20 Hz, 6H, C_{Ar}-CH₃). ¹³C NMR (126 MHz, DMSO): δ 139.28, 137.82, 136.08, 135.89-135.12(m), 134.62, 133.57 - 133.07 (m), 132.72-132.02 (m), 131.95, 131.87, 131.30, 130.85, 130.72, 130.64, 130.18, 130.11, 129.62-129.01 (m), 128.92, 128.68, 128.64, 127.45, 125.79,

121.45, 99.65, 96.54, 96.37, 95.27, 93.97, 91.89, 49.10 (CH₂P=O), 37.67, 32.59, 30.28, 29.93, 21.67, 20.83, 17.91, 15.06. ³¹P NMR (202 MHz, DMSO): δ 28.32 (P=O), 26.18 (d, *J* = 11.3 Hz), 25.05 (d, *J* = 12.4 Hz). Anal. calcd for C₅₁H₅₃Cl₂O₅P₃Ru: C, 60.59; H, 5.28. Found: C, 60.61; H, 5.25%. ESI-MS (*m/z*): calcd for [Ru₂-Cl+1-ClO₄]⁺ 877.2; found: 877.8. ESI-MS (*m/z*): calcd for [Ru₂-Cl+23-ClO₄] 899.2; found: 899.9.

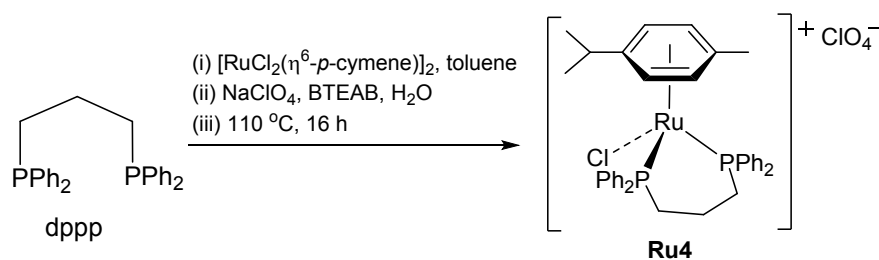
Safety warning: When using perchlorates at elevated temperatures, strict control of the amount used is advised as there is a possibility of explosion.

2.3 Synthesis of Ru3



Using the same procedure as described in route **B** for the synthesis of **Ru2**, **Ru3** was isolated as a pale green solid (1.58 g, 77%) ¹H NMR (500 MHz, DMSO) δ 7.61 (d, *J* = 7.4 Hz, 7H), 7.56 – 7.41 (m, 20H), 7.32 – 7.25 (m, 2H), 7.18 (t, *J* = 7.1 Hz, 1H), 6.28 – 6.10 (m, 2H), 5.75 – 5.38 (m, 2H), 3.16 (dd, *J* = 14.7, 6.9 Hz, 1H), 2.30 (s, 3H), 2.18 – 1.95 (m, 3H), 1.57 (s, 1H), 1.44 (s, 1H), 0.89 (s, 2H), 0.78 (s, 2H), 0.70 (d, *J* = 7.2 Hz, 3H), 0.61 (d, *J* = 7.2 Hz, 3H), 0.53 – 0.29 (m, 2H). ¹³C NMR (126 MHz, DMSO) δ 137.82, 136.07, 135.31, 135.26, 134.31, 133.41, 132.66, 132.13, 132.02, 131.85, 131.34, 130.92, 130.72, 130.65, 130.03, 129.96, 129.66, 129.54, 129.46, 129.38, 129.28, 129.24, 129.18, 129.10, 129.01, 128.96, 128.68, 128.67, 128.60, 125.79, 101.04, 98.89, 94.80, 93.63, 86.84, 85.99, 49.05 (CH₂P=O), 40.51, 40.35, 40.18, 40.01, 39.85, 39.68, 39.51, 30.37, 21.97, 21.52, 20.88, 20.72, 18.34, 16.84, 14.72. ³¹P NMR (202 MHz, DMSO) δ 28.65 (P=O), 25.12 (d, *J* = 26.92 Hz), 24.09 (d, *J* = 28.99 Hz). ESI-MS (*m/z*): calcd for [Ru₃-Cl+1-ClO₄]⁺ 890.2; found: 890.9. ESI-MS (*m/z*): calcd for [Ru₃-*p*-cymene-ClO₄]⁺: 791.1; found: 791.2.

2.4 Synthesis of **Ru4**



Using the same procedure as described in route **B** for the synthesis of **Ru2**, **Ru4** was isolated as a pale green solid (1.48 g, 94%) ^1H NMR (500 MHz, DMSO): δ 7.49 (dd, $J = 26.7, 9.3$ Hz, 20H), 6.25 (d, $J = 6.0$ Hz, 2H), 5.78 (d, $J = 6.1$ Hz, 2H), 3.14 (d, $J = 7.3$ Hz, 2H), 2.67-2.64 (m, 1H), 1.29 (t, $J = 7.2$ Hz, 4H), 1.16 (s, 3H), 0.71 (d, $J = 6.9$ Hz, 6H). ^{13}C NMR (126 MHz, DMSO): δ 137.04, 136.84, 136.63, 134.47, 134.43, 134.19, 134.14, 134.10, 133.95, 133.76, 133.70, 133.18, 133.06, 133.02, 132.98, 132.42, 132.06, 131.95, 131.67, 131.18, 130.82, 130.78, 130.74, 130.70, 130.63, 129.54, 129.35, 129.22, 129.17, 129.12, 129.08, 129.02, 128.99, 128.95, 128.91, 128.31, 126.59, 98.60, 94.94, 93.10, 93.06, 65.39 (C_{ether}), 40.35, 40.19, 40.02, 39.86, 39.69, 30.45, 20.89, 20.61, 15.65 (C_{ether}), 15.54, 7.96. ^{31}P NMR (202 MHz, DMSO): δ 29.90, 26.37. ESI-MS (m/z): Calcd for [**Ru4** +1- ClO_4] $^+$: 684.1; found: 684.4.

2.5 Using the ruthenium catalysts to promote the oxidation of triphenylphosphine

In order to explain the oxidation of the uncoordinated phosphine in **Ru2** and **Ru3**, the four different ruthenium complexes were tested as catalysts for the oxidation of PPh_3 in the presence of water over 24 h at 100 °C. Inspection of the results reveals conversions to triphenylphosphine oxide of 24% for $[\text{RuCl}_2(p\text{-cymene})]_2$, 94% for **Ru1**, 43% for **Ru2** and 97% for a mixture of $[\text{RuCl}_2(p\text{-cymene})]_2$ and triphos.

Table S2 Exploring the capacity of the ruthenium catalyst to mediate the oxidation of triphenylphosphine ^a

Entry	Ru-Cat	H_2O	OPPh_3^b

1	$[\text{RuCl}_2(p\text{-cymene})]_2$	none	none
2	$[\text{RuCl}_2(p\text{-cymene})]_2$	5 mL	24%
3	Ru1	none	none
4	Ru1	5 mL	94%
5	Ru2	none	none
6	Ru2	5 mL	43%
7	$[\text{RuCl}_2(p\text{-cymene})]_2$ + triphos	none	none
8	$[\text{RuCl}_2(p\text{-cymene})]_2$ + triphos	5 mL	97%
9 ^c	Ru1	5 mL	33%
10 ^c	$[\text{RuCl}_2(p\text{-cymene})]_2$	5 mL	none

^a Reaction conditions: Ru-cat (0.25 mmol), PPh₃ (1.31 g, 2.5 mmol), toluene (15 mL), water (5 mL), 100 °C, 24 h; ^b detected by HPLC; ^c 12 h

3. ¹H, ¹³C and ³¹P NMR spectra of Ru1 – Ru4

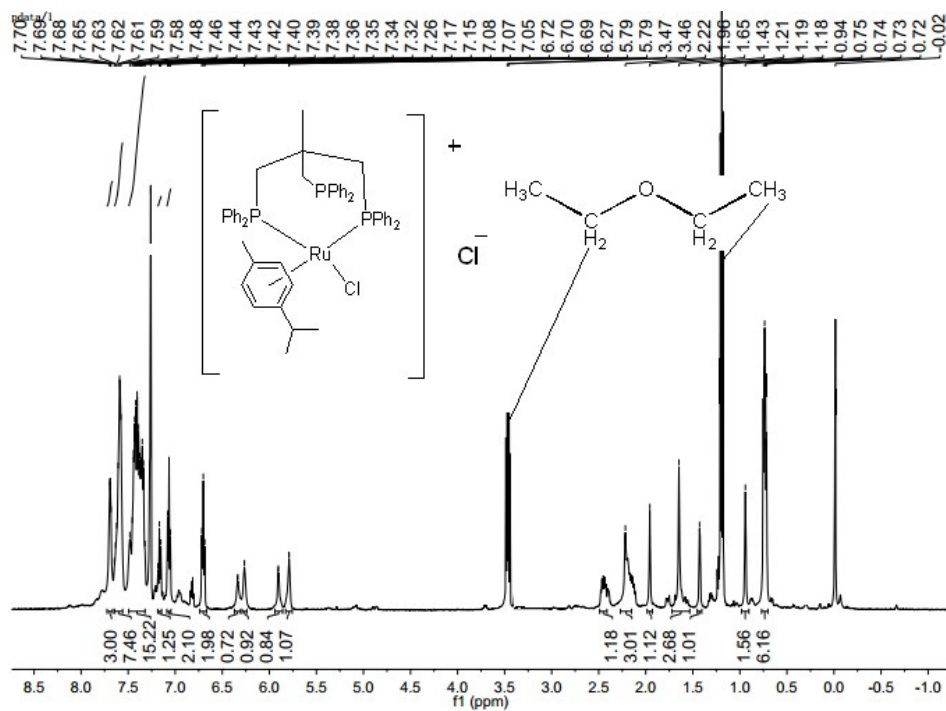


Fig. S1 ¹H NMR spectrum of **Ru1** in CDCl₃

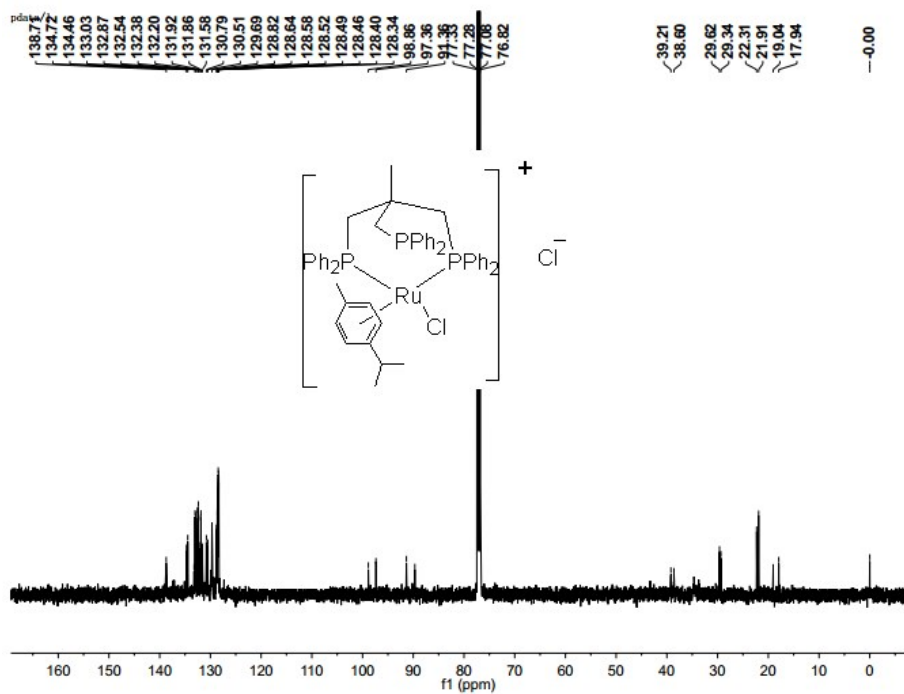


Fig. S2 ¹³C NMR spectrum of **Ru1** in CDCl₃

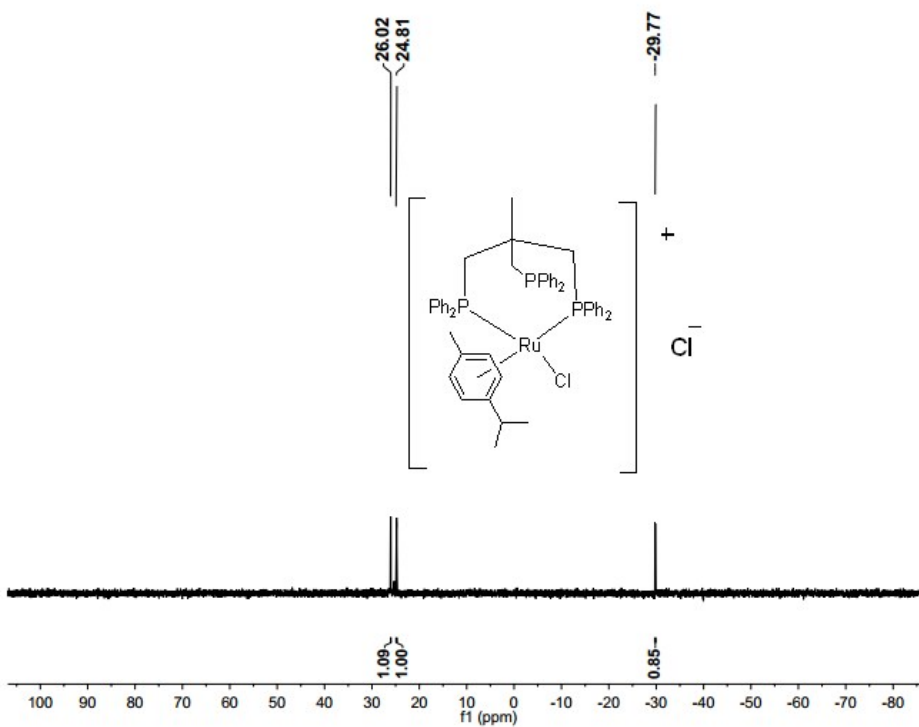


Fig. S3 ³¹P NMR spectrum of **Ru1** in CDCl₃

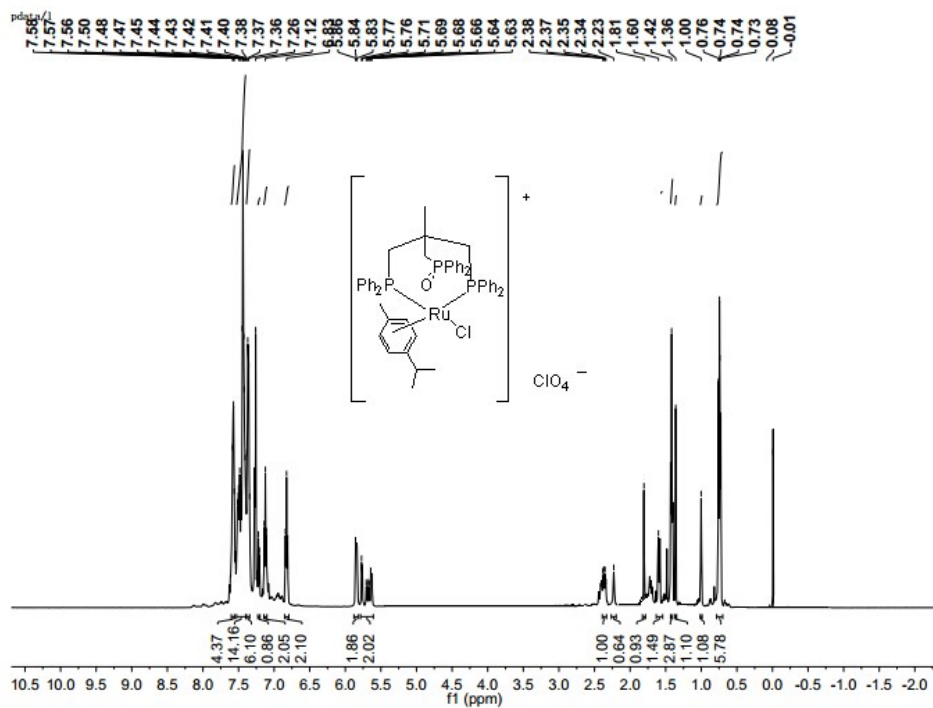


Fig. S4 ^1H NMR spectrum of **Ru2** in CDCl_3

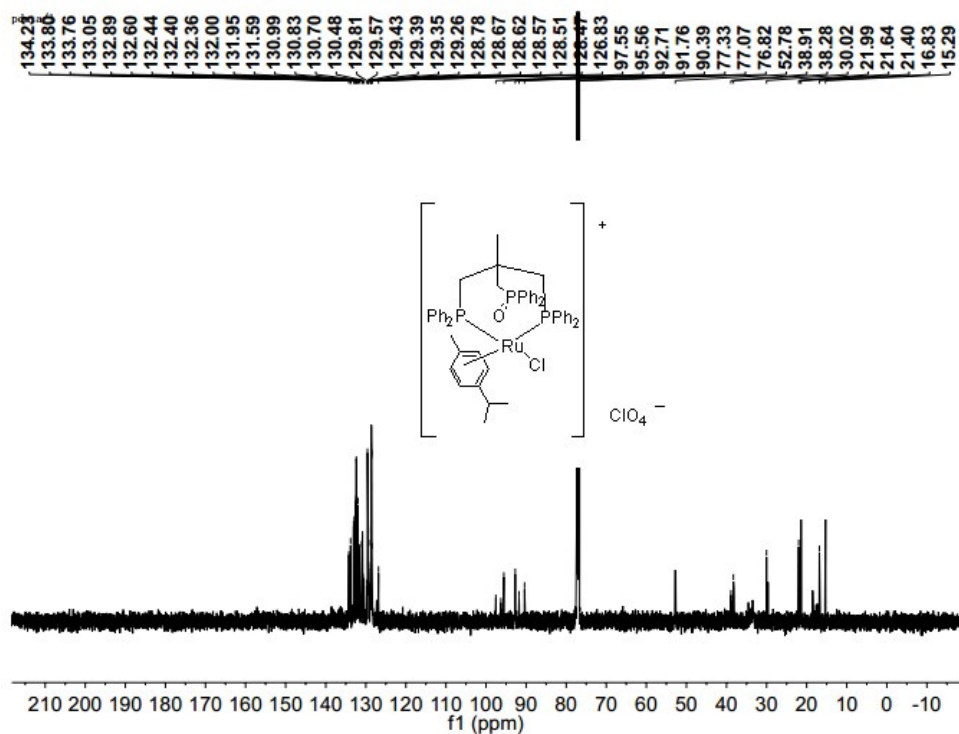


Fig. S5 ^{13}C NMR spectrum of **Ru2** in CDCl_3

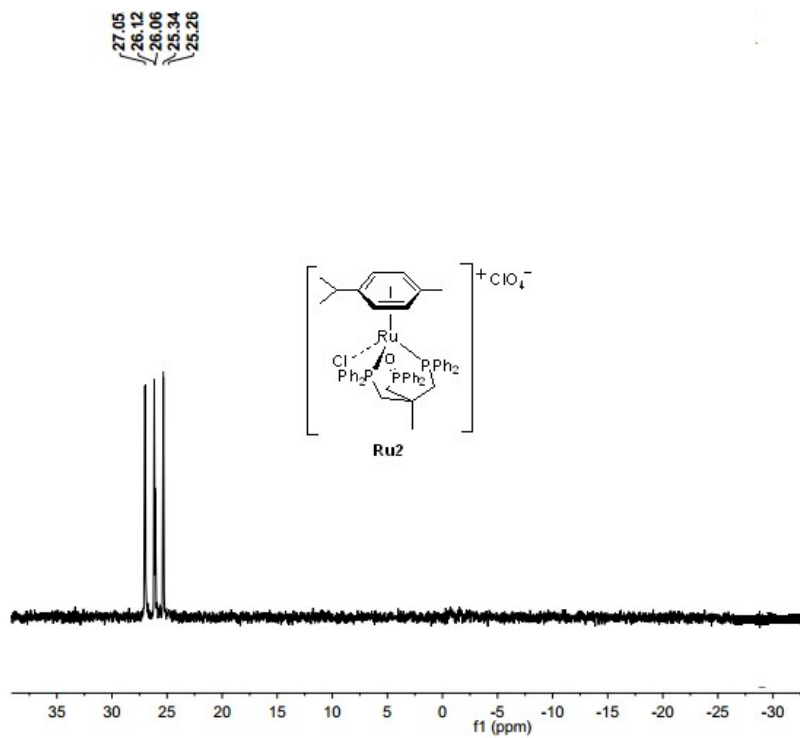


Fig. S6 ^{31}P NMR spectrum of **Ru2** in CDCl_3

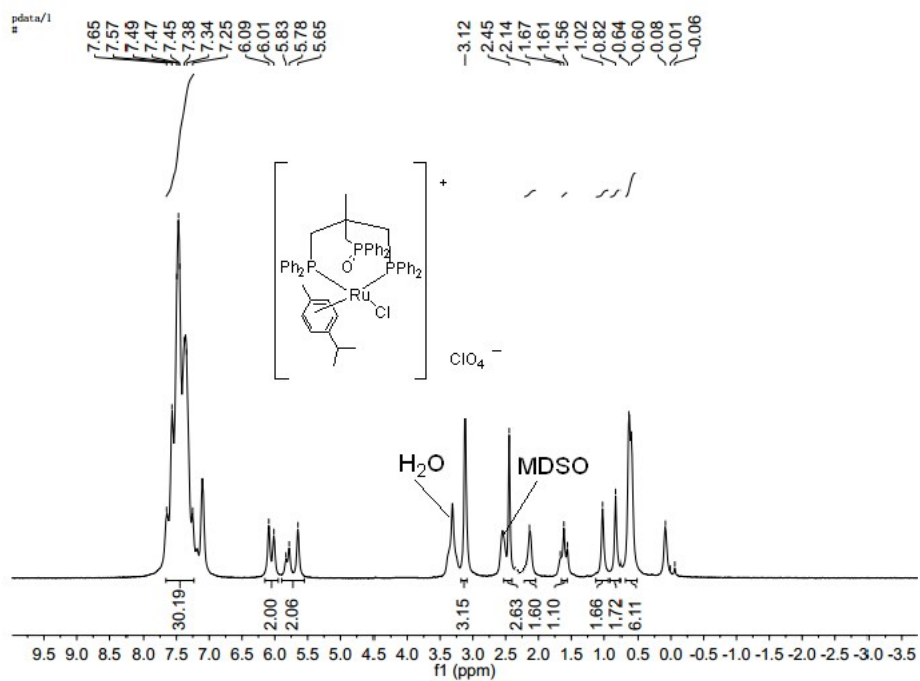


Fig. S7 ^1H NMR spectrum of **Ru2** in $\text{DMSO}-d_6$

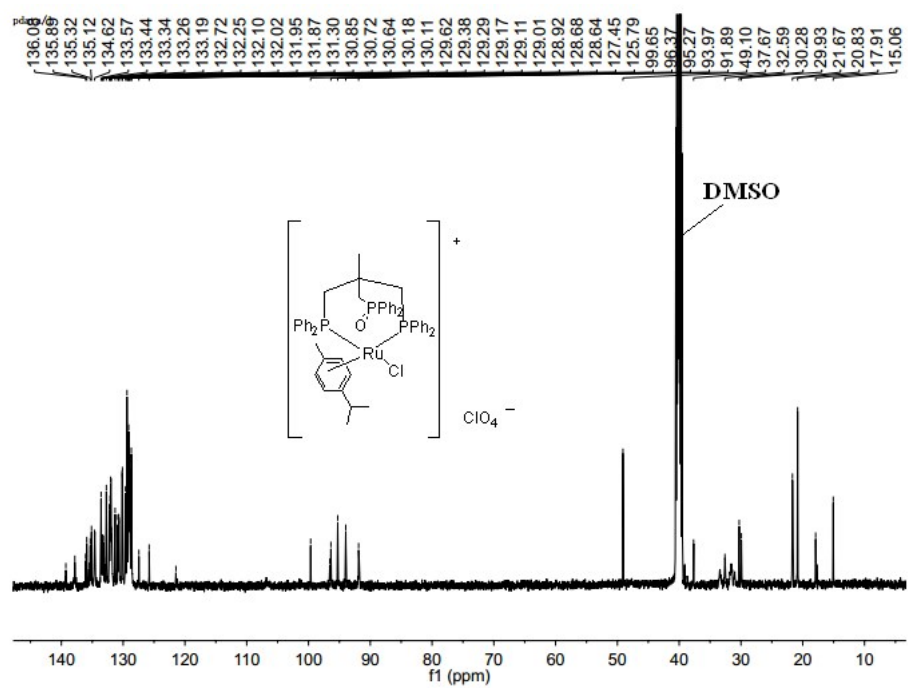


Fig. S8 ^{13}C NMR spectrum of **Ru2** in $\text{DMSO-}d_6$

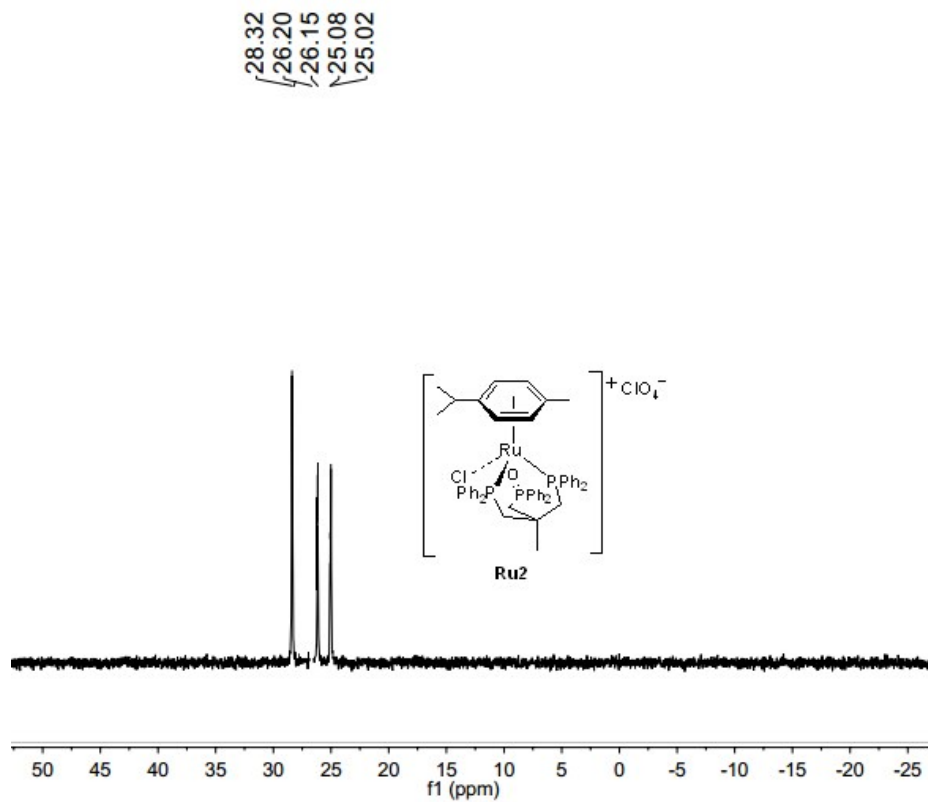


Fig. S9 ^{31}P NMR spectrum of **Ru2** in $\text{DMSO-}d_6$

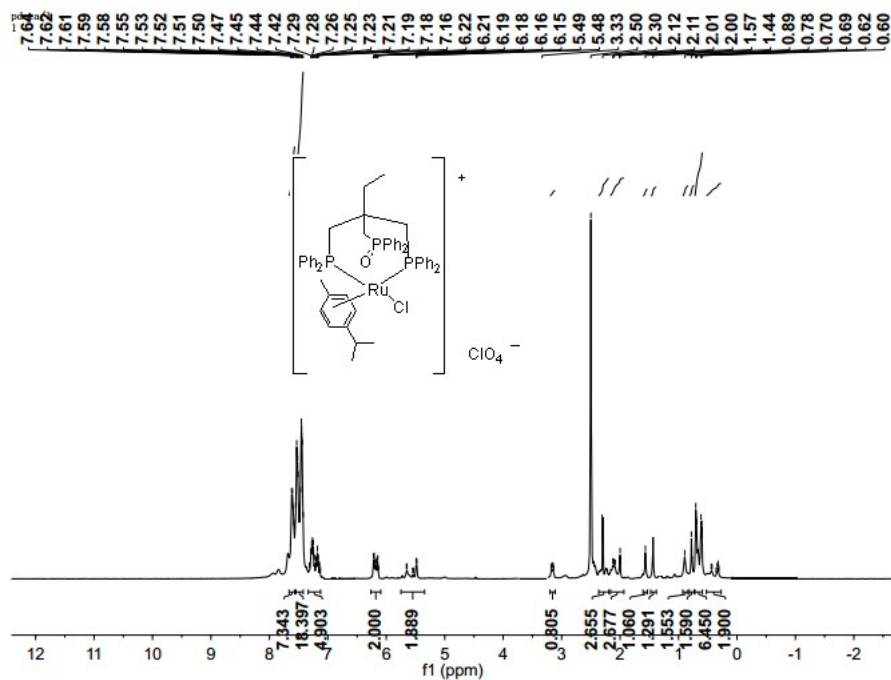


Fig. S10 The ^1H NMR spectrum of **Ru3** in $\text{DMSO-}d_6$

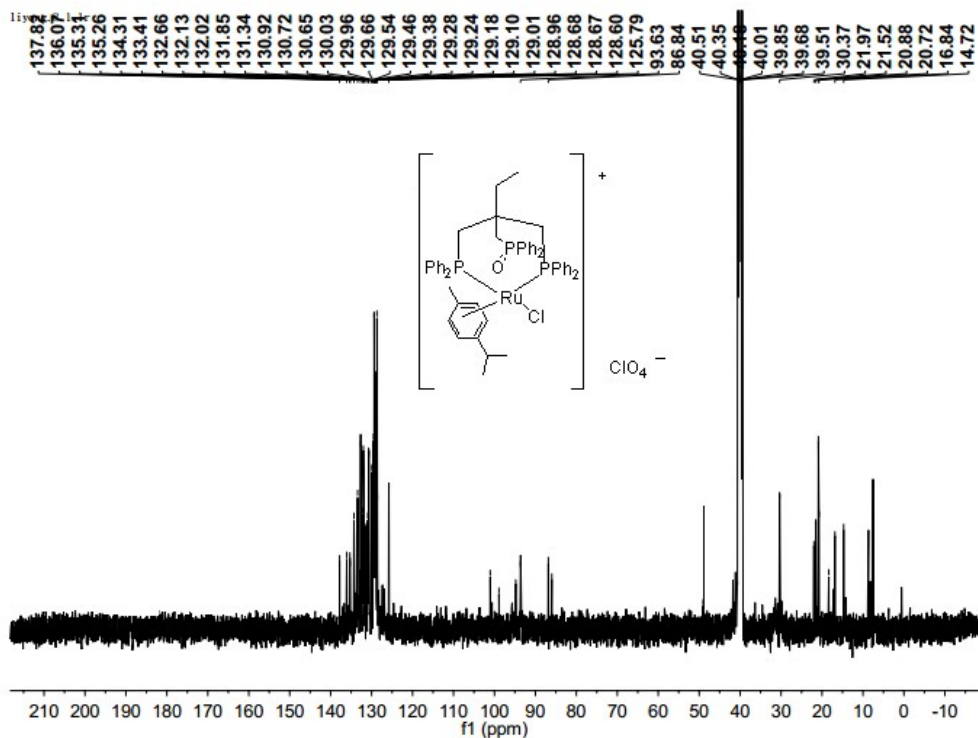


Fig. S11 ^{13}C NMR spectrum of **Ru3** in $\text{DMSO-}d_6$

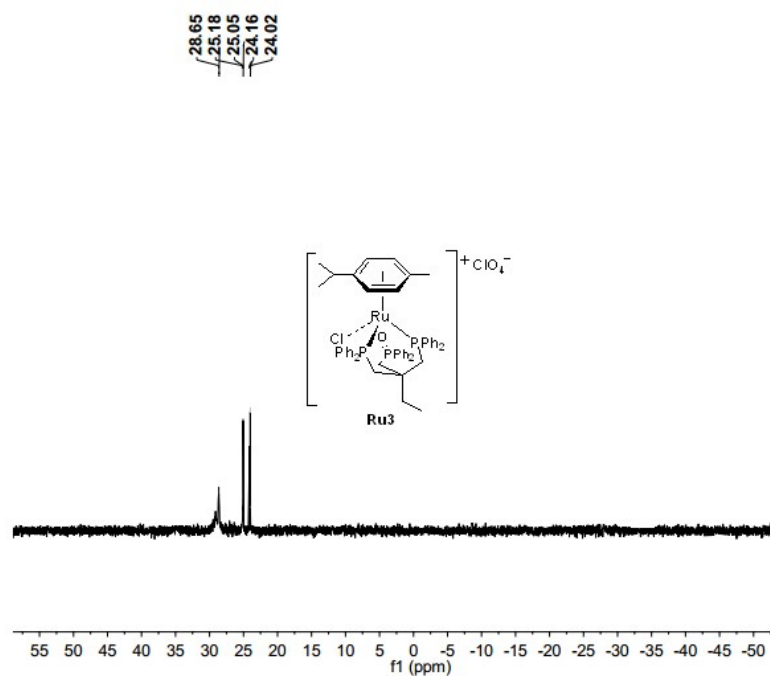


Fig. S12 ^{31}P NMR spectrum of **Ru3** in $\text{DMSO-}d_6$

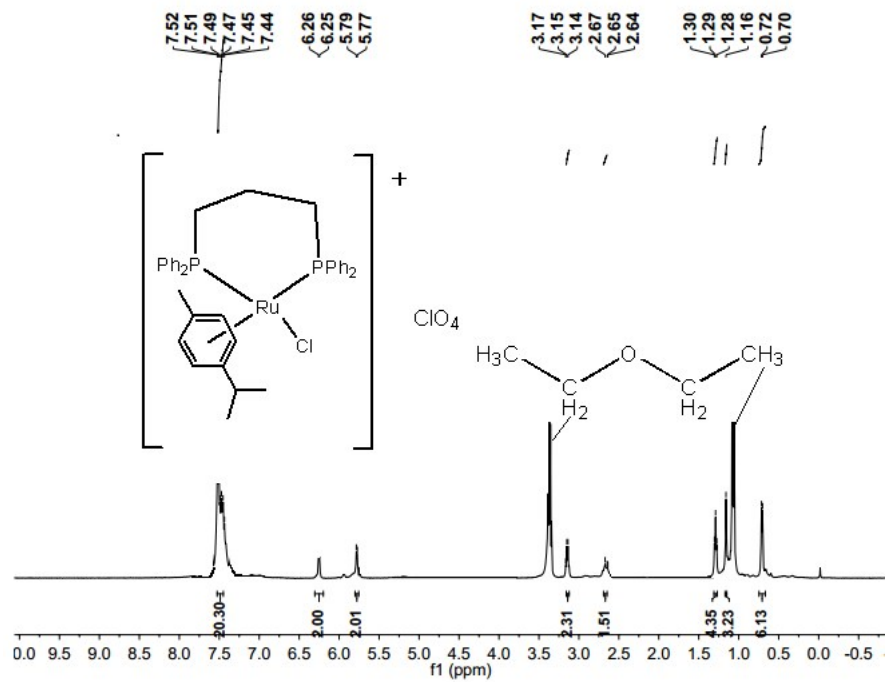


Fig. S13 ^1H NMR spectrum of **Ru4** in $\text{DMSO-}d_6$

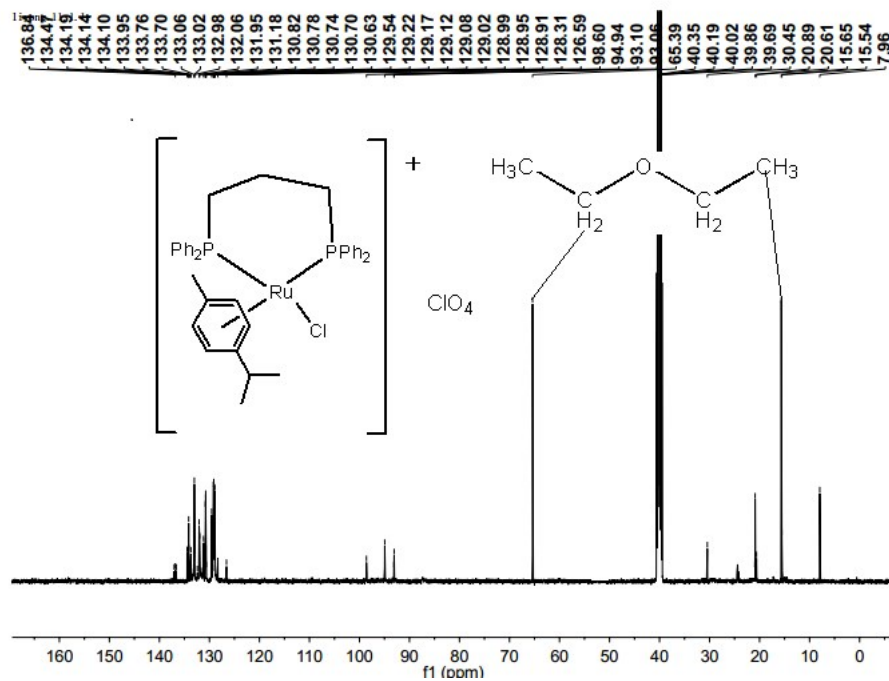


Fig. S14 ¹³C NMR spectrum of **Ru4** in DMSO-*d*₆

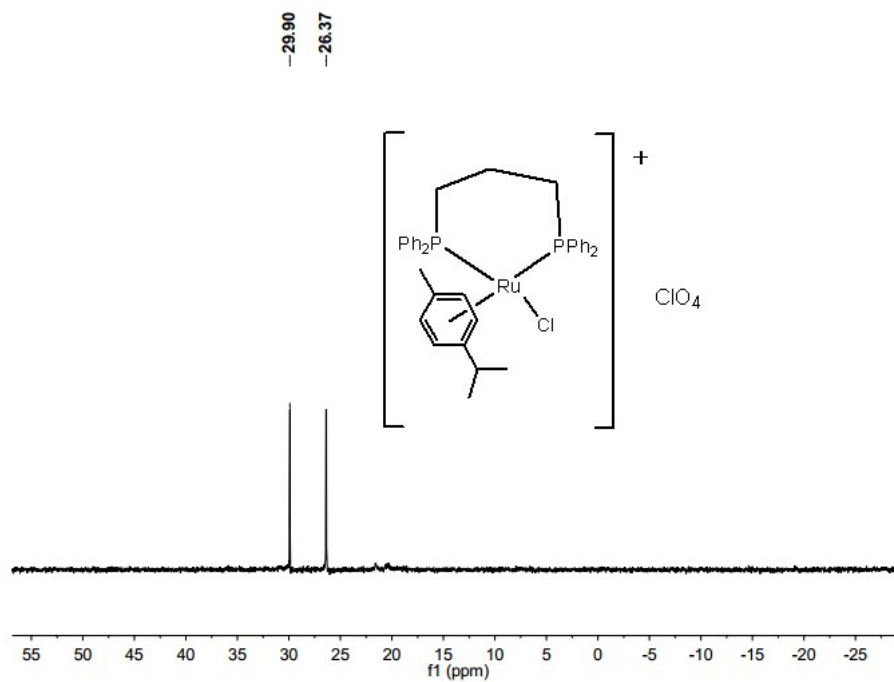


Fig. S15 ³¹P NMR spectrum of **Ru4** in DMSO-*d*₆

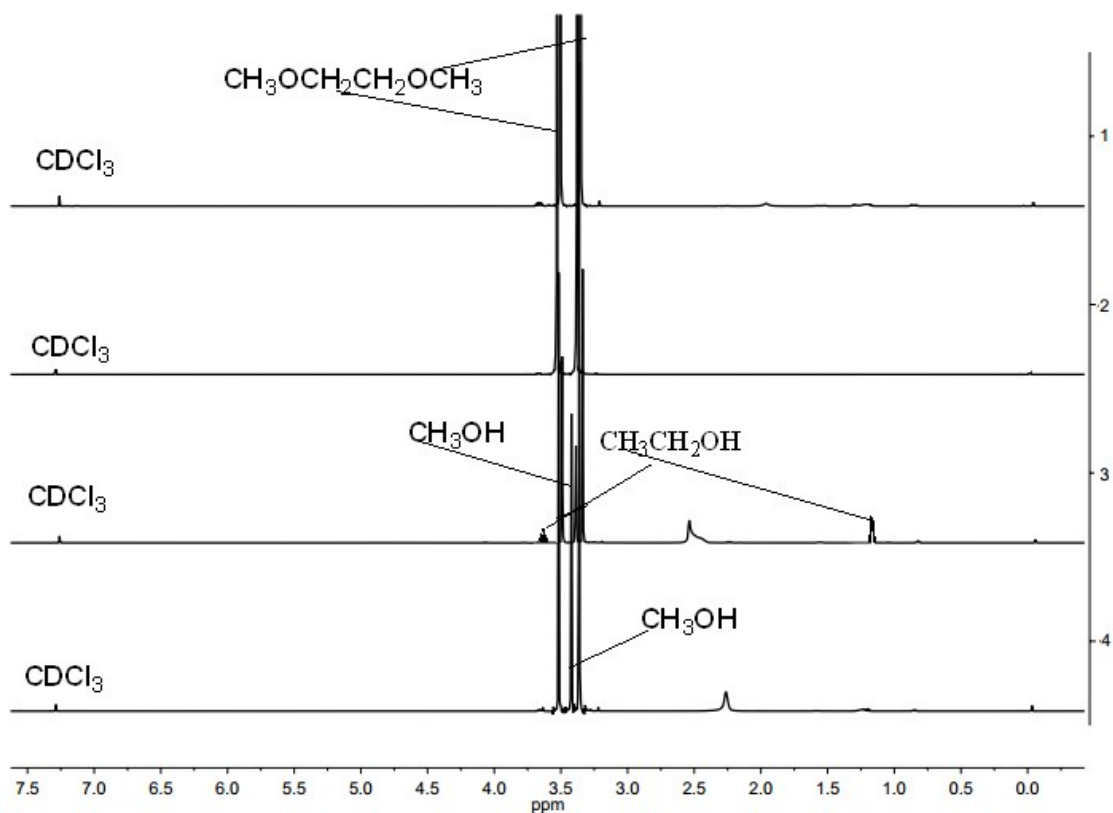
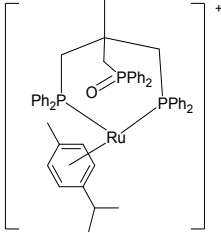
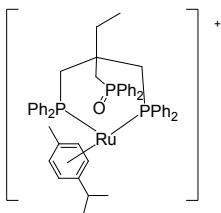
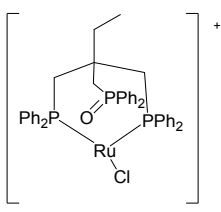
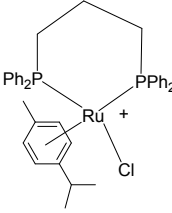


Fig. S16 Stacked ¹H NMR spectra (1 – 4) showing the identification of MeOH in spectra 3 and 4 (in CDCl₃). Spectrum 1: before the reaction. Spectrum 2: conditions, **Ru2** (10.0 μmol), P_{CO2} = 12 bar (at RT), P_{H2} = 68 bar (at RT), S:C ratio = 100:1, 1,2-dimethoxyethane (10 mL), after 20 h (entry 17, Table 1). Spectrum 3: conditions, decanoic acid (1.0 mmol), **Ru2** (10.0 μmol), P_{CO2} = 12 bar (at RT), P_{H2} = 68 bar (at RT), 1,2-dimethoxyethane (2.5 mL), S:C ratio = 100:1, after 20 h (entry 11, Table 1). Spectrum 4: conditions, decanoic acid (1.0 mmol), **Ru2** (10 μmol), P_{CO2} = 12 bar (at RT), P_{H2} = 68 bar (at RT), 1,2-dimethoxyethane (10 mL), S:C ratio = 100:1, after 20 h (entry 4, Table 1).

4. Identification of Ru2 - Ru4 and their fragments by using ESI-MS

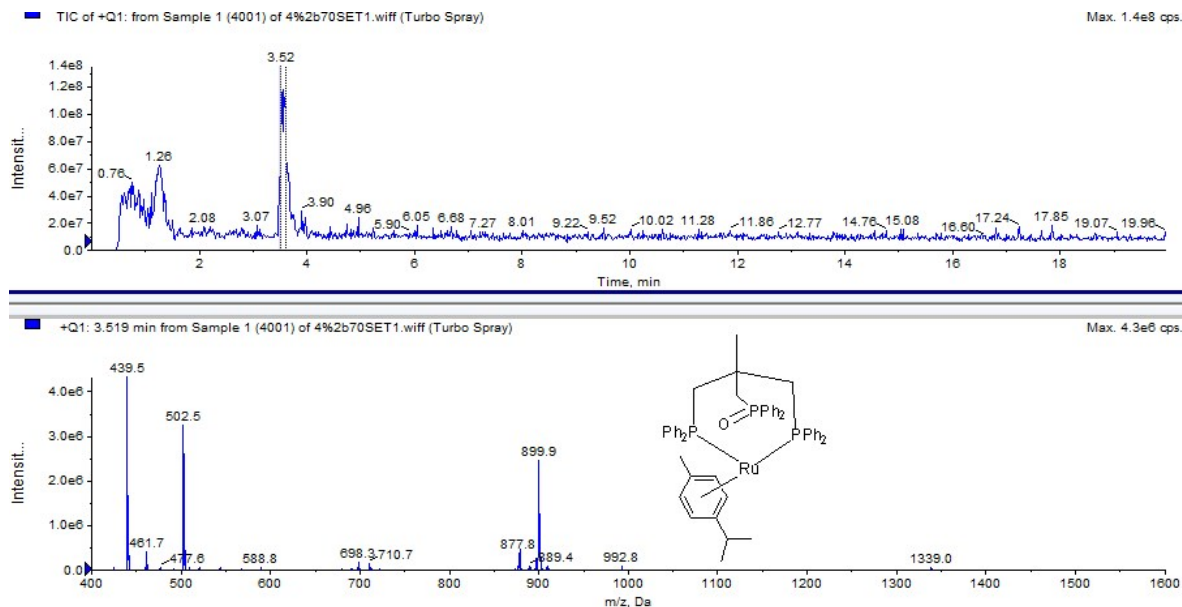
ESI-MS was performed on a 3200 QTRAP 1200 infinity series instrument using an Agilent ZORBAX SB-C18 column (dimensions in mm: 150 × 4.6): acetonitrile: water = 70:30, flow rate = 1 mL/min, electronic energy = 70 eV, Q1MS scan range = 100 ~ 1000.

Table S3 Species detected by ESI mass spectrometry;^a the corresponding spectra are given below

Intermediate	ESI detected species	<i>m/z</i> value	Structural assignment
Ru2	$[\mathbf{Ru2}\text{-Cl+H-ClO}_4]^+$,	877.8.	
	$[\mathbf{Ru2}\text{-Cl+23-ClO}_4]^+$	899.9	
Ru3	$[\mathbf{Ru3}\text{-Cl-ClO}_4]^+$,	890.9,	
	$[\mathbf{Ru3}\text{-}p\text{-cymene-ClO}_4]^+$	791.2	
Ru4	$[\mathbf{Ru4}\text{+H-ClO}_4]^+$	684.4	
			

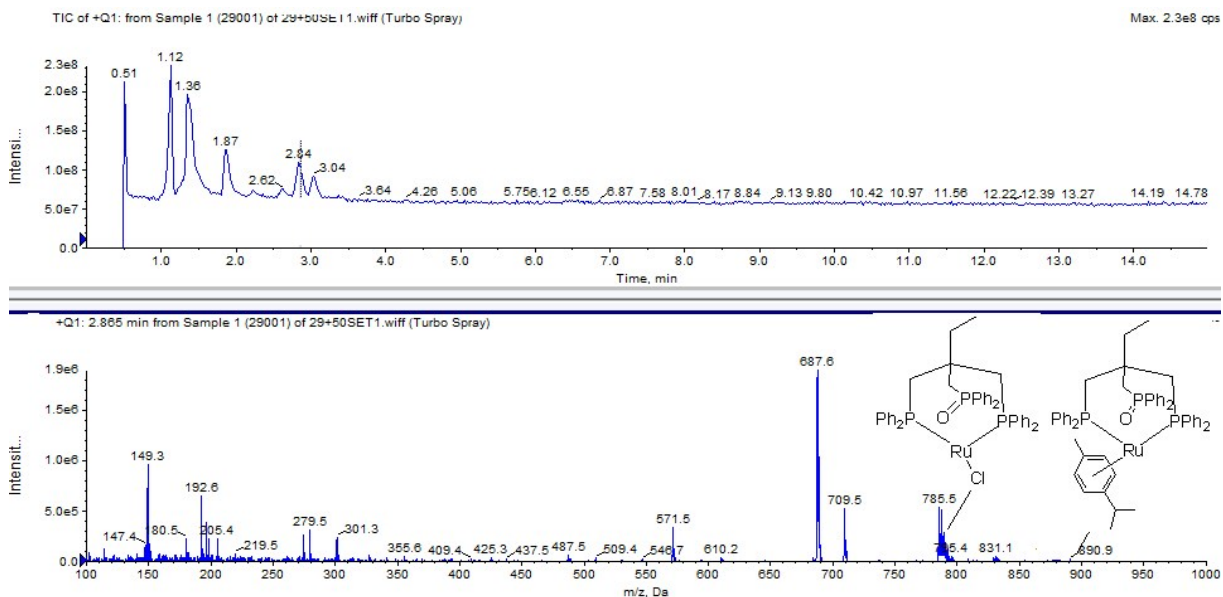
^a ESI mass spectra of **Ru2 - Ru4** in MeCN (1 mL) recorded using a 3200 QTRAP 1200 infinity series instrument. MeCN:H₂O = 70:30, flow rate = 1 mL/min, electronic energy = 70 eV, Q1MS scan range = 100 - 1000.

4.1. The LC and mass spectrum (m/z) of **Ru2** in MeCN



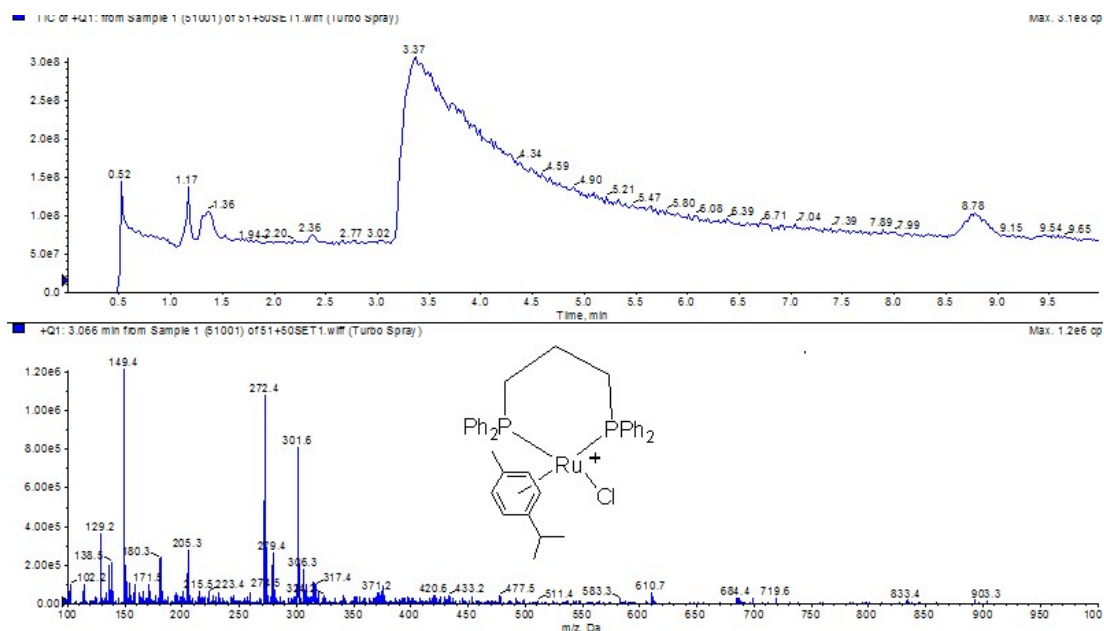
ESI mass spectrum of **Ru2** in MeCN (1 mL) recorded using the 3200 QTRAP 1200 infinity series instrument. MeCN:H₂O = 70:30, flow rate = 1 mL/min, electronic energy = 70 eV, Q1MS scan range = 400 - 1600. The base peak corresponds to [**Ru2**-Cl-CIO₄]⁺ at m/z 877.8 and [**Ru2**-Cl+23-CIO₄]⁺ at m/z 899.9.

4.2 The LC and mass spectrum of **Ru3** in MeCN



ESI mass spectrum of **Ru3** in MeCN (1 mL) recorded using the 3200 QTRAP 1200 infinity series instrument. MeCN:H₂O = 70:30, flow rate = 1 mL/min, electronic energy = 50 eV, Q1MS scan range = 100 - 1000. The base peak corresponds to [**Ru3**-Cl-CIO₄]⁺ at m/z 890.0 and [**Ru3**-*p*-cymene-CIO₄]⁺ at m/z 791.2.

4.3. The LC and mass spectrum of **Ru4** in MeCN



ESI mass spectrum of **Ru4** in MeCN (1 mL) recorded using the 3200 QTRAP 1200 infinity series instrument. MeCN:H₂O = 70:30, flow rate = 1 mL/min, electronic energy = 50 eV, Q1MS scan range = 100 - 1000. The base peak corresponds to [**Ru4**+H-ClO₄]⁺ at *m/z* 684.4.

5. Catalytic study, GC-MS spectra for the products and various data

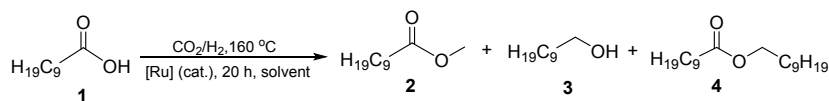
5.1 Catalytic study

Under an atmosphere of argon, a stainless steel 100 mL autoclave, equipped with a magnetic stir bar, was charged with **Ru1** – **Ru4** (2.5 - 10 μmol) and the solvent to be used (2.5 – 5 mL). A solution of the carboxylic acid (1 mmol) in the solvent (5 – 25 mL) was then added *via* a syringe. The autoclave was purged by three cycles of pressurization/venting with CO₂ (5 - 10 bar), and then pressurized with the desired mixture of CO₂ and H₂. The autoclave was heated to the desired temperature and the contents stirred. After the pre-determined reaction time, the autoclave was cooled to room temperature and the pressure slowly released. The reaction mixture was filtered through a plug of silica gel and then analyzed by GC and GC-MS. The full set of data is tabulated in Table 1, while Table S4 below collects the results obtained using solely **Ru2** as the catalyst.

In case of entries 3 and 4 in Table S4 (and Table 1), the experiments were performed three times

with a conversion error of less than $\pm 0.2\%$. For entry 3, the conversion/selectivity showed a modest variation, while for entry 4 the differences in conversion/selectivity were negligible.

Table S4 Evaluation of **Ru2** as a catalyst for the hydrogenation of CO₂, in the presence of decanoic acid (**1**), to give methyl decanoate (**2**);^a entries 3 and 4 were each repeated three times.

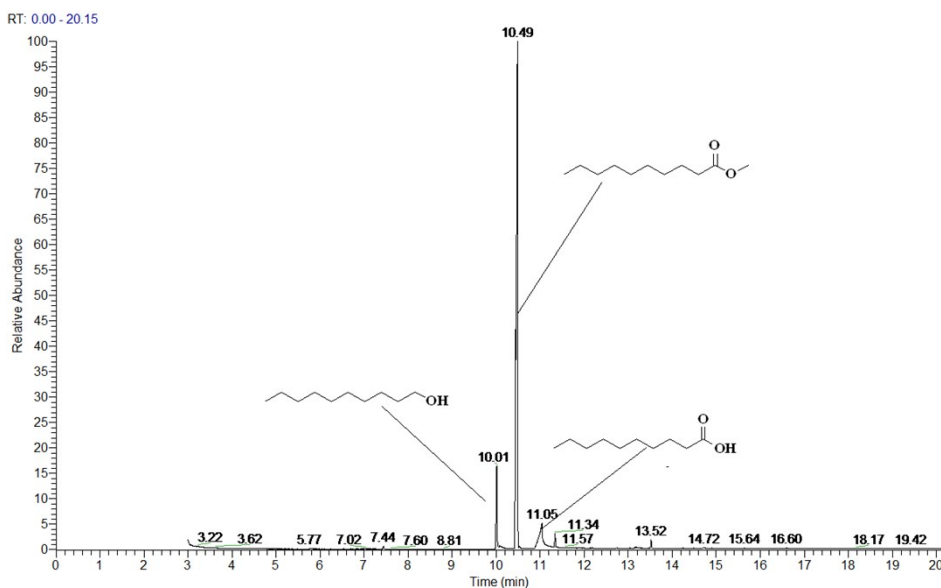


Entry	[Ru]	CO ₂ :H ₂ (bar)	Conv. (%) ^b	2/3/4 (% conv. to each) ^b
1	Ru2	12:70	91.3	83.2/7.8/0
2	Ru2	12:70	91.5	83.5/7.5/0
3	Ru2	12:70	91.7	83.4/8.3/0
4	Ru2	12:68	99.2	99.2/0/0
5	Ru2	12:68	99.4	99.4/0/0
6	Ru2	12:68	99.6	99.6/0/0

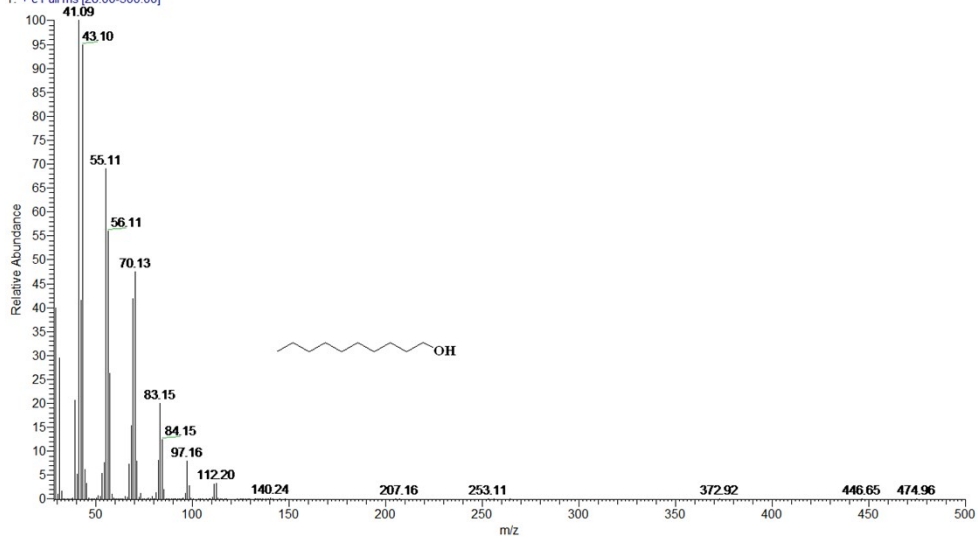
^a Conditions: decanoic acid (1.0 mmol), **Ru2** (10.0 μmol), solvent (10 mL), P_{H₂} = 68 - 70 bar (at RT), P_{CO₂} = 12 bar (at RT), Temp. = 160 °C, Time = 20 h, S:C = 100, DME is 1,2-dimethoxyethane; ^b The conversion, with reference to decanoic acid (**1**), was determined by GC (using mesitylene as the internal standard) and by GC-MS

5.2 GC-MS spectra of the products and data

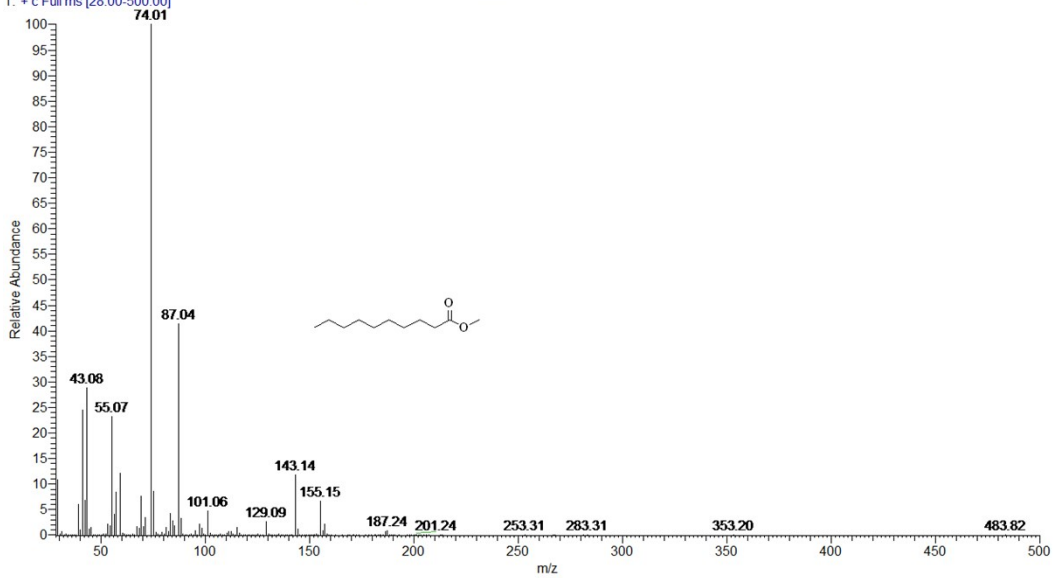
5.2.1 Gas chromatogram and mass spectra for entry 3, Table 1



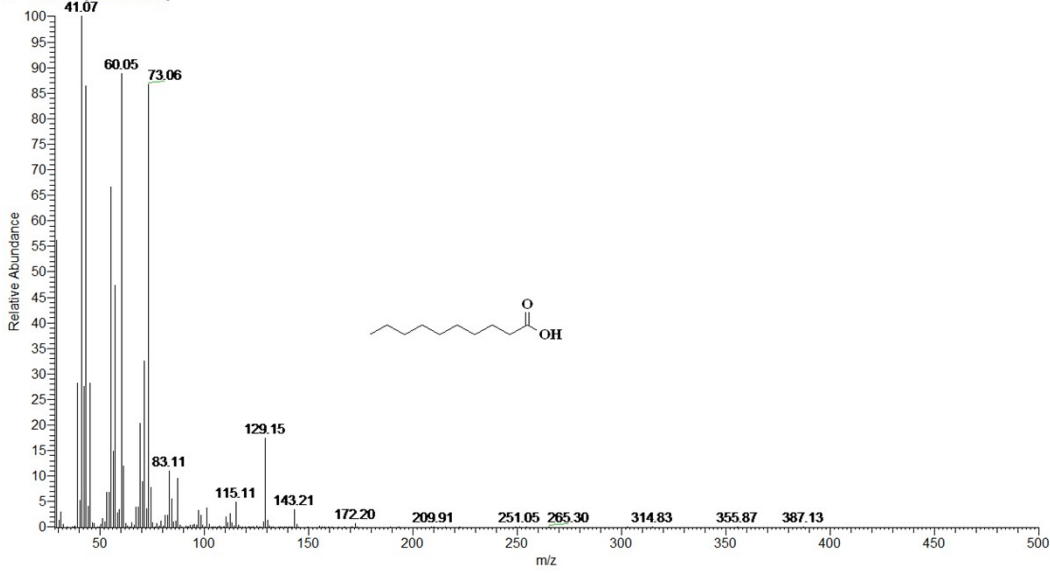
160615-3 #2725 RT: 10.01 AV: 1 NL: 2.24E7
T: + c Full ms [28.00-500.00]



160615-3 #2907 RT: 10.48 AV: 1 SB: 165 10.54-10.77, 10.15-10.34 NL: 2.52E8
T: + c Full ms [28.00-500.00]



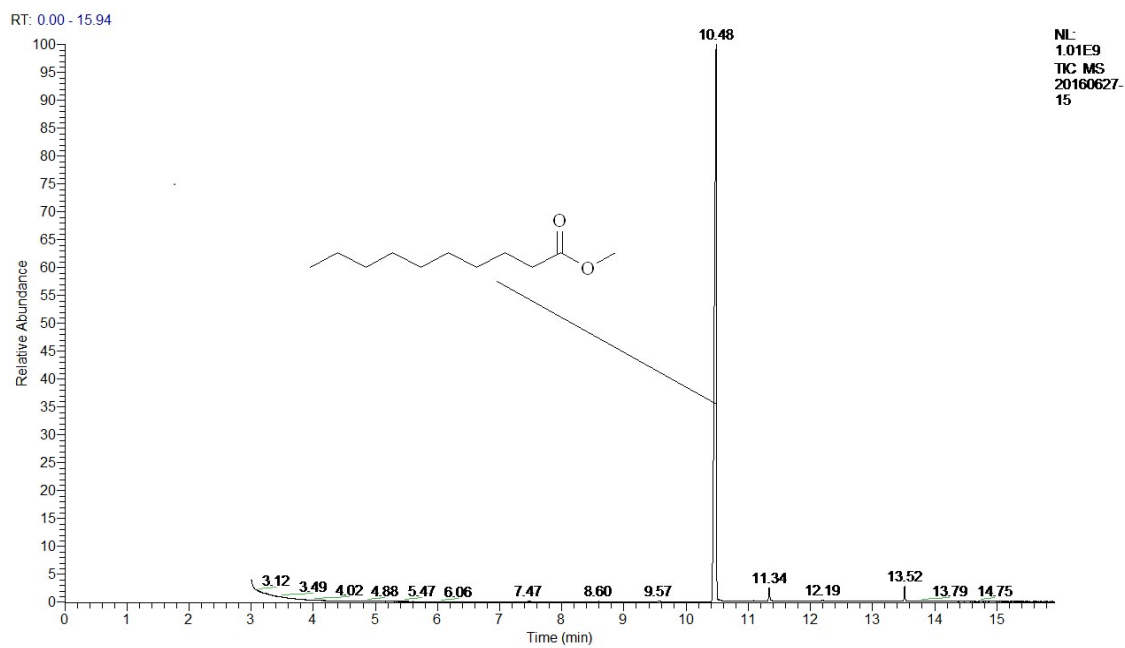
160615-3 #3124 RT: 11.04 AV: 1 SB: 78 11.11-11.22, 10.81-10.89 NL: 4.95E6
 T: + c Full ms [28.00-500.00]



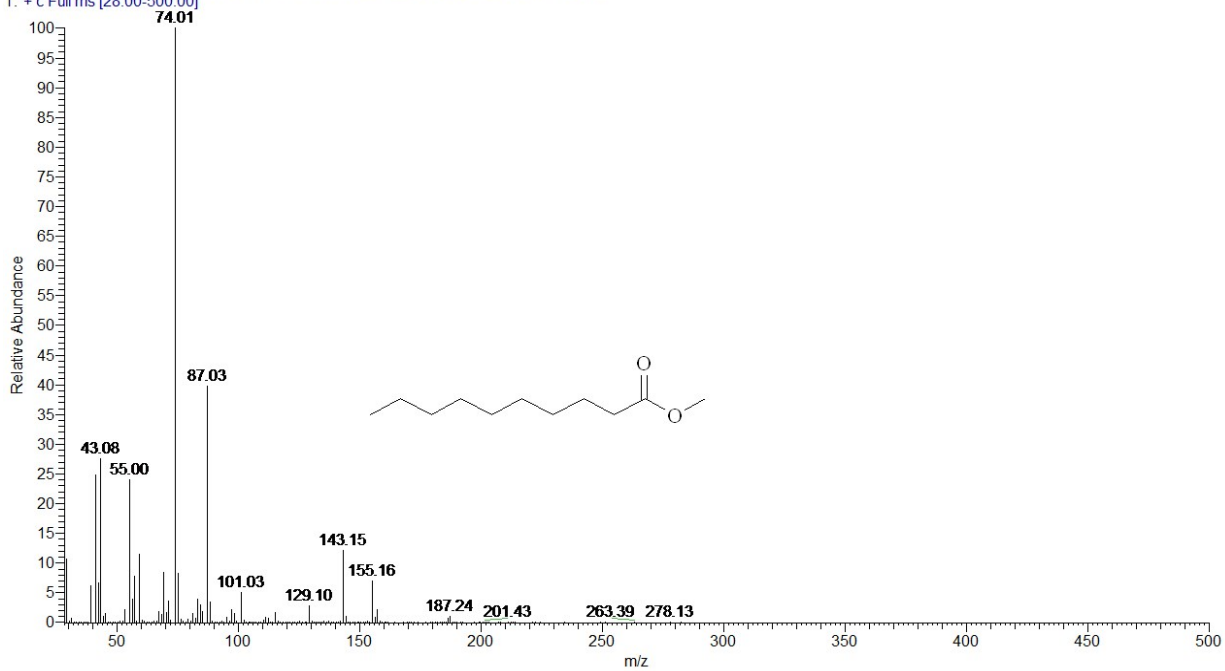
PEAK LIST 160615-3.RAW RT: 10.59 - 11.90

Apex RT	Start RT	End RT	Area	%Area	Height	%Height
10.01	9.98	10.03	2.10E+08	7.56	1.49 E+08	13.03
10.49	10.42	10.5	2.33E+09	83.34	9.57+08	83.14
11.05	10.86	11.13	2.53E +08	9.1	4.41E+07	3.84

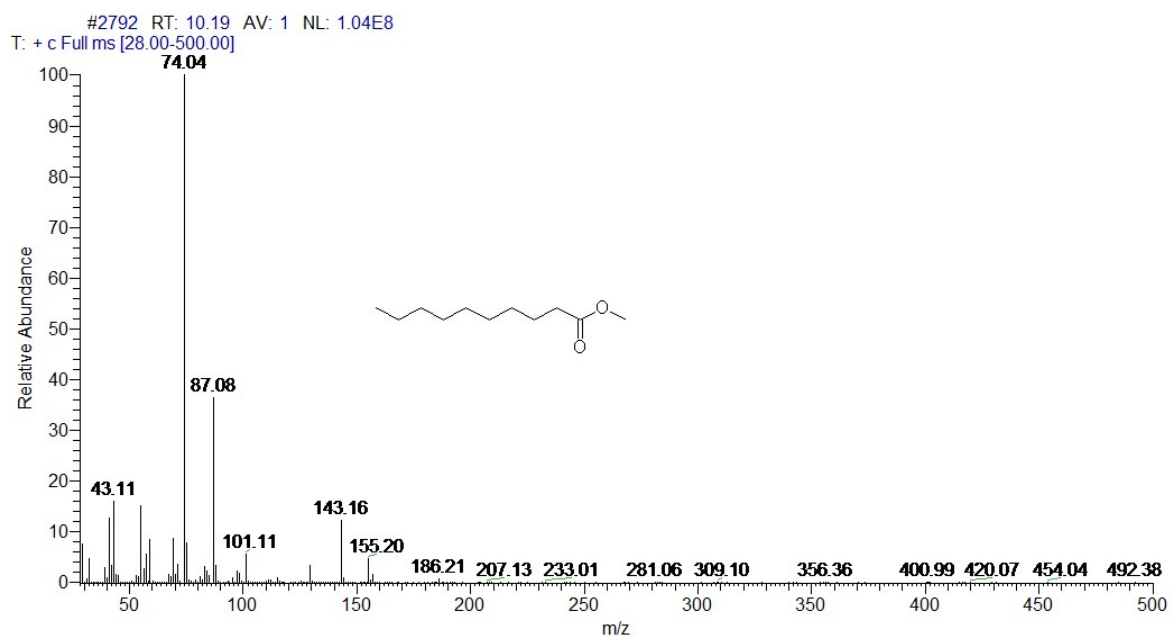
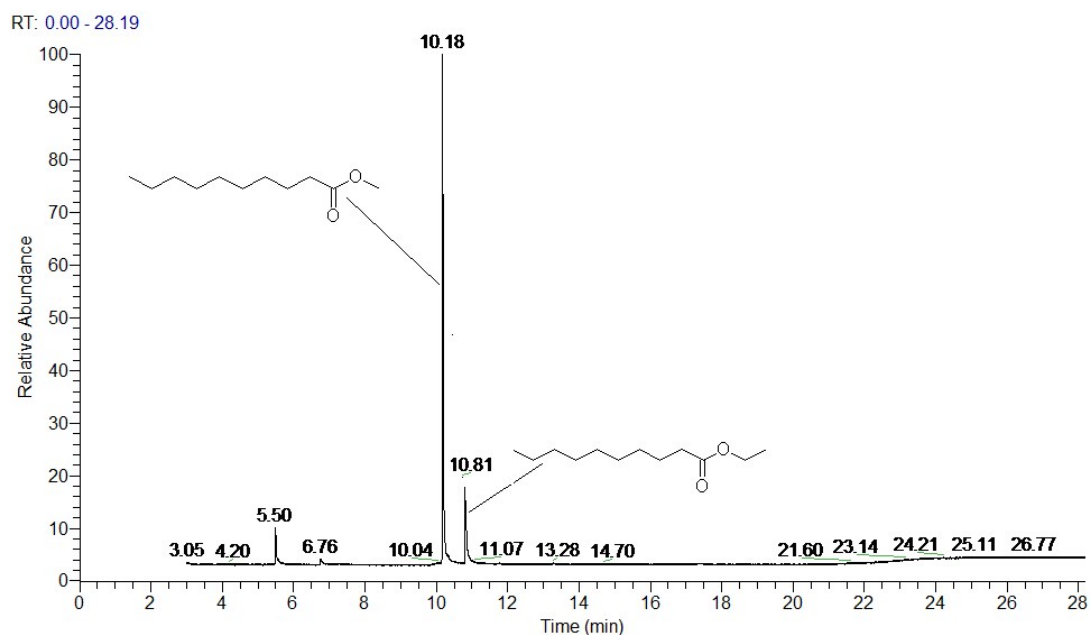
5.2.2 Gas chromatogram and mass spectrum for entry 4, Table 1

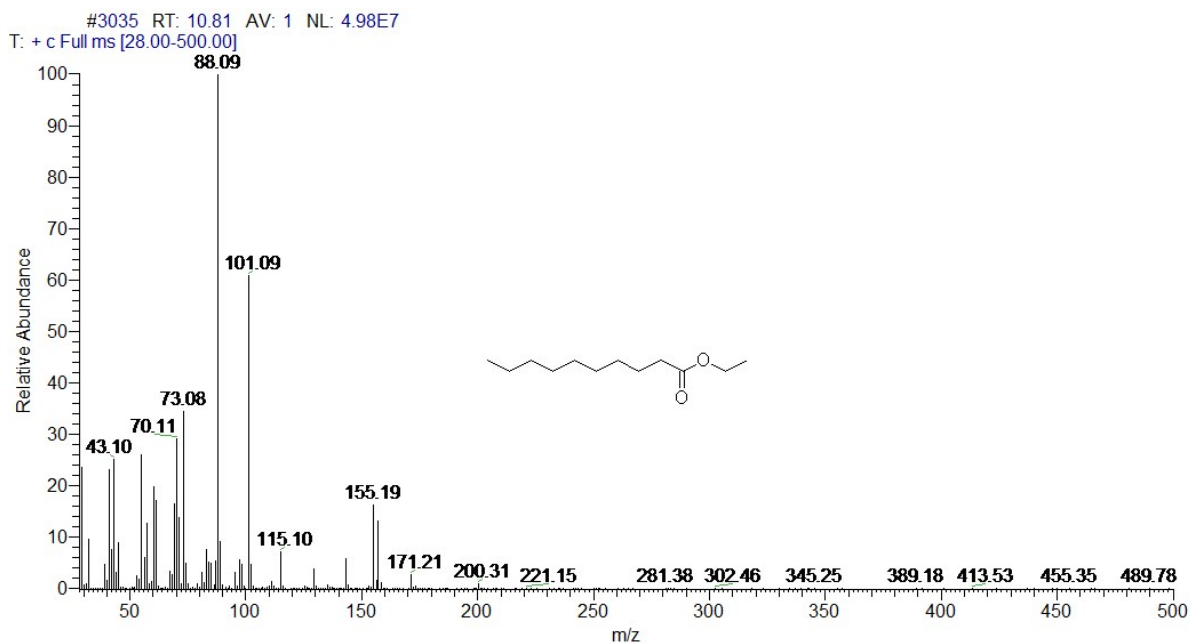


20160627-15 #2908 RT: 10.48 AV: 1 SB: 60 10.54-10.64, 10.33-10.38 NL: 2.80E8
T: + c Full ms [28.00-500.00]



5.2.3 Gas chromatogram and mass spectra for entry 11, Table 1

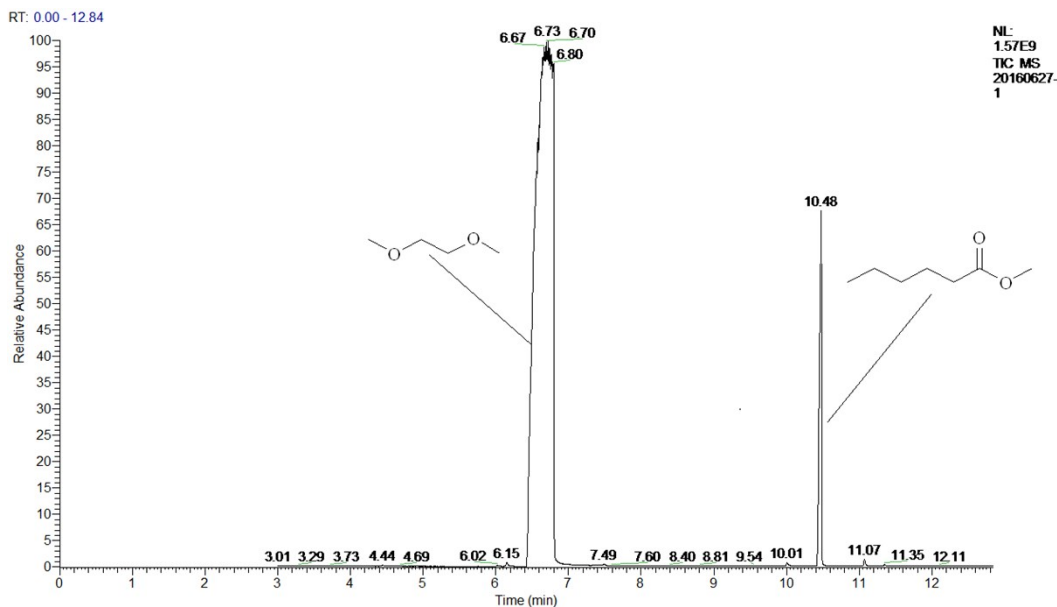




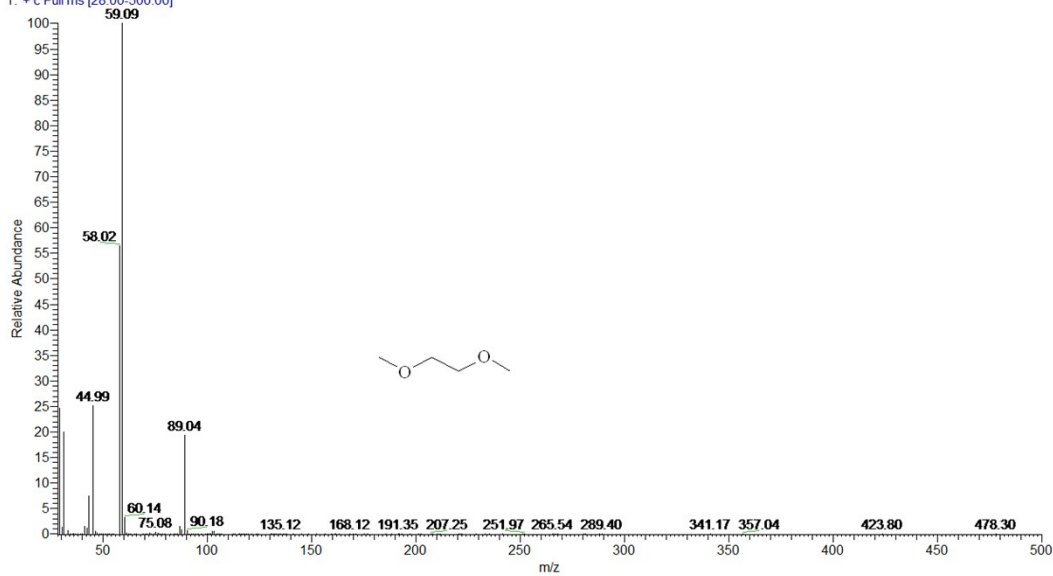
PEAK LIST RT: 6.90 - 14.67

Apex RT	Start RT	End RT	Area	%Area	Height	%Height
10.18	10.13	10.42	11.4E+09	95.4	68.9E+08	95.9
10.81	10.78	11.03	5.53E+08	4.6	2.89E+08	4.1

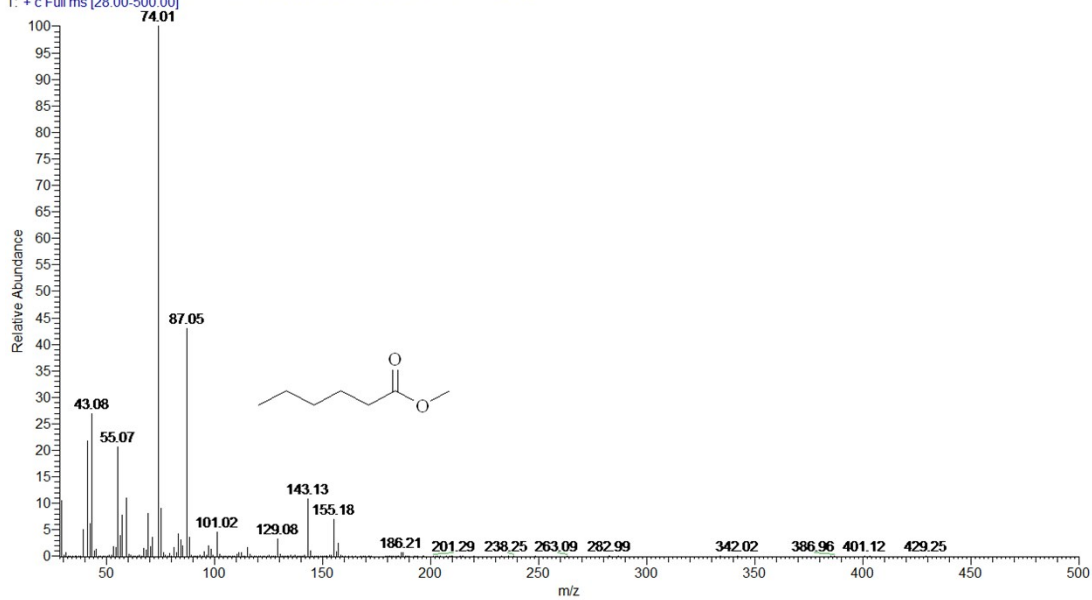
5.2.4 Gas chromatogram and mass spectra for entry 3, Table 2



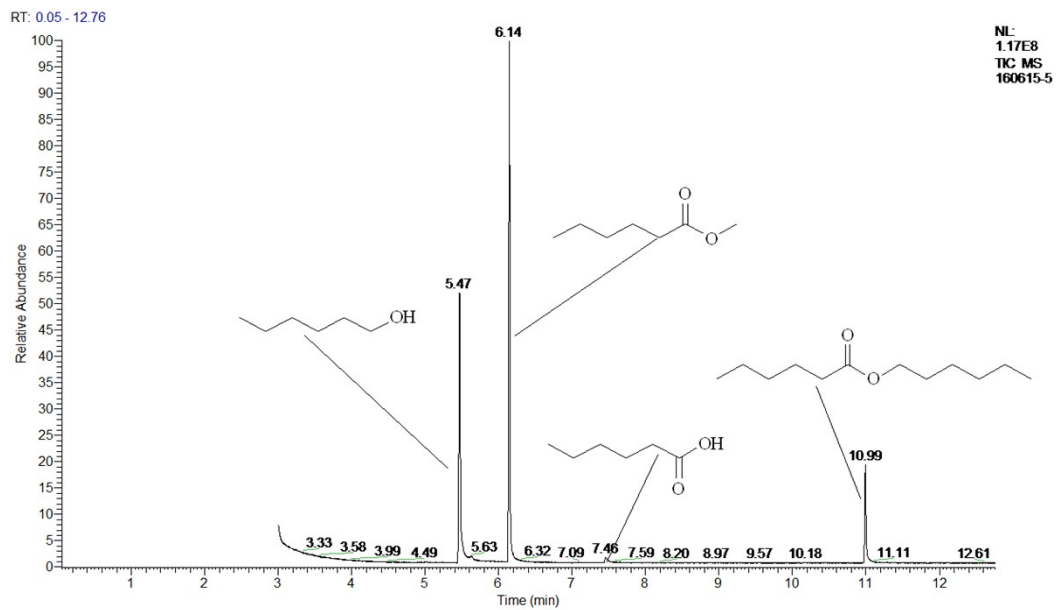
20160627-1 #1429 RT: 6.68 AV: 1 SB: 45 10.53-10.60, 10.37-10.41 NL: 5.61E8
T: + c Full ms [28.00-500.00]



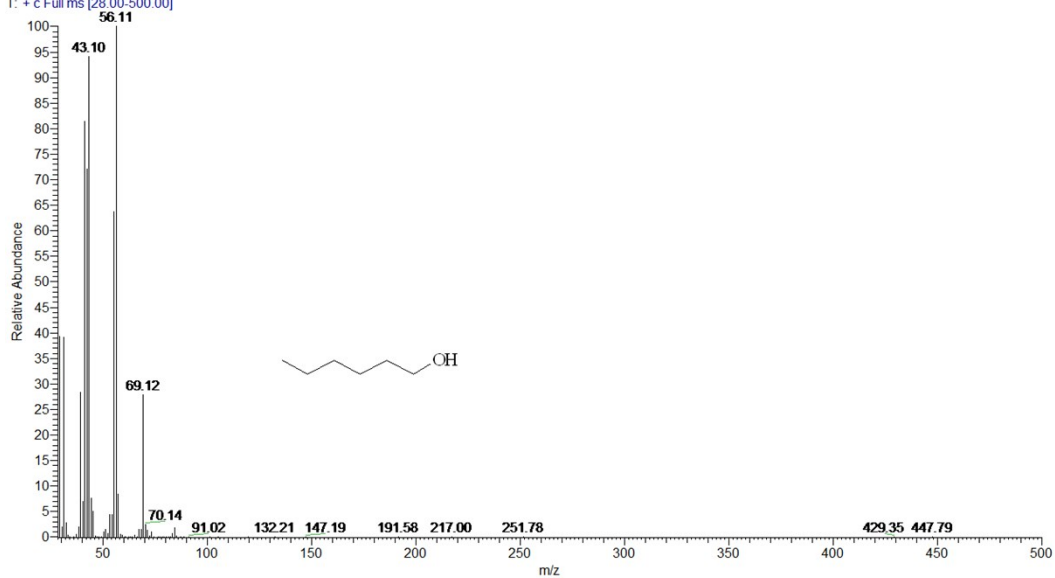
20160627-1 #2902 RT: 10.47 AV: 1 SB: 45 10.53-10.60, 10.37-10.41 NL: 2.60E8
T: + c Full ms [28.00-500.00]



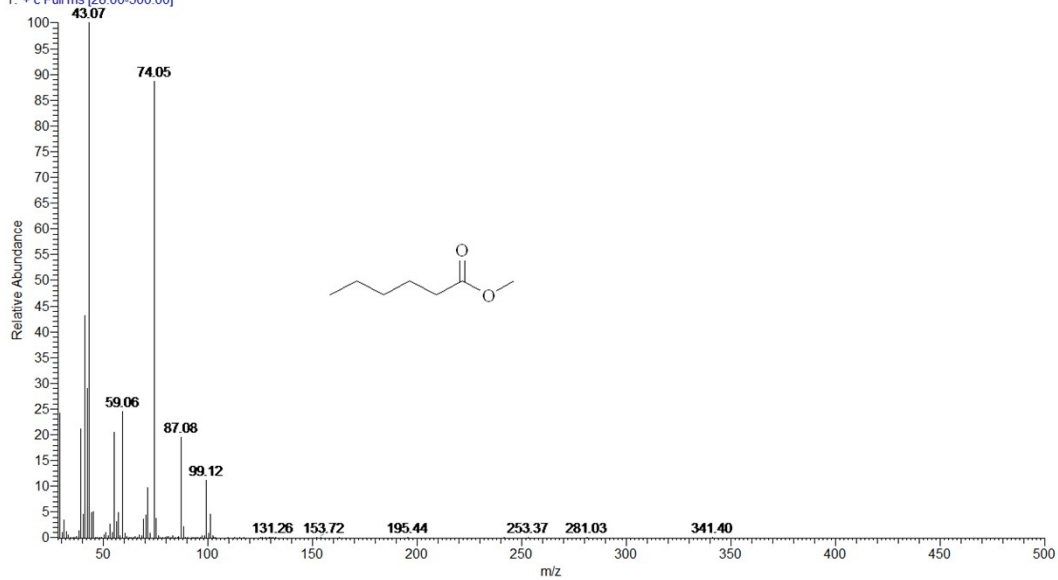
5.2.5 Gas chromatogram and mass spectra for entry 4, Table 2



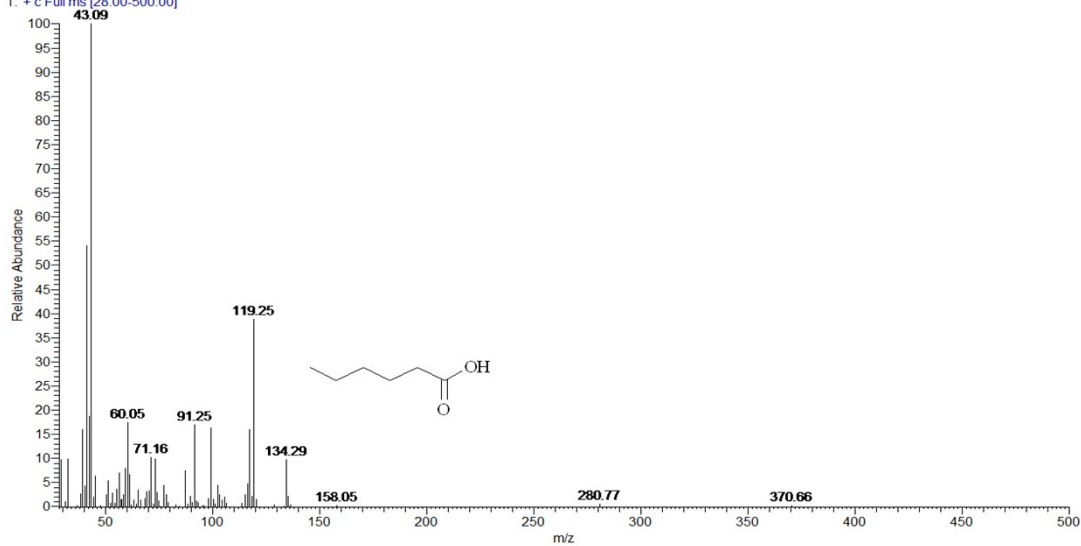
160615-5 #959 RT: 5.47 AV: 1 NL: 9.84E6
T: + c Full ms [28.00-500.00]



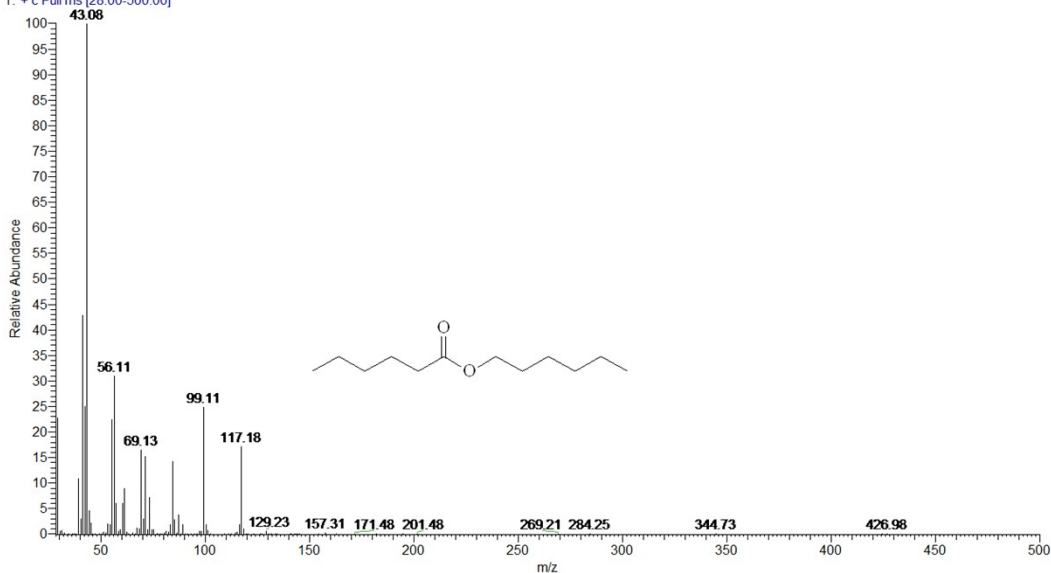
160615-5 #1222 RT: 6.14 AV: 1 NL: 2.53E7
T: + c Full ms [28.00-500.00]



160615-5 #1732 RT: 7.46 AV: 1 SB: 86 7.58-7.70, 7.25-7.35 NL: 2.28E5
T: + c Full ms [28.00-500.00]



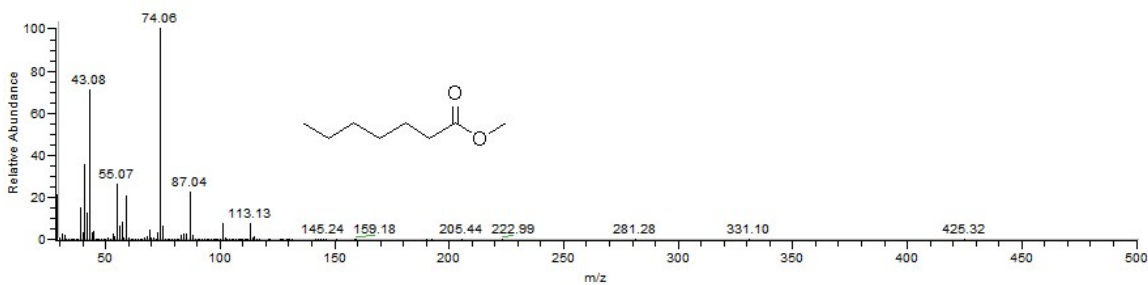
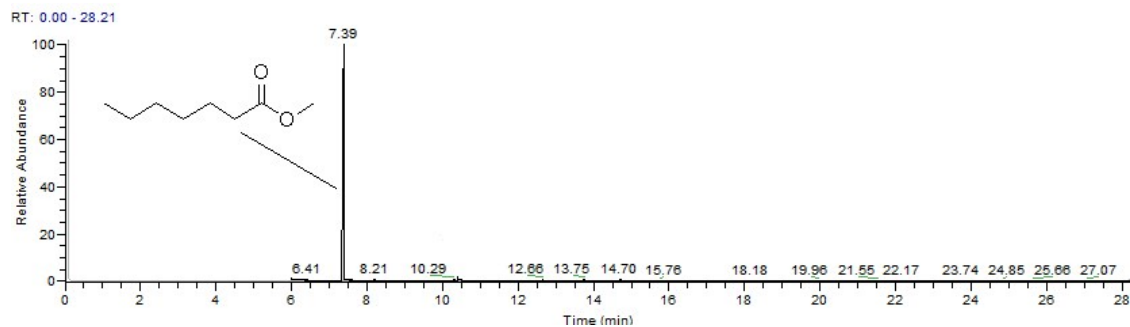
160615-5 #3105 RT: 10.99 AV: 1 SB: 79 11.10-11.20, 10.76-10.87 NL: 5.16E6
 T: + c Full ms [28.00-500.00]



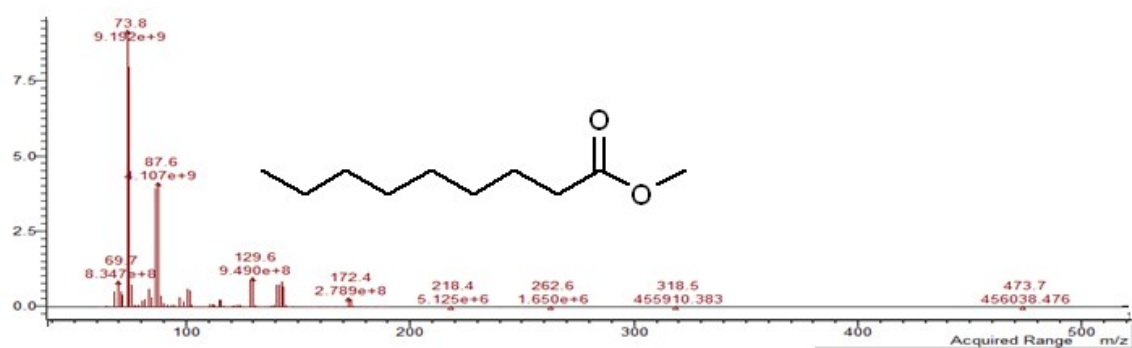
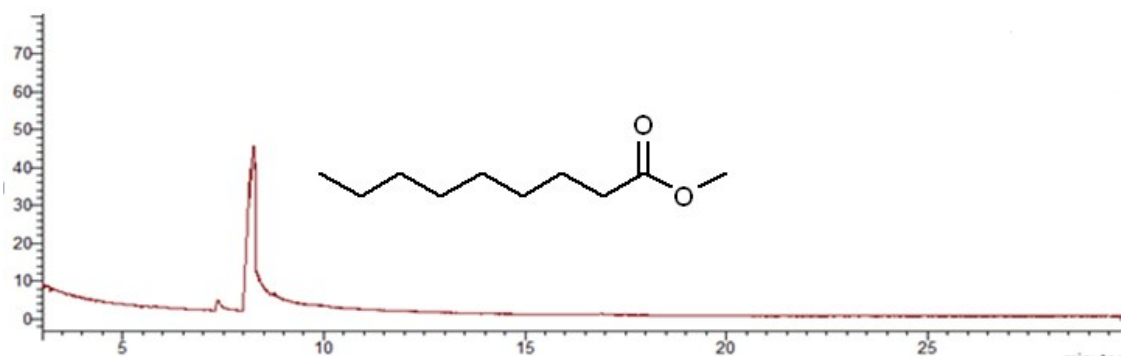
PEAK LIST RT: 10.18 - 12.30

Apex RT	Start RT	End RT	Area	%Area	Height	%Height
5.47	5.44	5.5	7.53E+07	33.28	5.85E+07	30.04
6.14	6.12	6.18	1.24E+08	54.77	1.15E+08	58.85
10.99	10.97	11.04	2.70E+07	11.94	2.16E+07	11.11

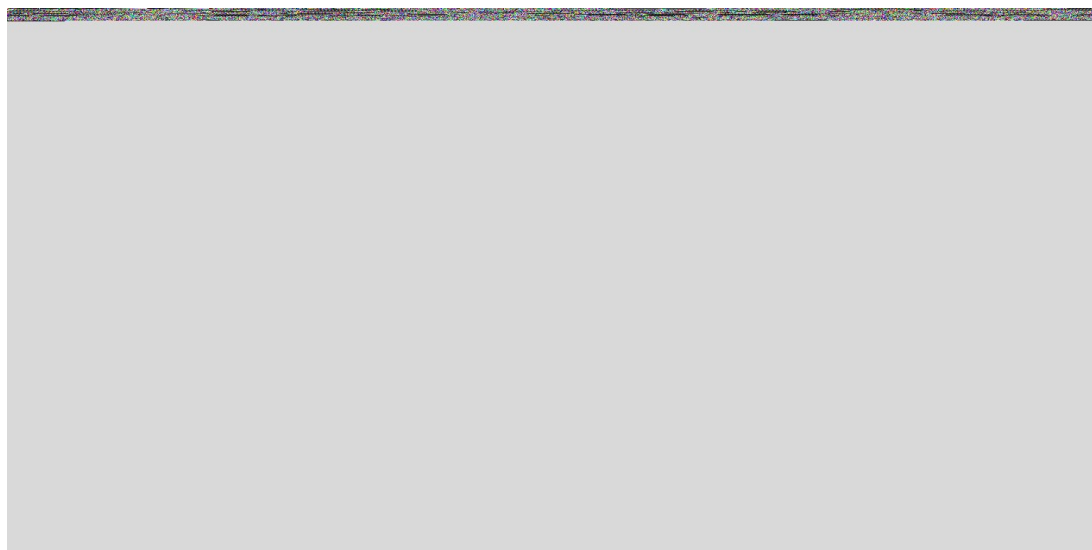
5.2.6 Gas chromatogram and mass spectrum for entry 5, Table 2



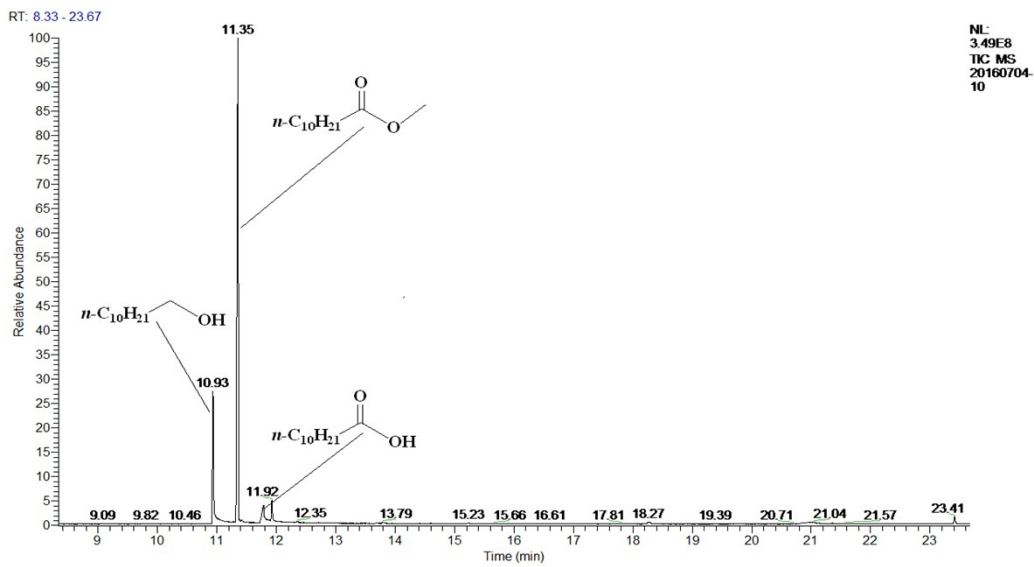
5.2.7 Gas chromatogram and mass spectrum for entry 6, Table 2



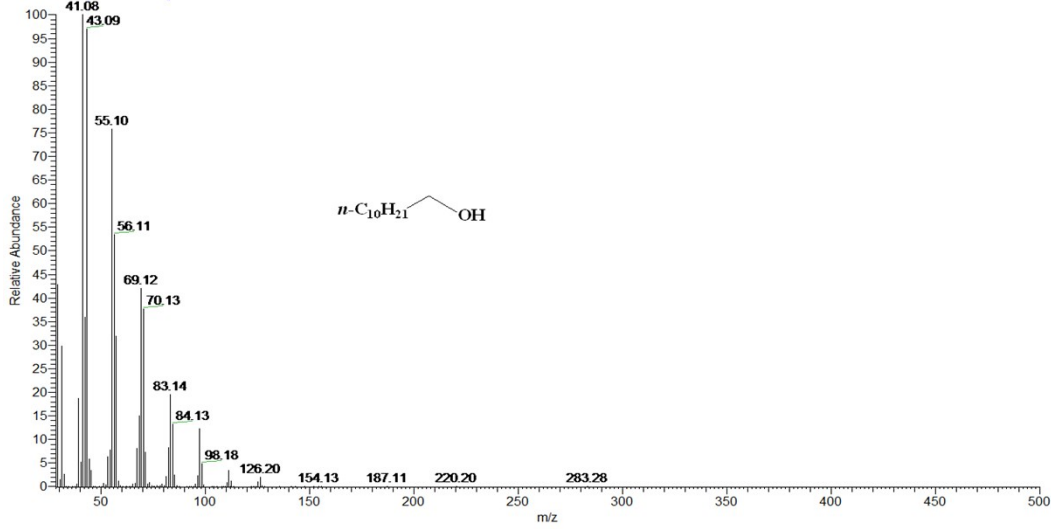
5.2.8 Gas chromatogram and mass spectrum for entry 7, Table 2



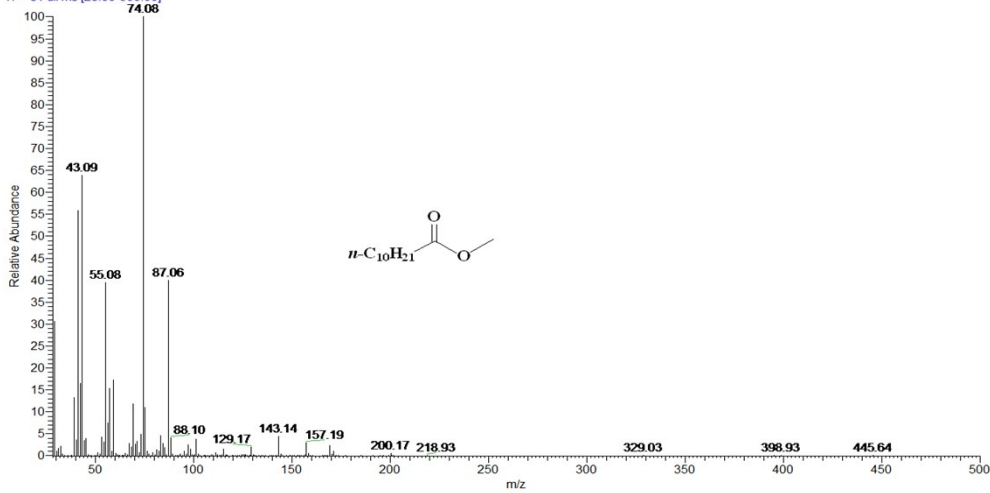
5.2.9 Gas chromatogram and mass spectra for entry 8, Table 2



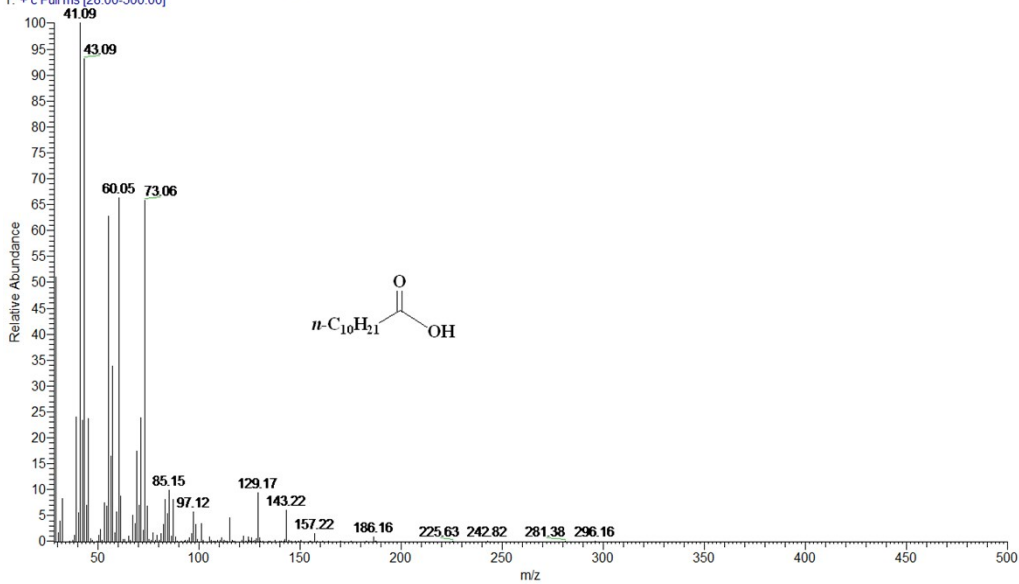
20160704-10 #2891 RT: 10.94 AV: 1 NL: 6.70E6
T: + c Full ms [28.00-500.00]



20160704-10 #3040 RT: 11.33 AV: 1 NL: 8.96E6
T: + c Full ms [28.00-500.00]



20160704-10 #3216 RT: 11.78 AV: 1 NL: 1.66E6
T: + c Full ms [28.00-500.00]

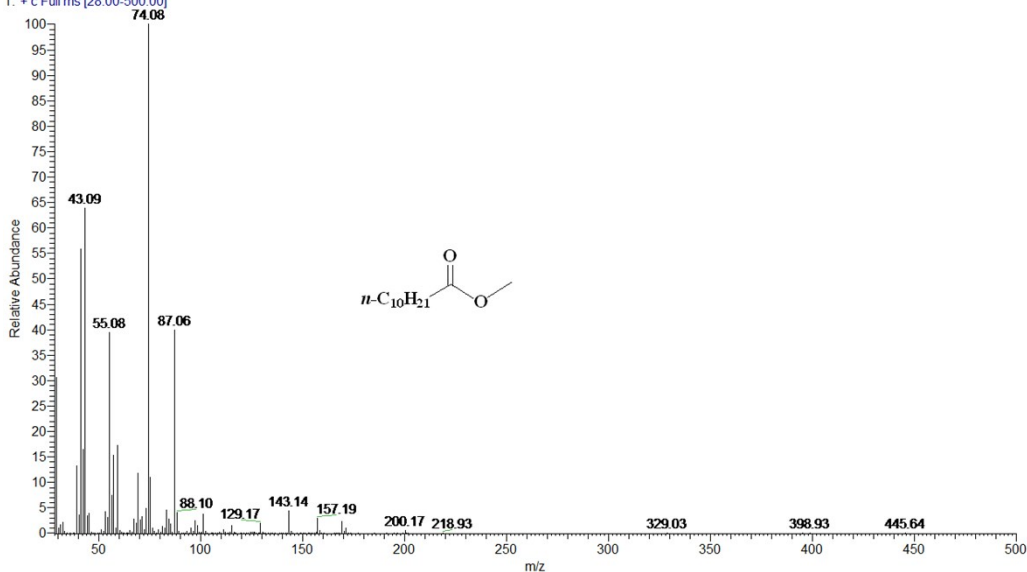


PEAK LIST RT: 10.38 - 11.81

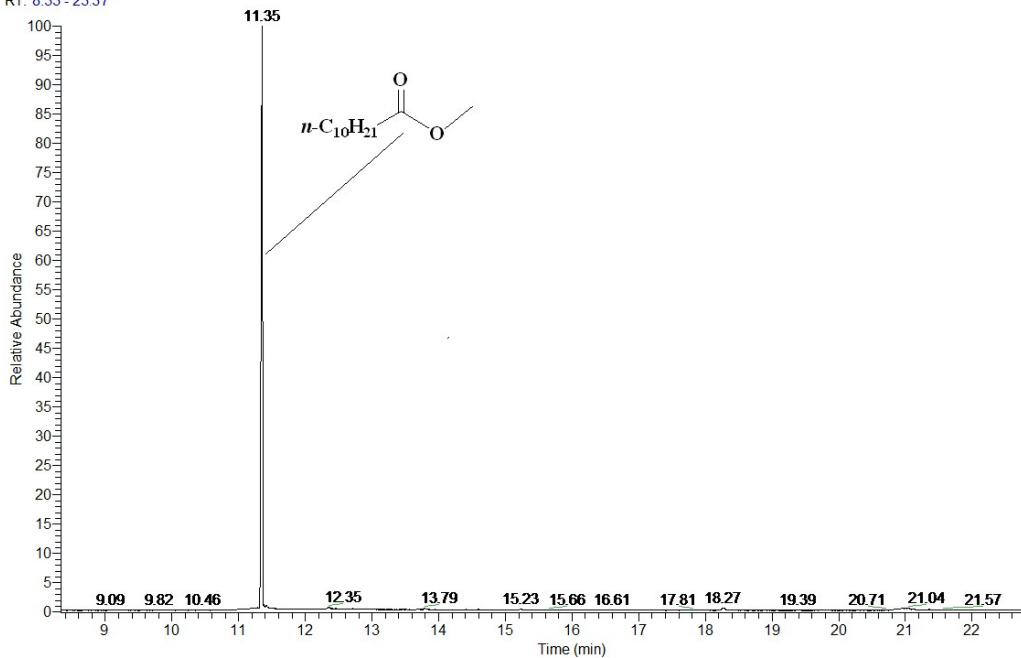
Apex RT	Start RT	End RT	Area	%Area	Height	%Height
10.93	10.91	10.95	9.29E+07	15.34	8.75E+07	19.75
11.35	11.31	11.37	4.90E+08	80.89	3.46E+08	78.03
11.78	11.72	11.8	2.29E+07	3.78	9.85E+06	2.22

5.2.10 Gas chromatogram and mass spectra for entry 9, Table 2

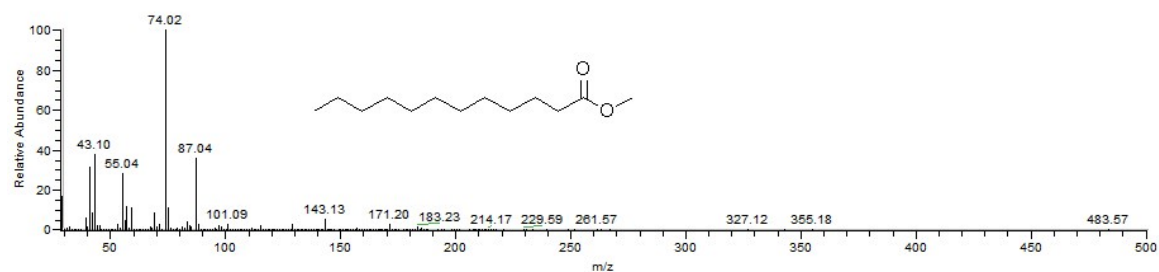
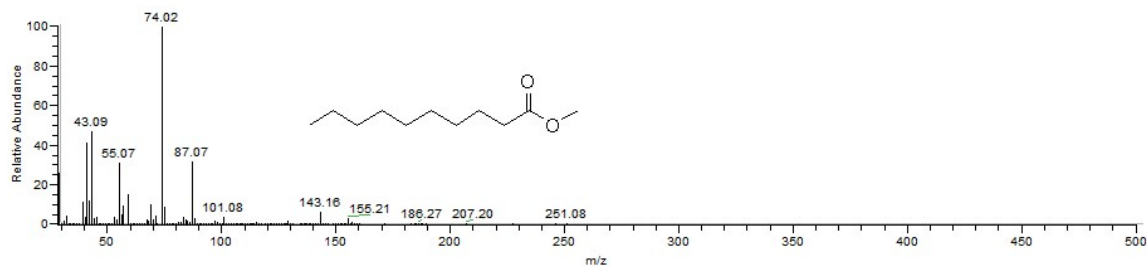
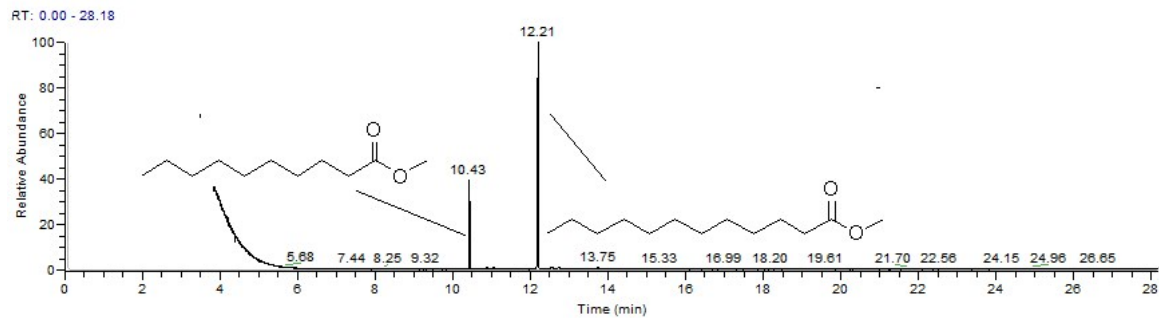
20160706-10 #3060 RT: 11.33 AV: 1 NL: 8.96E6
T: + c Full ms [28.00-500.00]



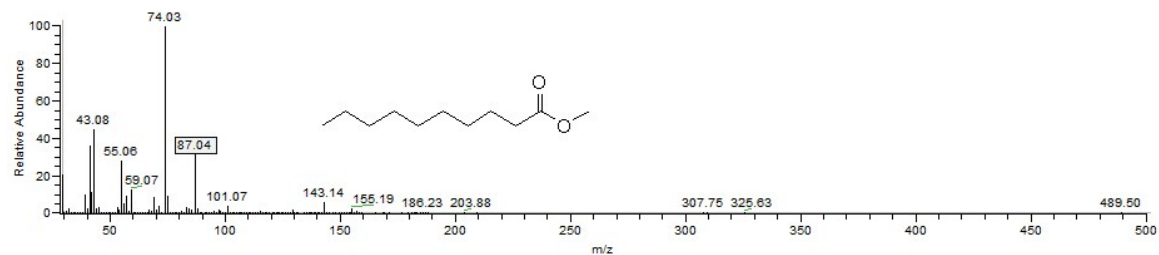
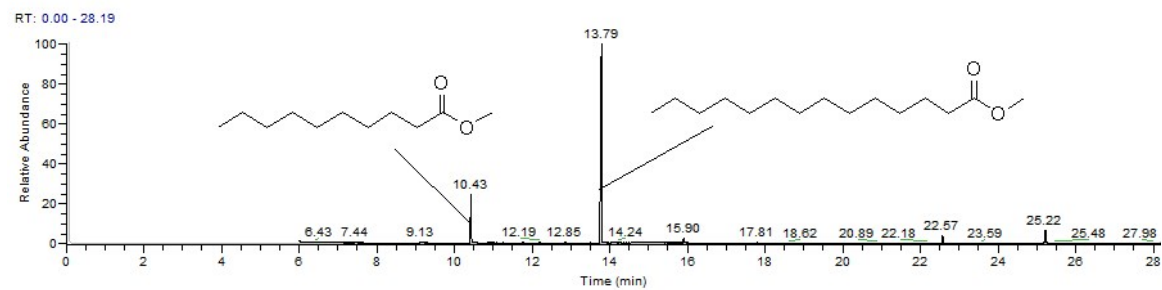
RT: 8.33 - 23.37

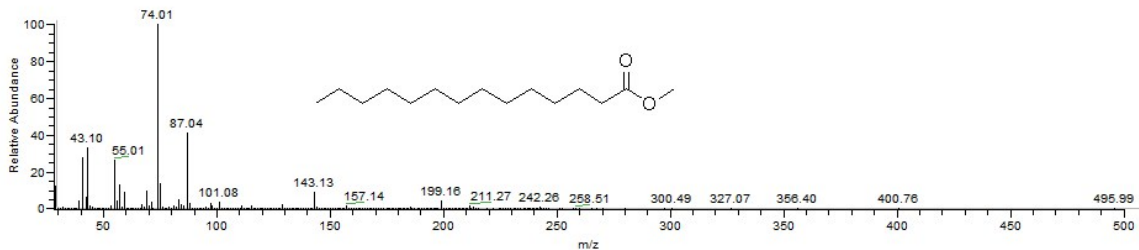


5.2.11 Gas chromatogram and mass spectra for entry 10, Table 2

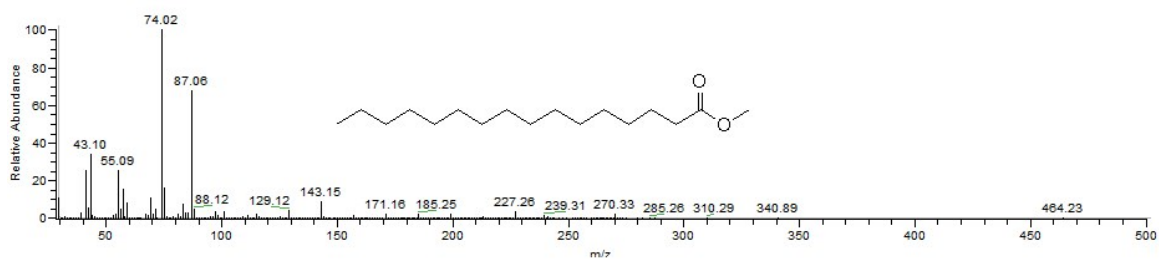
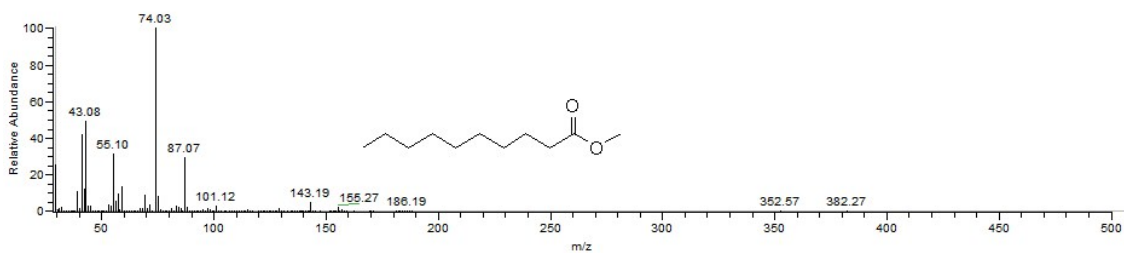
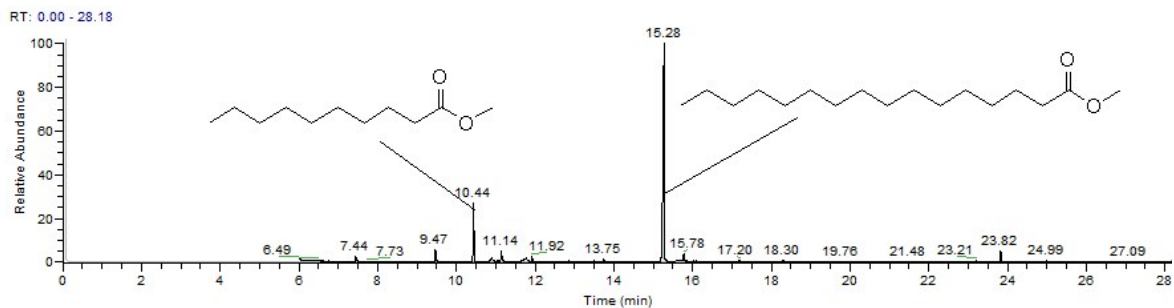


5.2.12 Gas chromatogram and mass spectra for (entry 11, Table 2)



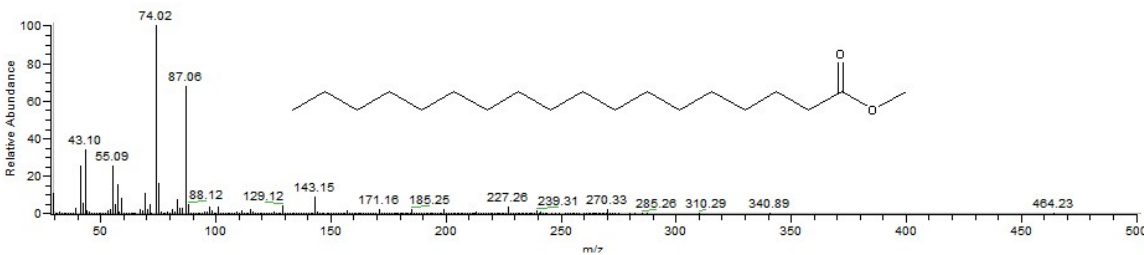
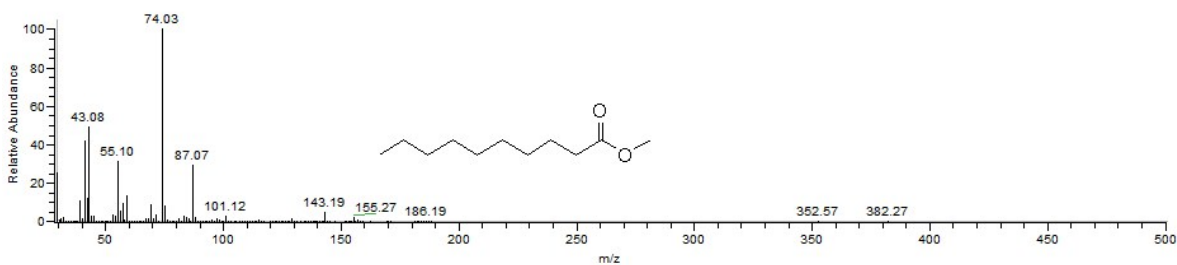
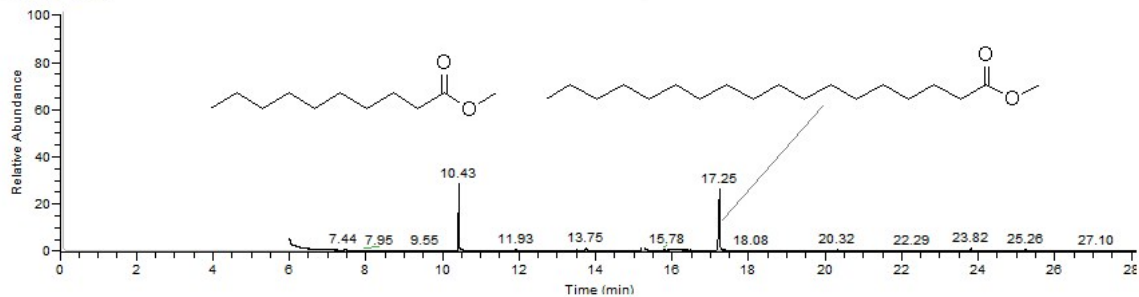


5.2.13 Gas chromatogram and mass spectra for entry 12, Table 2



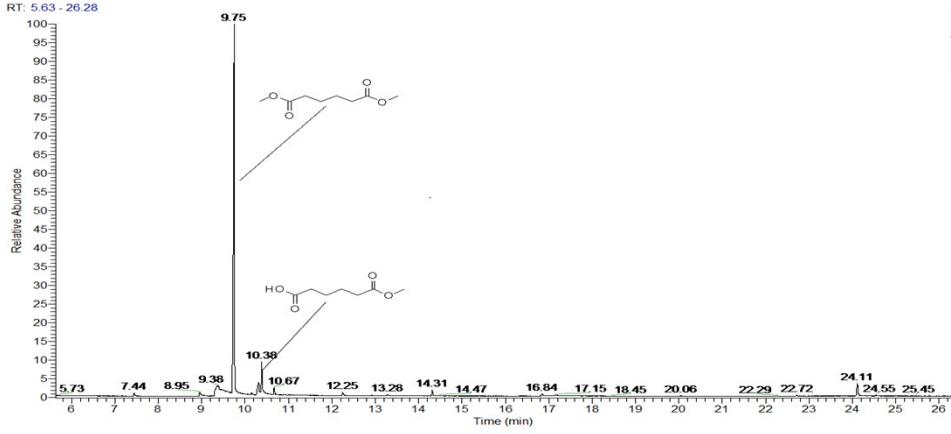
5.2.14 Gas chromatogram and mass spectra for entry 13, Table 2

RT: 0.00 - 28.17



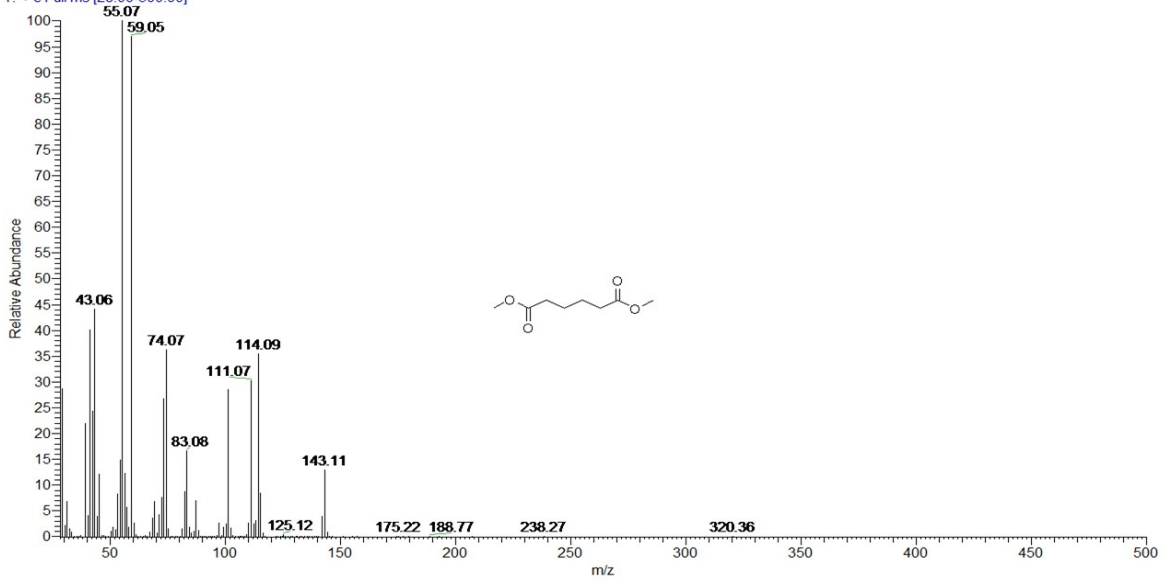
5.2.15 Gas chromatogram and mass spectra for entry 14, Table 2

RT: 5.83 - 26.28

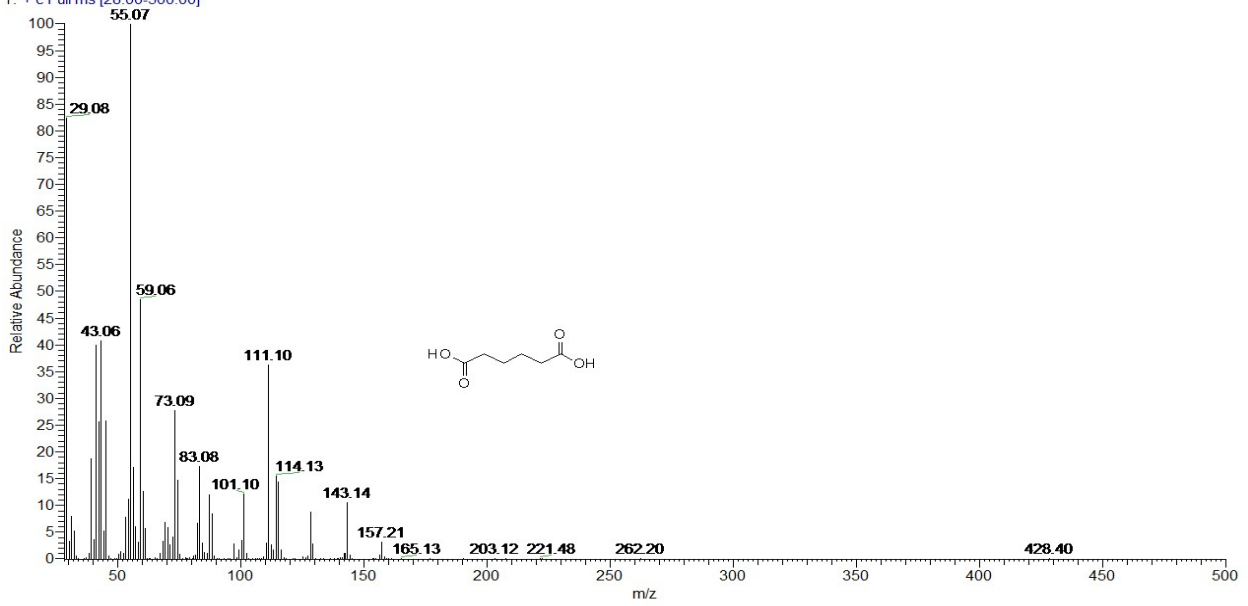


NL
2.94E8
TIC MS
20160704
11

20160704-11 #2422 RT: 9.73 AV: 1 NL: 2.49E7
 T: + c Full ms [28.00-500.00]



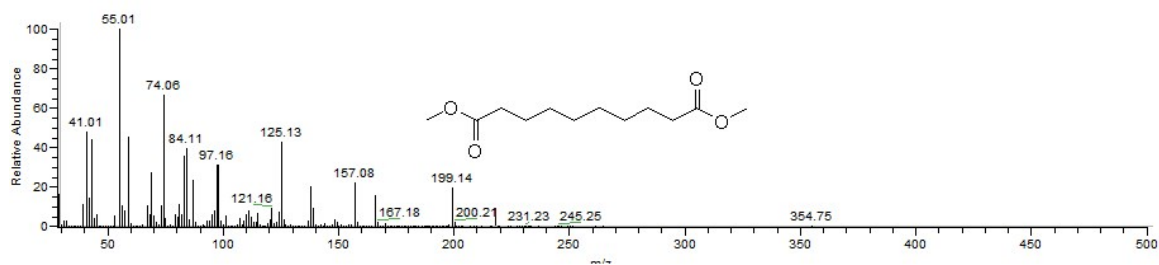
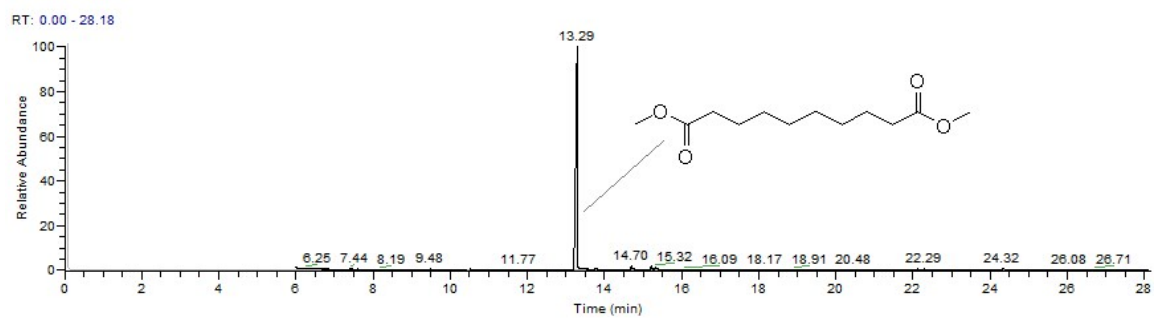
20160704-11 #2674 RT: 10.38 AV: 1 NL: 3.61E6
 T: + c Full ms [28.00-500.00]



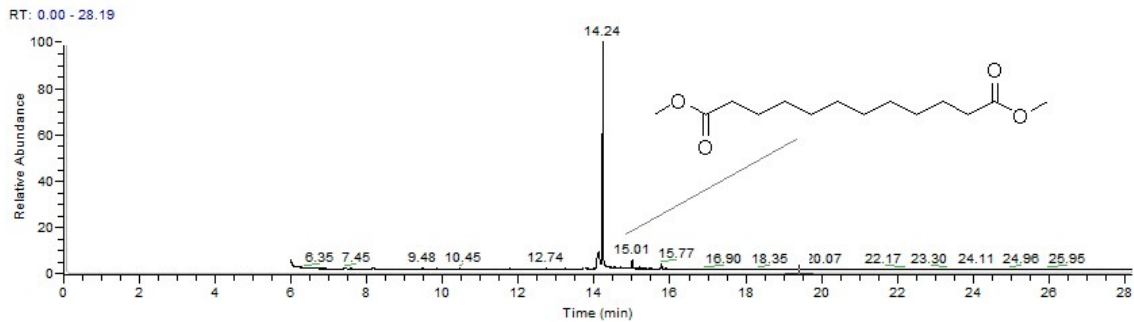
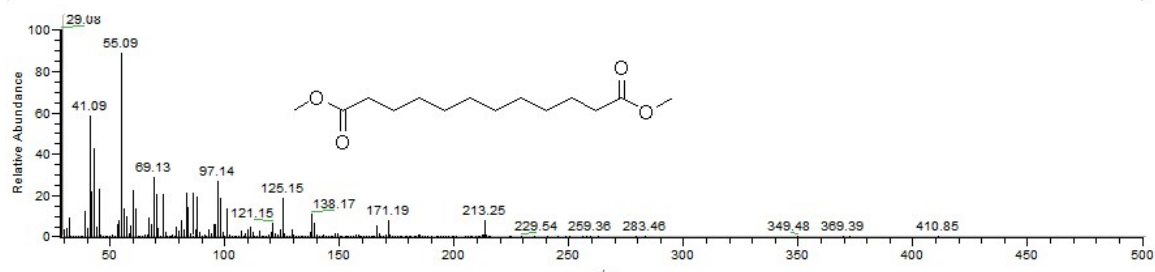
PEAK LIST RT: 10.03 - 10.67

Apex RT	Start RT	End RT	Area	%Area	Height	%Height
9.75	9.69	9.77	4.90E+08	94.62	2.86E+08	90.1
10.38	10.36	10.41	2.79E+07	5.38	2.35E+07	7.4

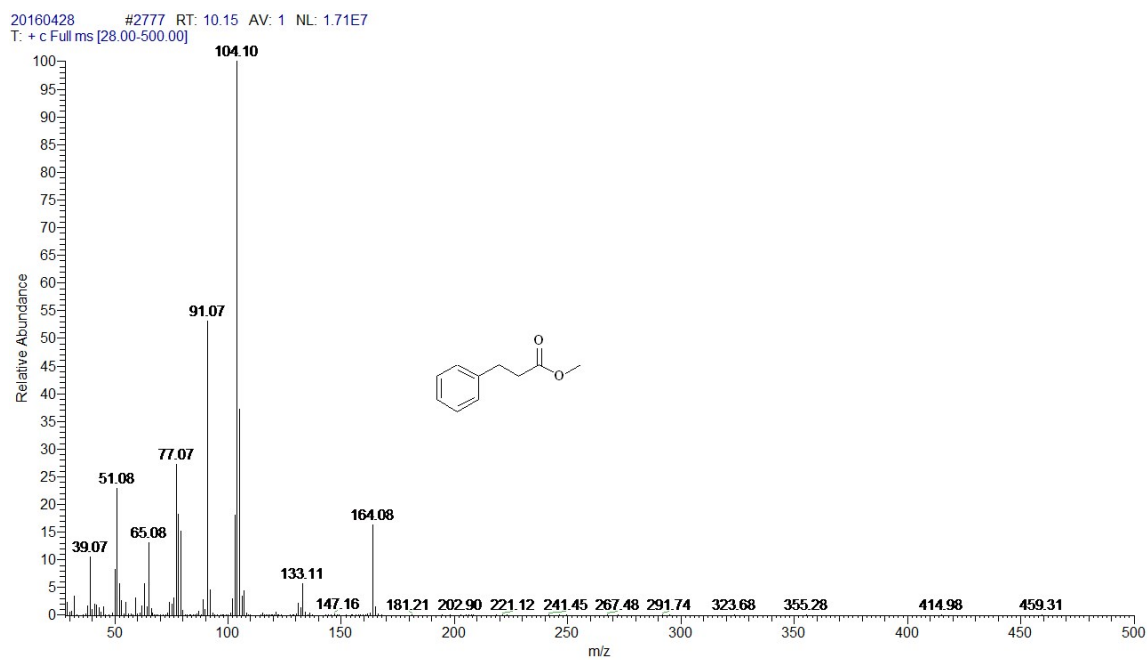
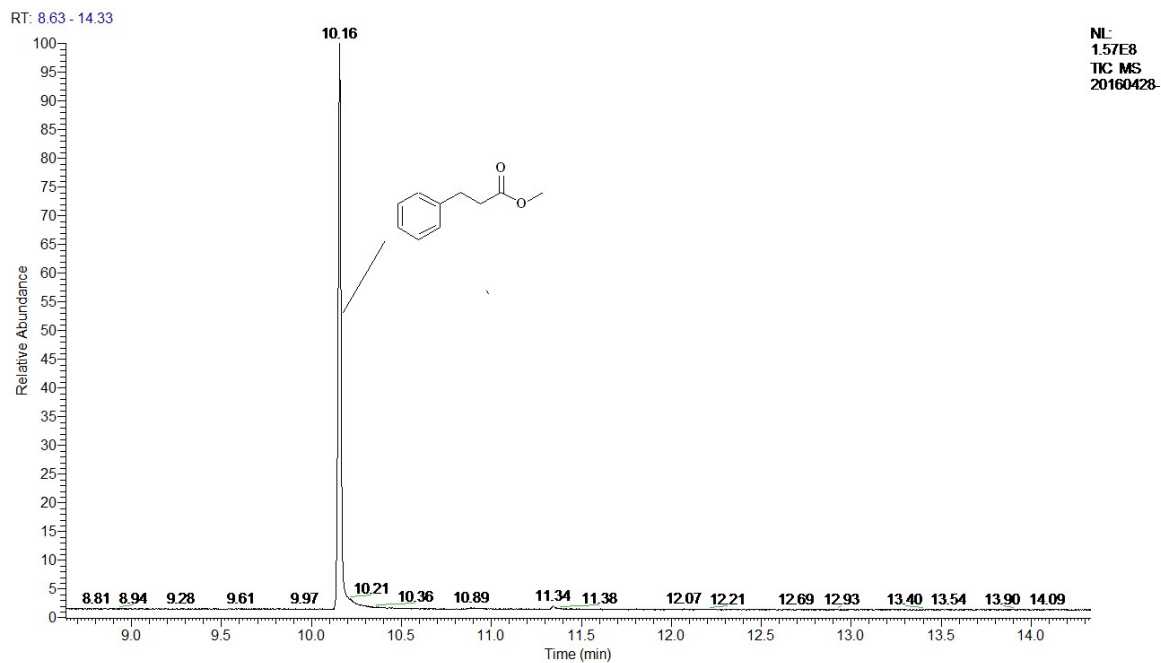
5.2.16 Gas chromatogram and mass spectrum for entry 15, Table 2



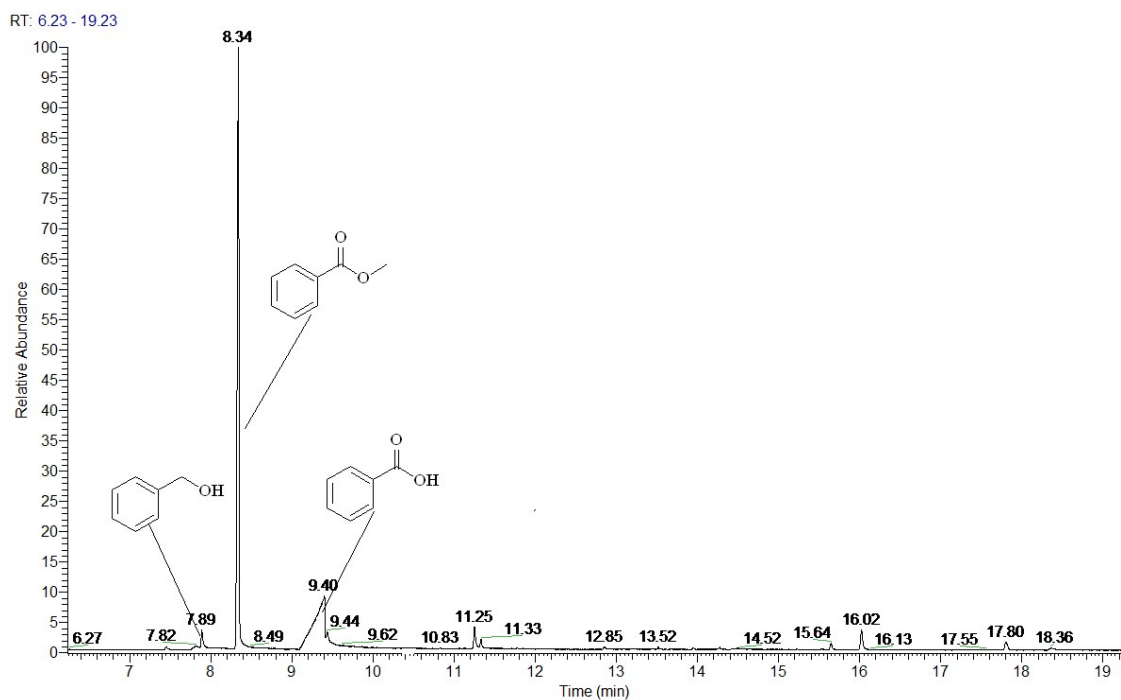
5.2.17 Gas chromatogram and mass spectrum for entry 16, Table 2



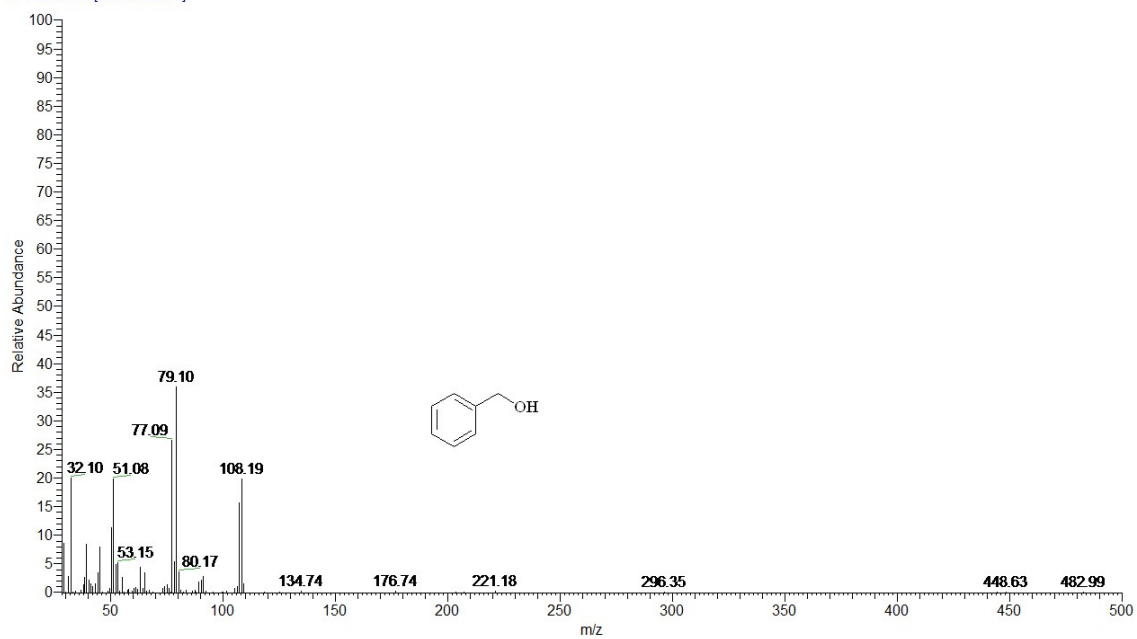
5.2.18 Gas chromatogram and mass spectrum for entry 17, Table 2



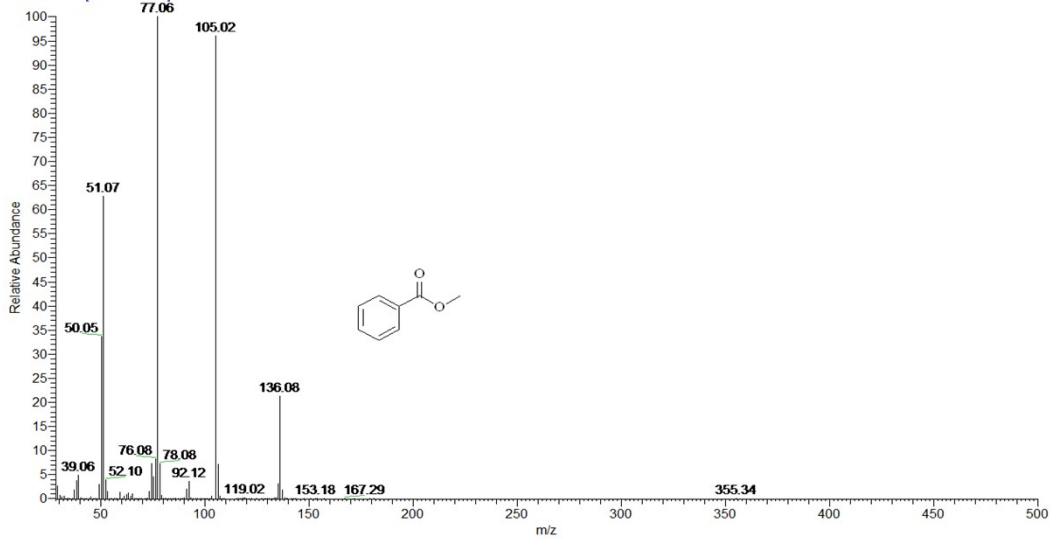
5.2.19 GC-MS spectrum for methyl benzoate [6a, Table 3 (S:C = 500:1)]



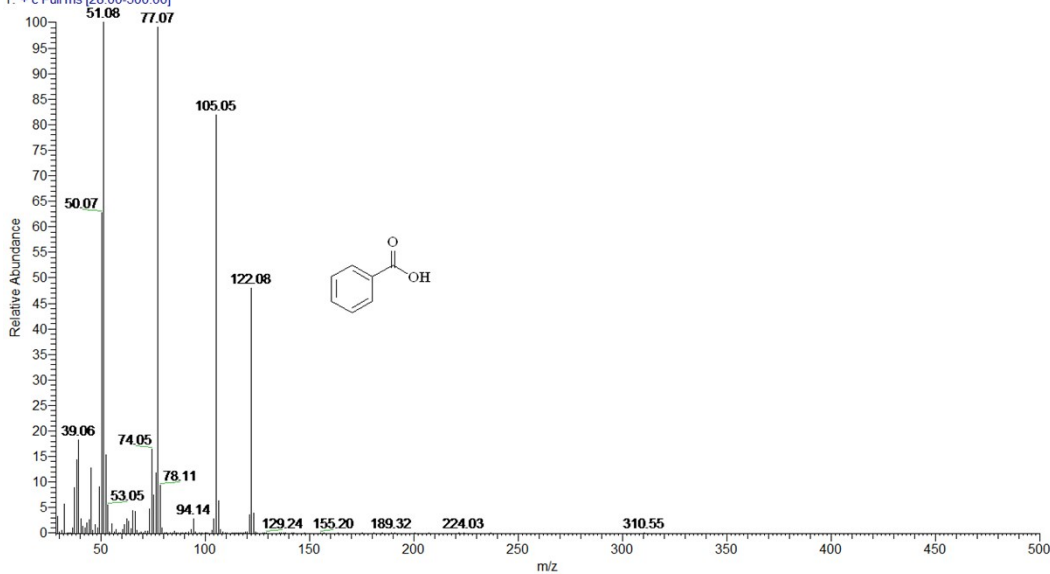
20160704-12 #1676 RT: 7.81 AV: 1 NL: 7.54E5
T: + c Full ms [28.00-500.00]



20160704-12 #1881 RT: 8.34 AV: 1 NL: 5.52E7
 T: + c Full ms [28.00-500.00]



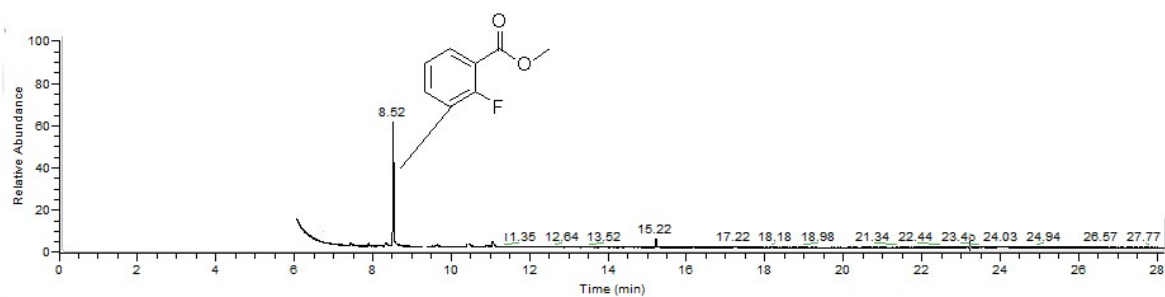
20160704-12 #2281 RT: 9.37 AV: 1 NL: 2.87E6
 T: + c Full ms [28.00-500.00]



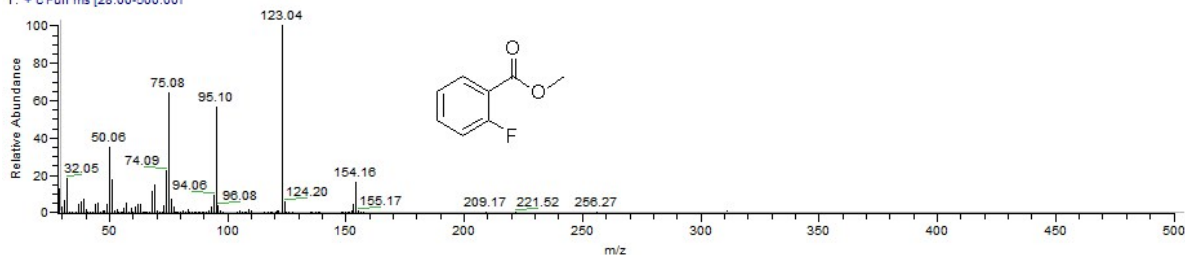
PEAK LIST 20160704-12.RAW

Apex RT	Start RT	End RT	Area	%Area	Height	%Height
7.89	7.86	7.90	1.38E+06	0.30	2.36E+05	0.10
8.34	8.30	8.37	3.20E+08	69.53	2.20E+08	93.22
9.40	9.09	9.42	1.38E+08	30.17	1.57E+07	6.68

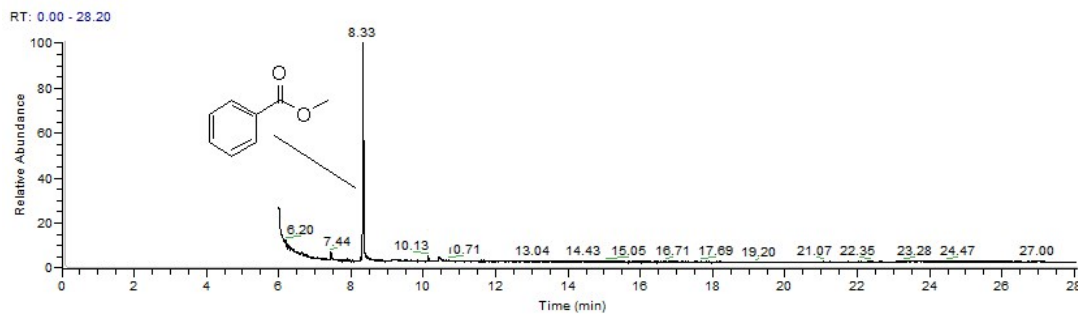
5.2.20 GC-MS spectrum for methyl 2-fluorobenzoate (6b, Table 3)



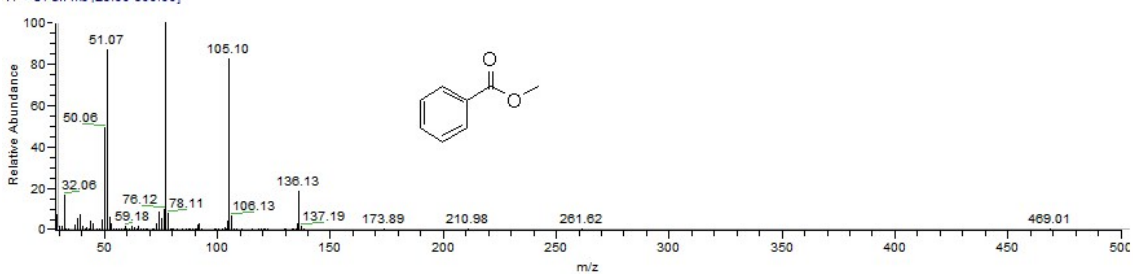
RT: 8.54 AV: 1 NL: 2.71E6
T: + c Full ms [28.00-500.00]



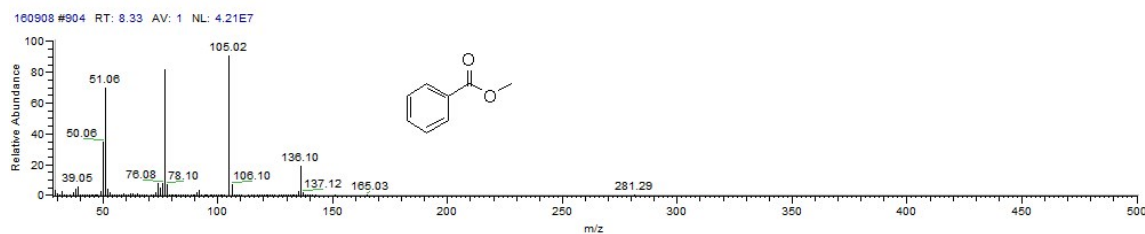
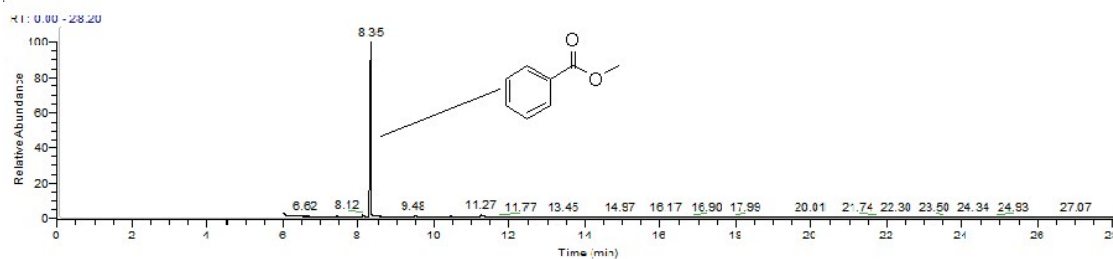
5.2.21 GC-MS spectrum for methyl 2-chlorobenzoate (6c, Table 3) – only methyl benzoate (6a) identified



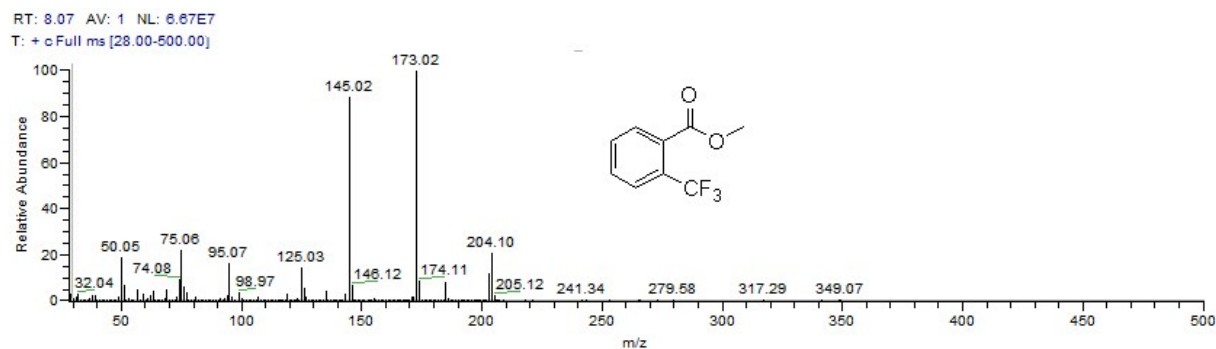
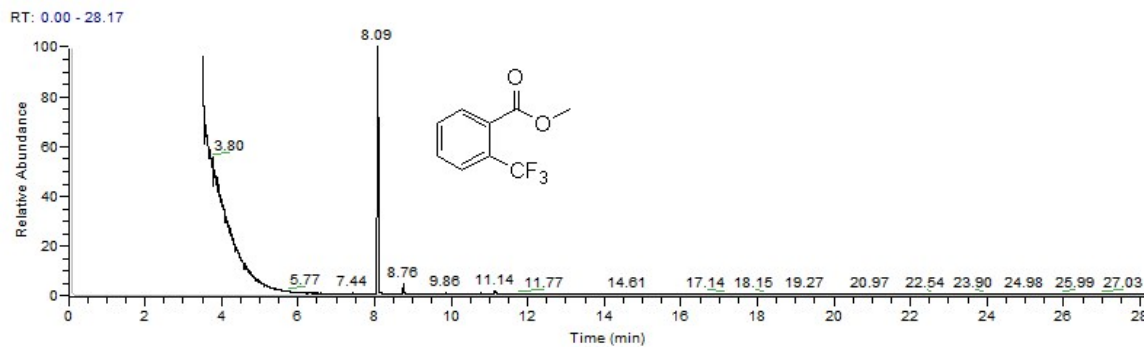
RT: 8.31 AV: 1 NL: 3.08E6
T: + c Full ms [28.00-500.00]



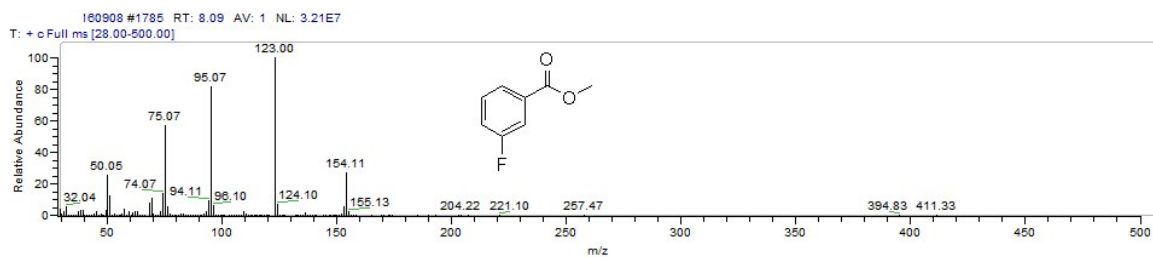
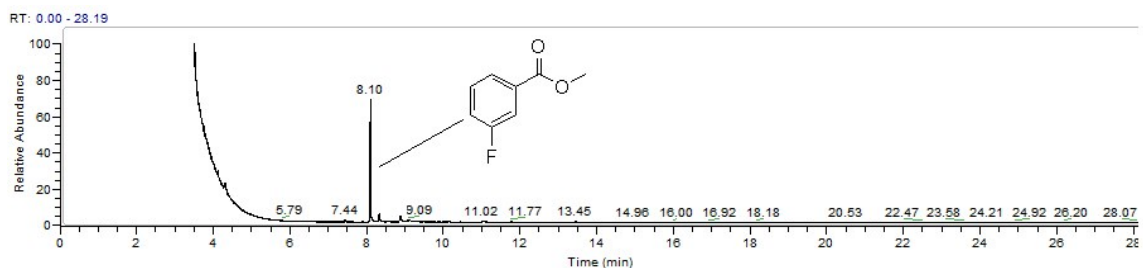
5.2.22 GC-MS spectrum for methyl 2-bromobenzoate (6d, Table 3) – only methyl benzoate (6a) identified



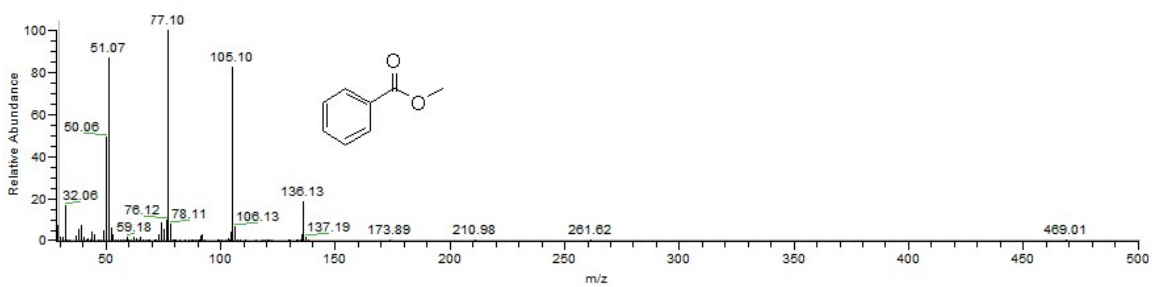
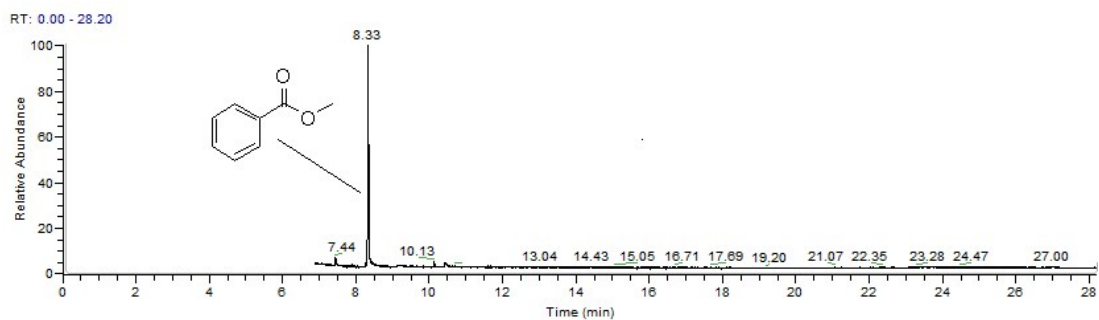
5.2.23 GC-MS spectrum for methyl 2-(trifluoromethyl)benzoate (6e, Table 3)



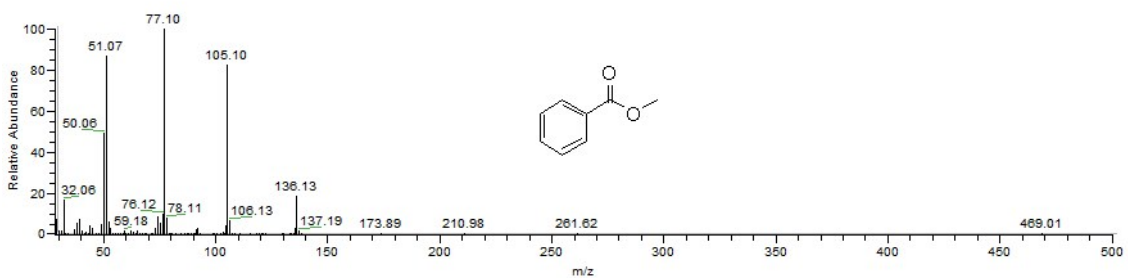
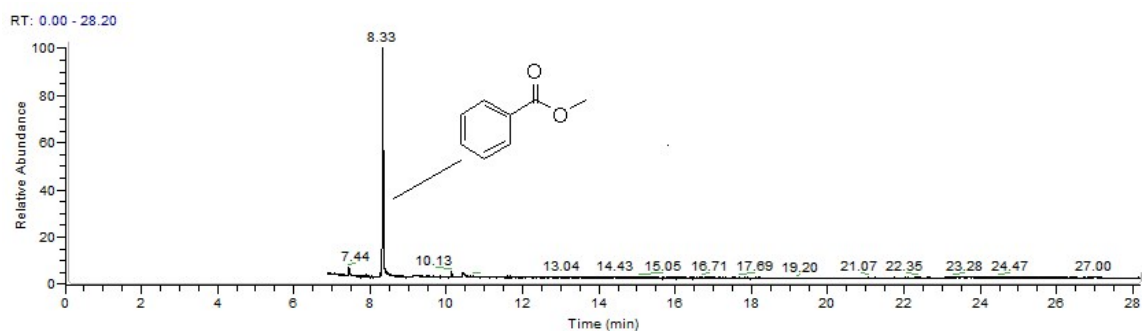
5.2.24 GC-MS spectrum for methyl 3-fluorobenzoate (6f, Table 3)



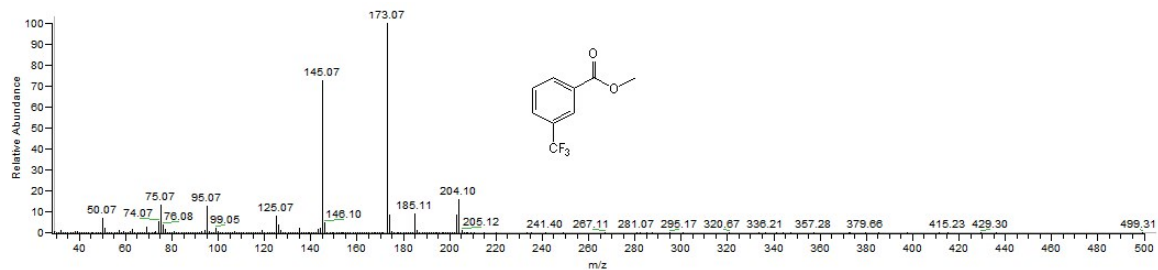
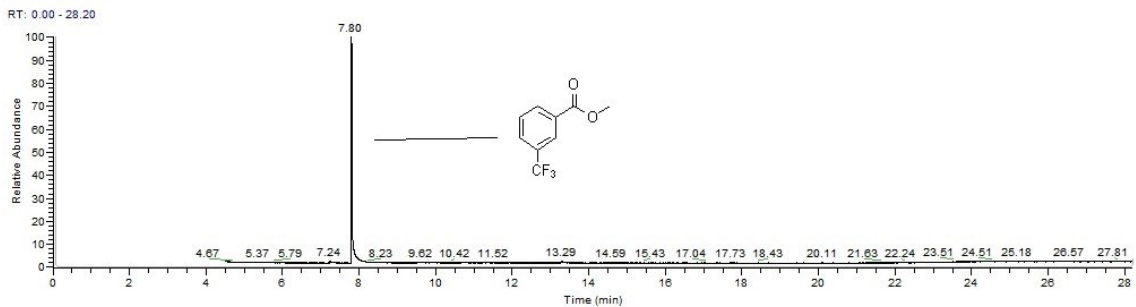
5.2.25 GC-MS spectrum for methyl 3-chlorobenzoate (6g, Table 3) – only methyl benzoate (6a) identified



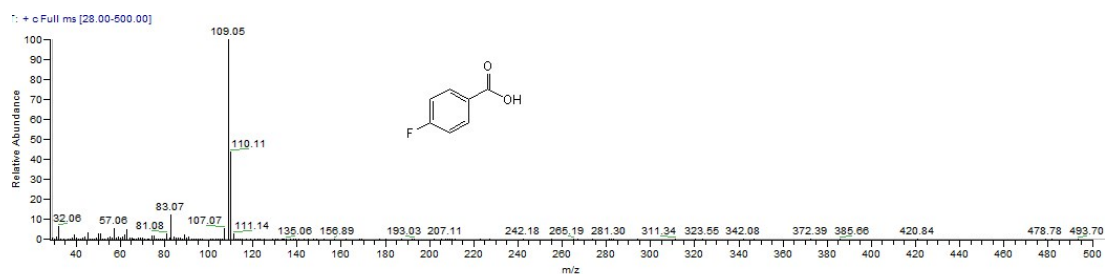
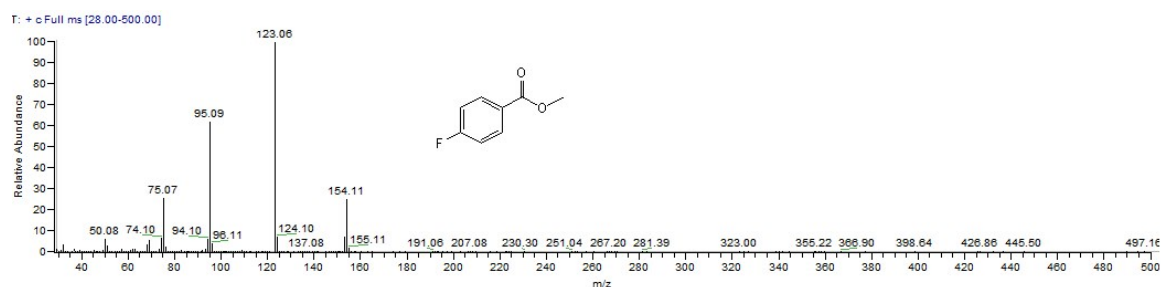
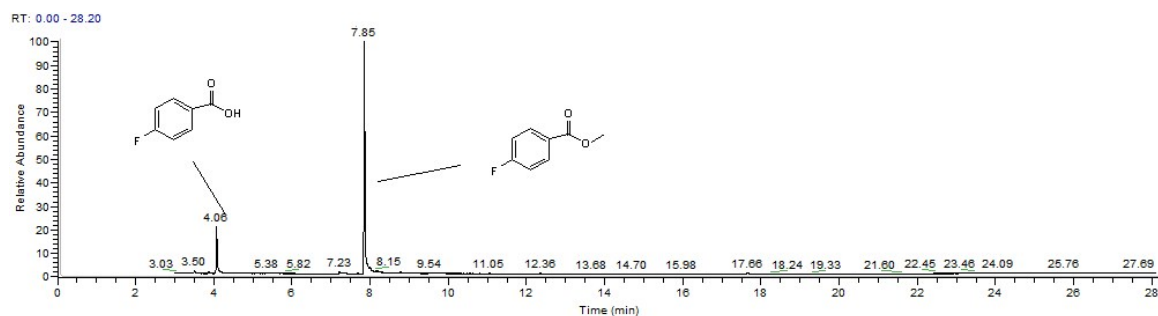
5.2.26 GC-MS spectrum for methyl 3-bromobenzoate (6h, Table 3) – only methyl benzoate (6a) identified



5.2.27 GC-MS spectrum for methyl 3-(trifluoromethyl)benzoate (6i, Table 3)



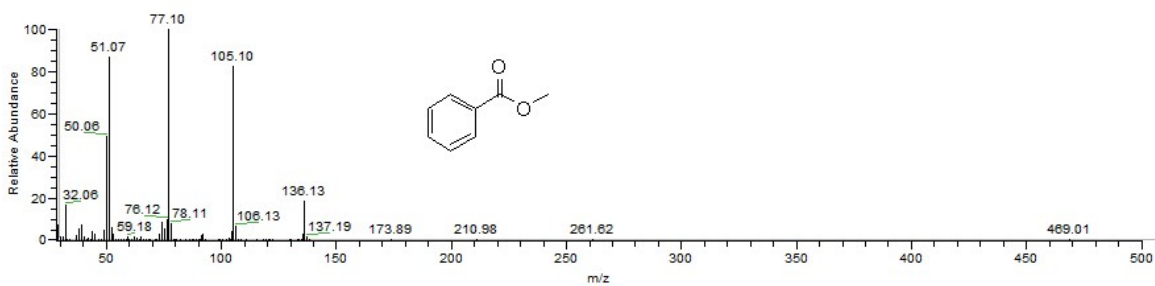
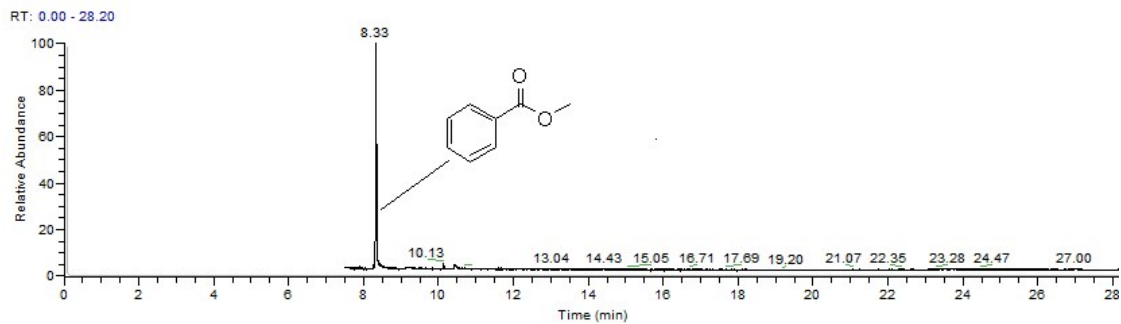
5.2.28 GC-MS spectrum for methyl 4-fluorobenzoate (6j, Table 3)



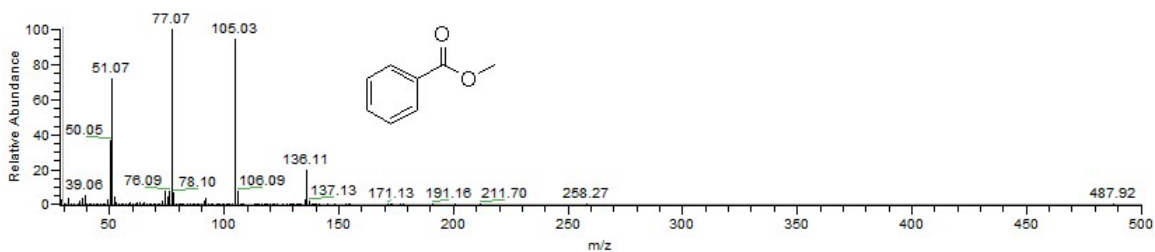
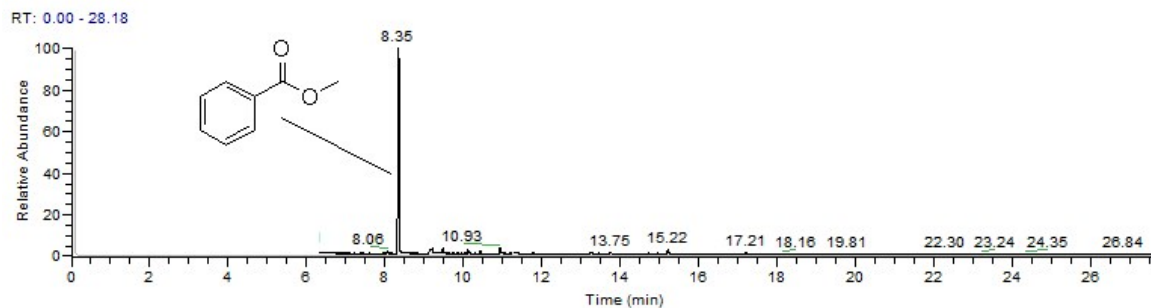
PEAK LIST RT: 0.00 - 28.20

Apex RT	Start RT	End RT	Area	%Area	Height	%Height
4.06	3.87	4.43	8.55E+08	21.69	2.93E+08	17.06
7.85	7.6	8.63	3.09E+09	78.31	1.42E+09	82.94

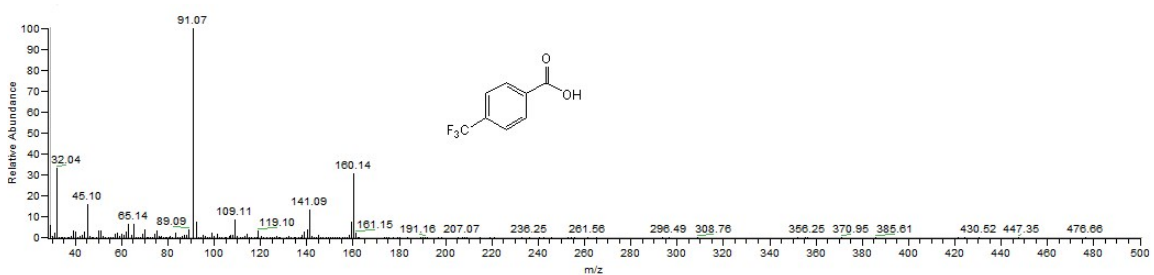
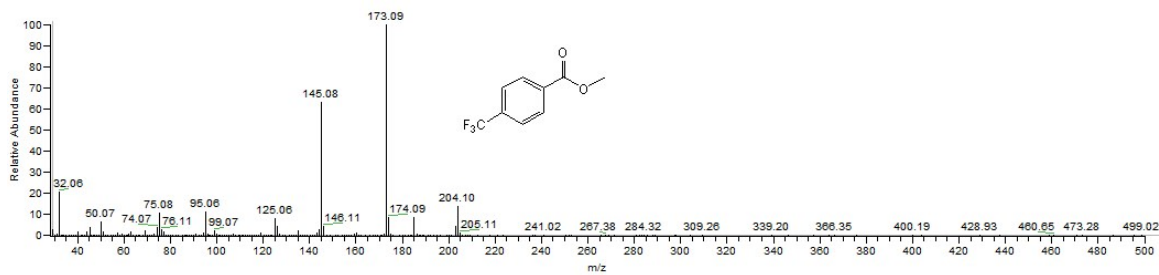
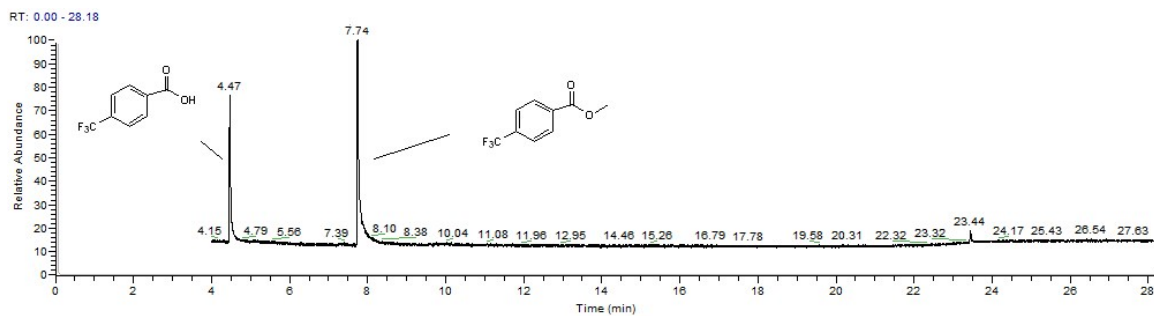
5.2.29 GC-MS spectrum for methyl 4-chlorobenzoate (6k, Table 3) – only methyl benzoate (6a) identified



5.2.30 GC-MS spectrum for methyl 4-bromobenzoate (6l, Table 3) – only methyl benzoate (6a) identified



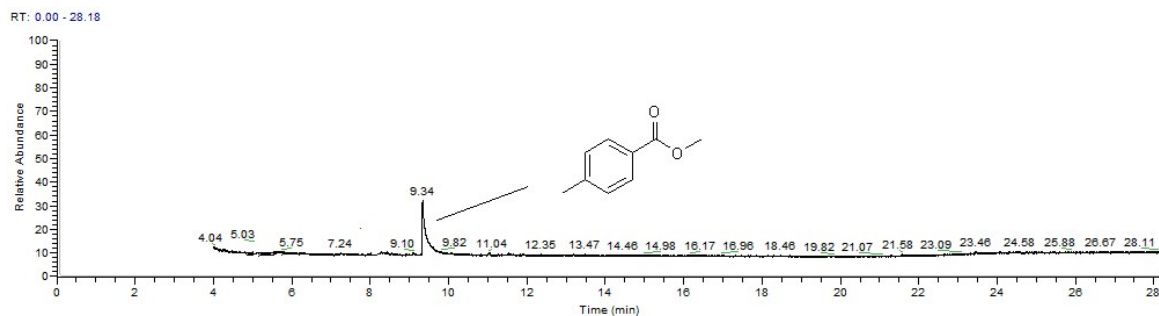
5.2.31 GC-MS spectrum for methyl 4-(trifluoromethyl)benzoate (6m, Table 3)

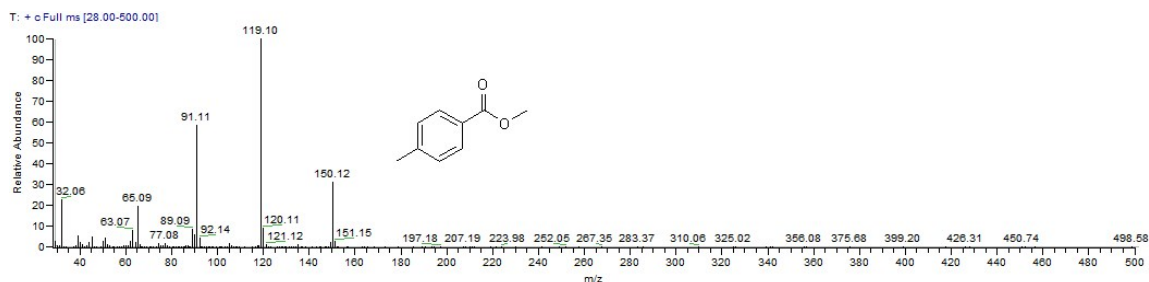


PEAK LIST RT: 0.00 - 28.18

Apex RT	Start RT	End RT	Area	%Area	Height	%Height
4.47	4.34	5.2	2.29E+08	26.85	9.48E+07	41.51
7.74	7.59	8.92	6.24E+08	73.15	1.34E+08	58.49

5.2.32 GC-MS spectrum for methyl 4-methylbenzoate (6n, Table 3)

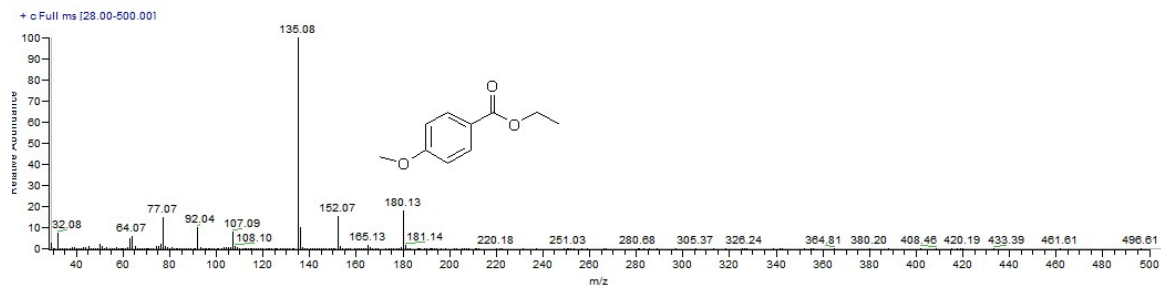
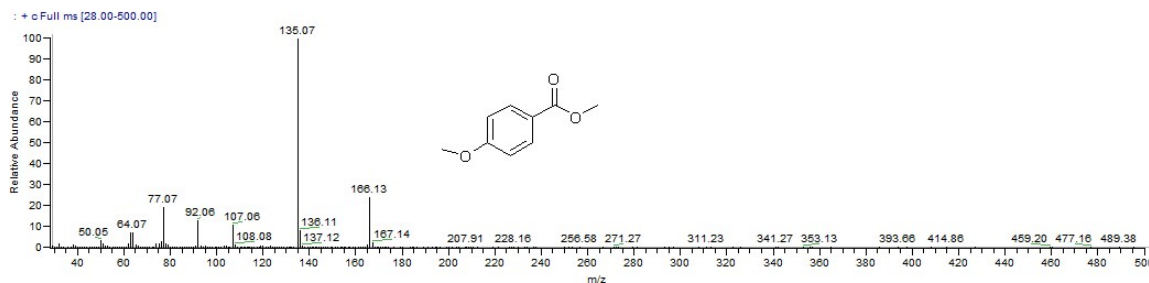
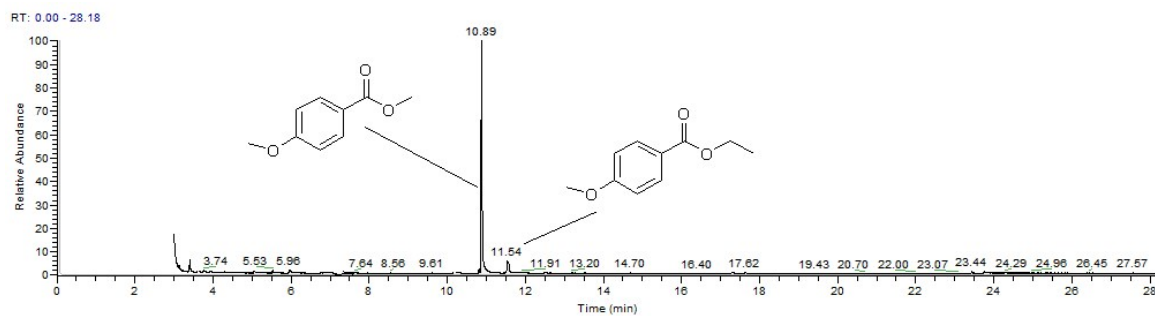




PEAK LIST RT: 0.00 - 28.18

Apex RT	Start RT	End RT	Area	%Area	Height	%Height
9.34	9.13	10.1	3.44E+08	100	5.05E+07	100

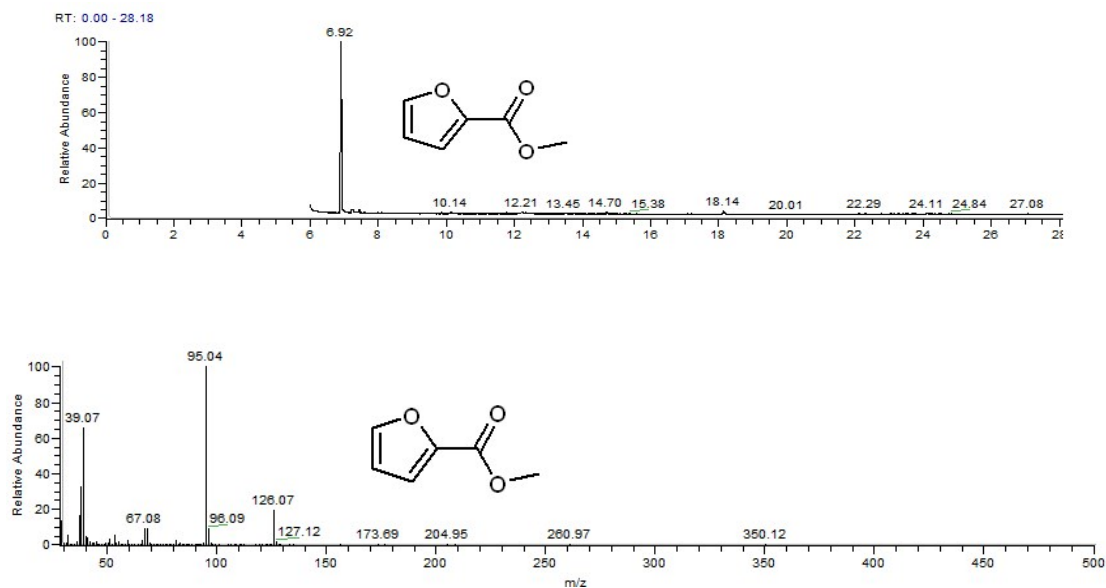
5.2.33 GC-MS spectrum for methyl 4-methoxybenzoate (6o and 6o', Table 3)



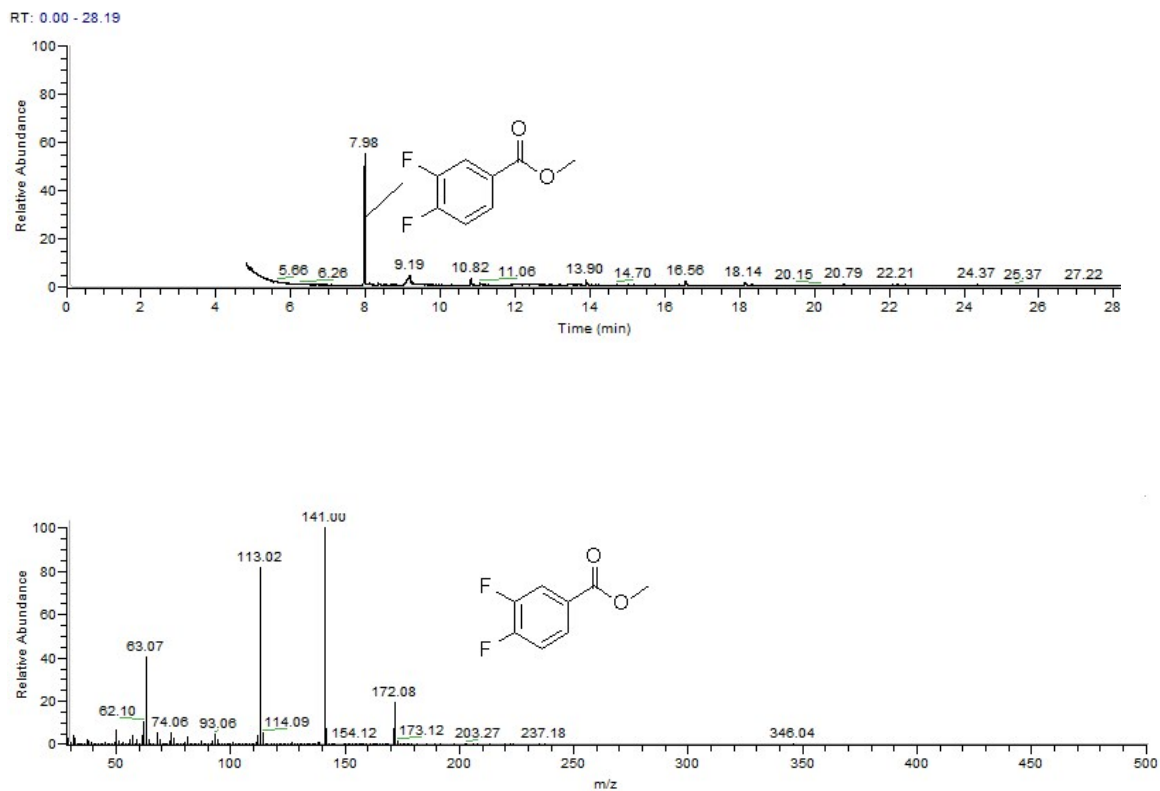
PEAK LIST RT: 0.00 - 28.18

Apex RT	Start RT	End RT	Area	%Area	Height	%Height
10.89	10.63	11.34	5.34E+09	82.28	2.48E+09	94.02
11.54	11.4	11.81	1.15E+09	17.72	1.58E+08	5.98

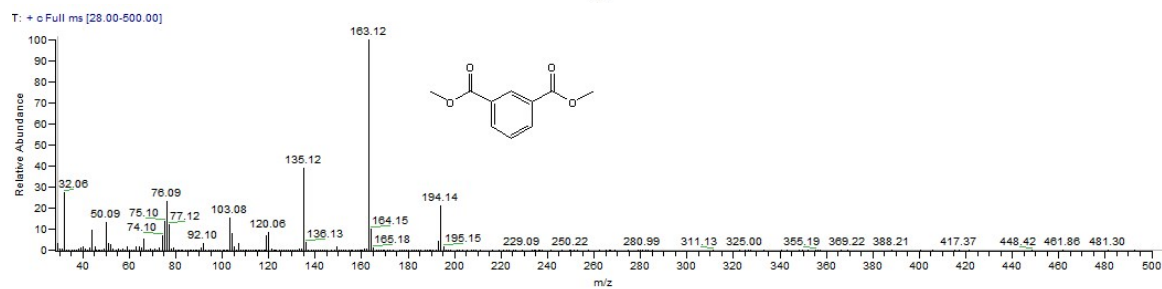
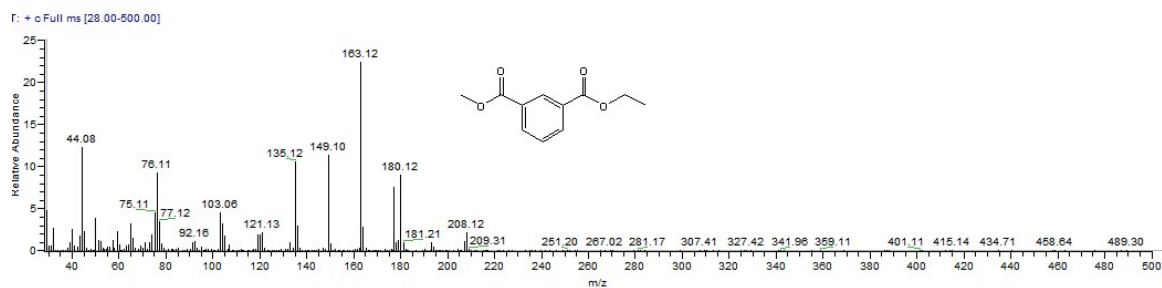
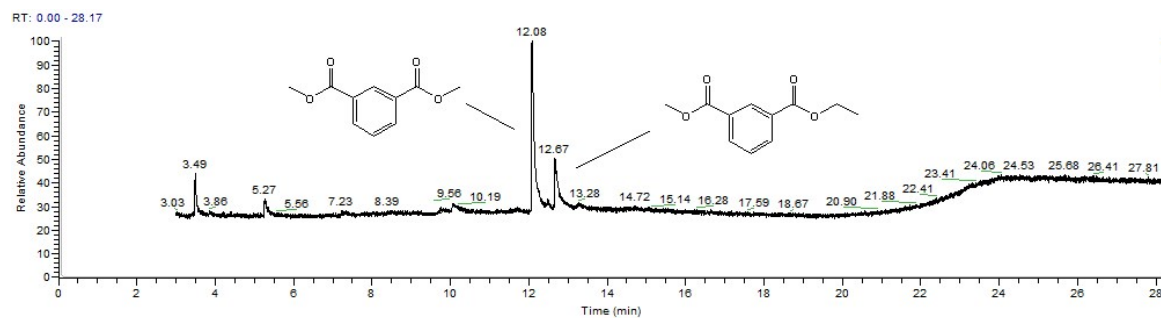
5.2.34. GC-MS spectrum for methyl furan-2-carboxylate (6p, Table 3)



5.2.35 GC-MS spectrum for methyl 3,4-difluorobenzoate (6q, Table 3)



5.2.36 GC-MS spectrum for dimethyl isophthalate (6r and 6r', Table 3)



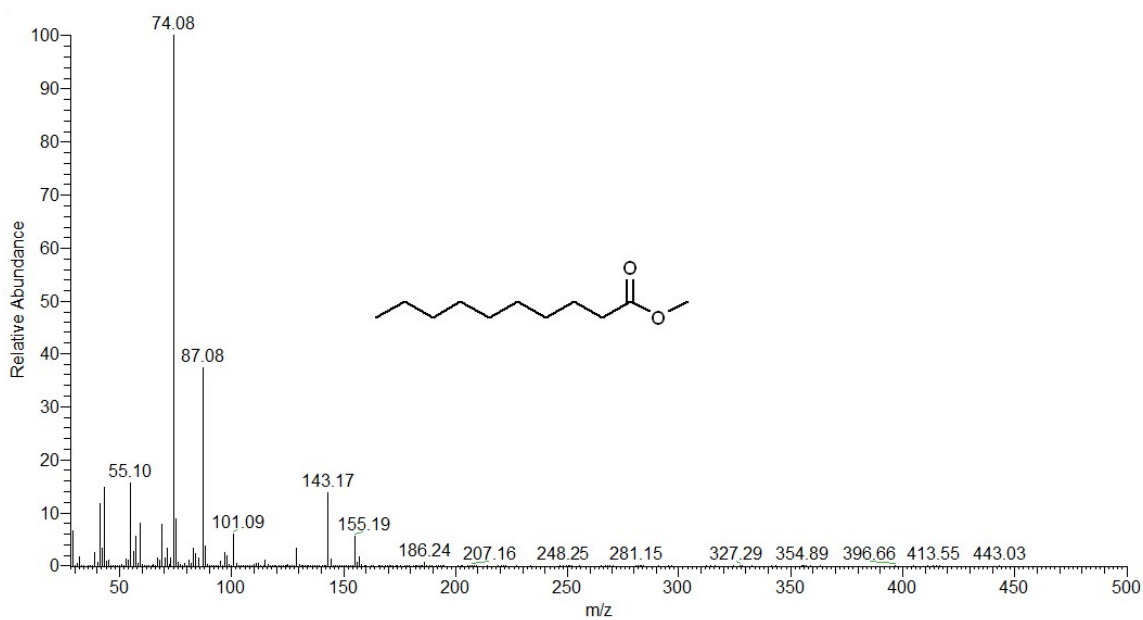
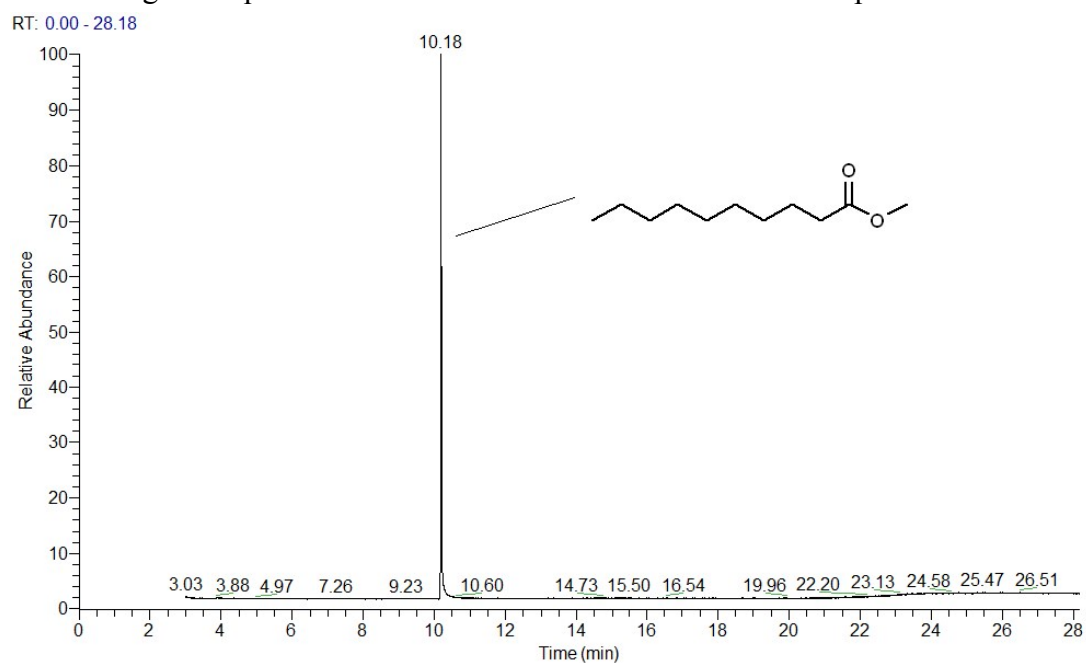
PEAK LIST RT: 0.00 - 28.17

Apex RT	Start RT	End RT	Area	%Area	Height	%Height
12.08	11.9	12.35	2.49E+08	65.33	5.37E+07	77.07
12.67	12.52	13.38	1.32E+08	34.67	1.60E+07	22.93

6. GC-MS and NMR spectra used in the mechanistic study

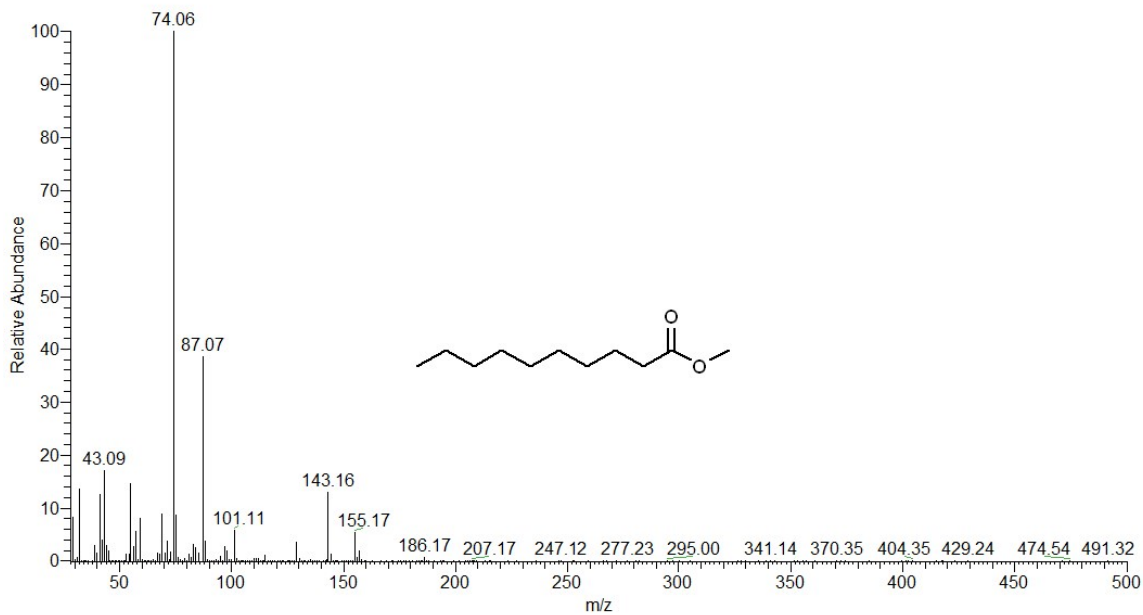
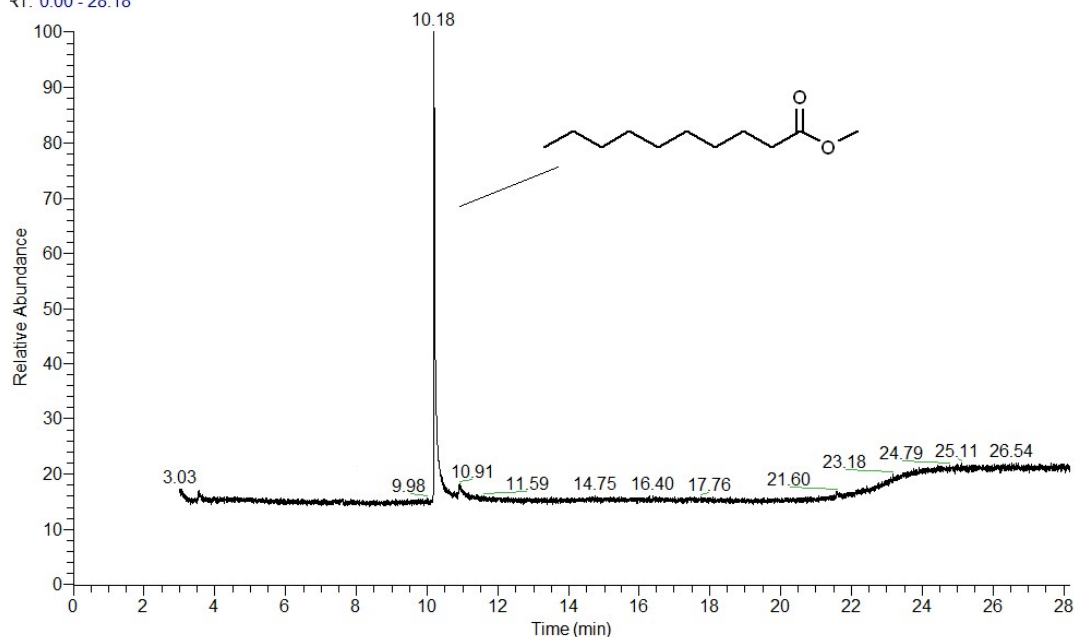
6.1 The mechanism of hydrogenation of carbon dioxide to methyl ester using MeOH, HCHO, HCOOH as the C1 source.

6.1.1 Using one equivalent of MeOH as the carbon source for the production of methyl decanoate



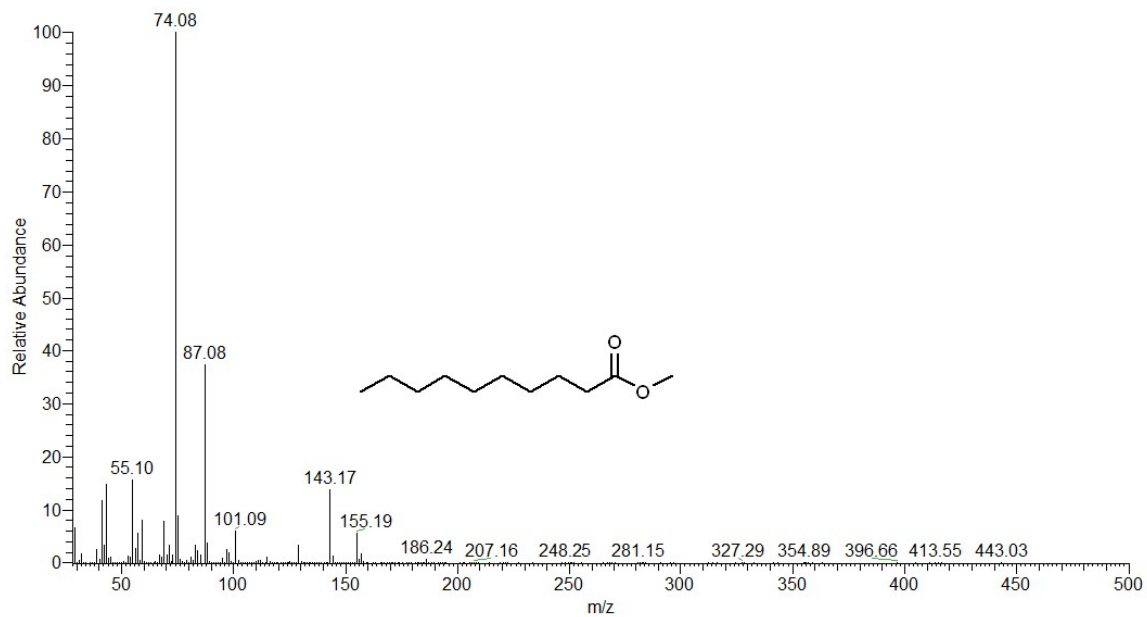
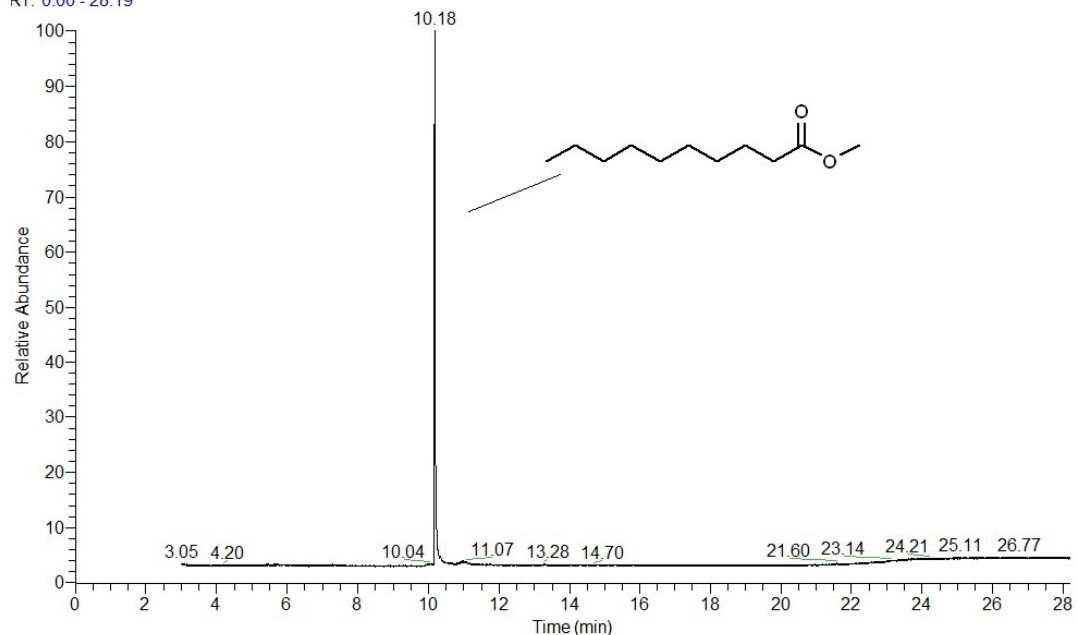
6.1.2 Using one equivalent of formaldehyde as the carbon source for the production of methyl decanoate

RT: 0.00 - 28.18



6.1.3. Using one equivalent of formic acid as the carbon source for the production of methyl decanoate

RT: 0.00 - 28.19



6.2. Standard concentration curve of MeOH in the reaction solution

Entry	Standard solution concentration (mg/mL) ^a	Peak area ratio (%) ^b
1	50.0	0.04809
2	62.5	0.05759
3	75.0	0.07275
4	87.5	0.08500
5	100.0	0.09716

^a Standard solution: 50 - 100 mg of methanol was dissolved in 1 mL of 1,2-dimethoxyethane (DME), dubbed a certain concentration of methanol standard solution; ^b Peak area ratio: By using the ratio of methanol to the solvent peak area in the gas chromatogram, the conversion was determined by GC (using mesitylene as the internal standard)

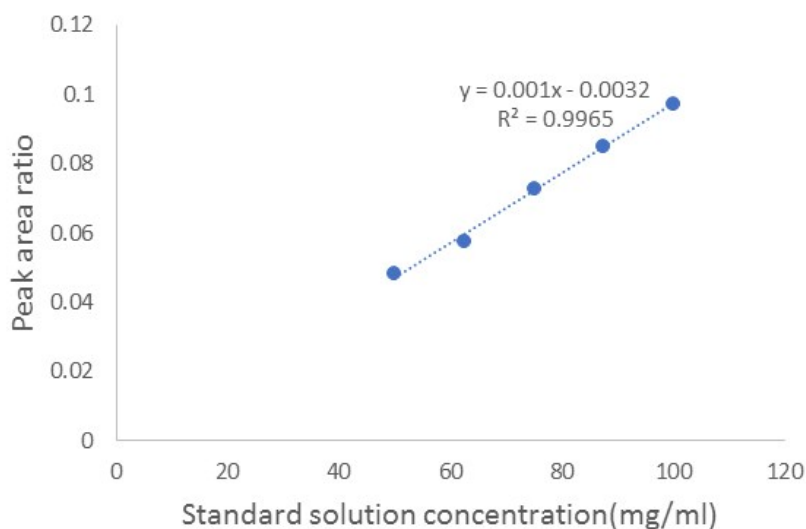


Fig. S17 Standard concentration curve of MeOH

6.3. Attempted identification of the ruthenium species formed following the Ru₂-mediated conversion of carbon dioxide to methyl decanoate

A 50 mL autoclave was charged with a solution of decanoic acid (1.36 g, 8.00 mmol) and **Ru₂** (0.40 g, 0.40 mmol) in 1,2-dimethoxyethane (10 mL). The autoclave was pressurized with 62 bar H₂ and 18 bar CO₂ and the reaction mixture stirred and heated for 20 h at 160 °C. On cooling to room temperature, the autoclave was vented and the 1,2-dimethoxyethane removed under reduced

pressure. Dichloromethane (1.0 mL) and diethylether (50 mL) were introduced yielding a pale yellow powder. After washing three times with diethyl ether (3 x 2 mL), the crude solid was filtered and dried under reduced pressure (0.12 g). The ^1H NMR and ^{31}P NMR data are detailed below and their spectra are shown in Figs S18 and S19.

^1H NMR (500 MHz, CDCl_3) δ 7.82-6.90 (m, 30H), 3.27 – 2.62 (m, 2H), 2.34-2.32 (m, 2H), 1.50 – 1.20 (m, 3H), 0.99-0.94 (m, 2H). ^{31}P NMR (202 MHz, CDCl_3) δ 31.29 (P=O), 29.14, 28.26, 27.05, 26.17 (d, J = 16.2 Hz), 25.86 (d, J = 16.2 Hz).

Analysis of the NMR spectra:

- Both NMR spectra show full consumption of **Ru2** (see Fig. S4 for the ^1H NMR spectrum of **Ru2**)
- No evidence of coordinated *para*-cymene aromatic peaks that occur between δ 5.0 and 6.5 in the ^1H NMR spectrum implying dissociation of free *para*-cymene. For comparison, see Fig. S4 for the ^1H NMR spectrum of **Ru2**.
- No hydride signals in the ^1H NMR spectrum could be detected ruling out the isolation of the proposed hydride species **I**. These data suggest that intermediate **I** is too short-lived to be observed on the NMR timescale.³
- Only unidentified Ru-phosphine species could be detected in the ^{31}P NMR spectrum; no signals corresponding to free phosphine signals were seen.
- However, the observations noted in the ^{31}P NMR spectrum cannot fully rule out the role, at some level, of ruthenium nanoparticulate species in the catalysis. Note: phosphine ligands have been reported to coordinate to the surface of ruthenium nanoparticles in a manner akin to a phosphine in a molecular complex by donation of electrons from the phosphorus atom.⁴

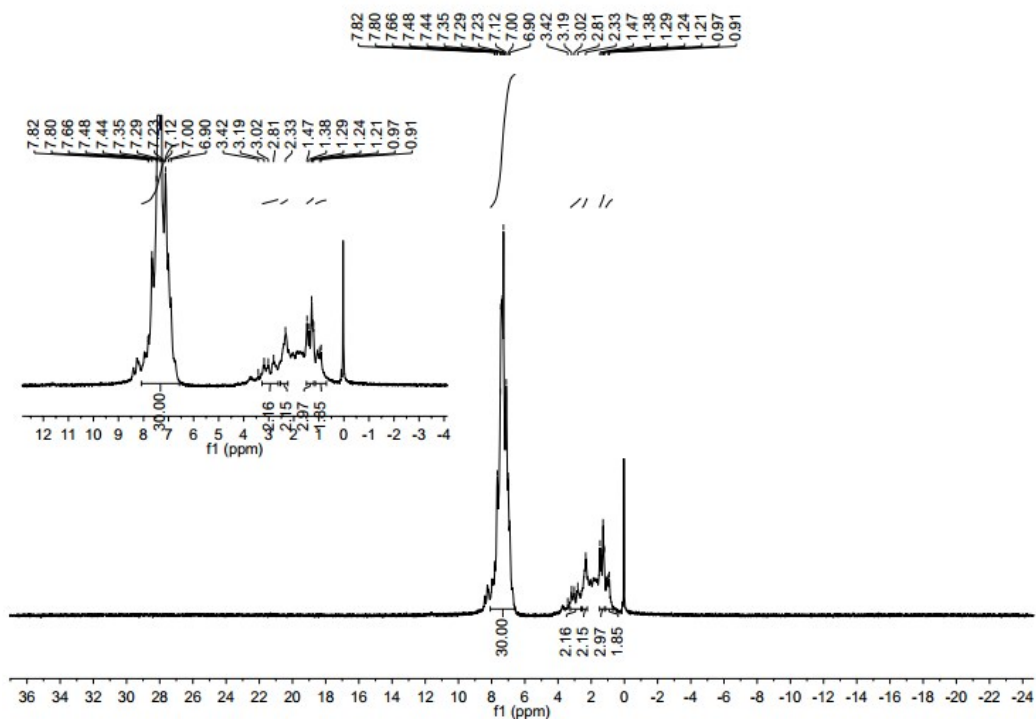
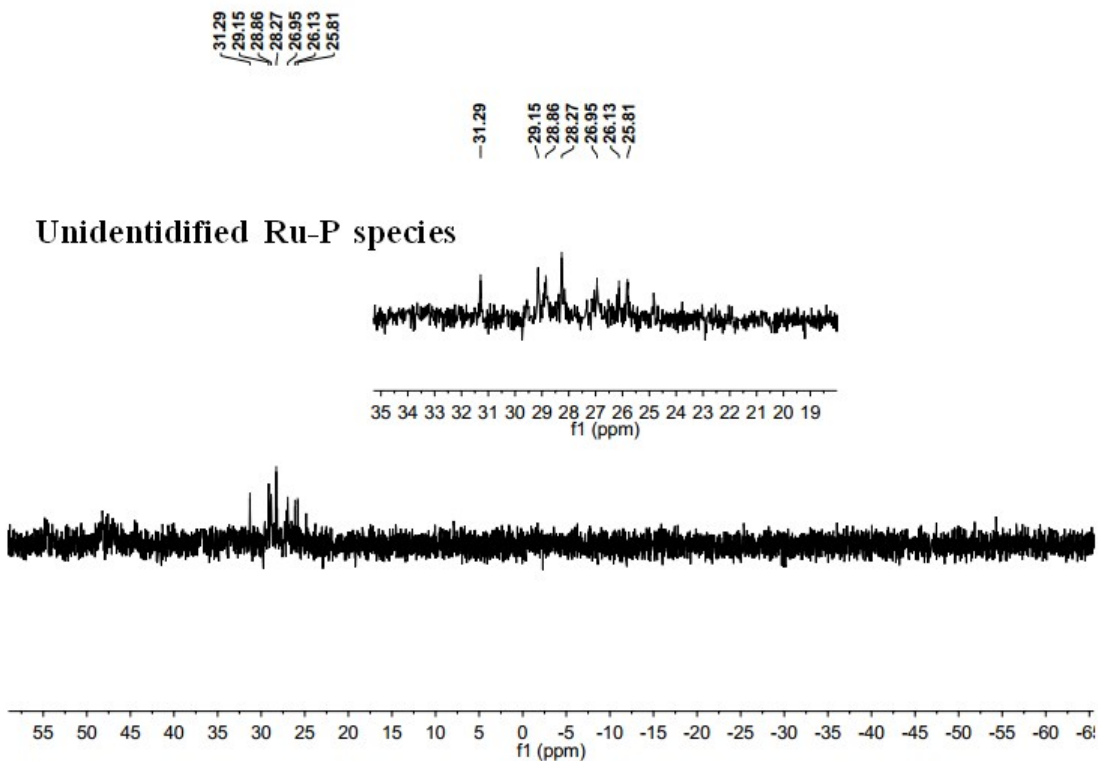


Fig. S18 ^1H NMR spectrum of the crude solid in CDCl_3



Unidentified Ru-P species

Fig. S19 ^{31}P NMR spectrum of the crude solid in CDCl_3

7. X-ray structure determination

Table S6 Crystal data and structure refinement for **Ru2** and **Ru3**.

Identification code	Ru2	Ru3
Empirical formula	C ₅₁ H ₅₃ Cl ₂ O ₅ P ₃ Ru	C ₅₂ H ₅₅ Cl ₂ O ₅ P ₃ Ru
Formula weight	1010.81	1024.90
Temperature/K	173.0	173.0
Crystal system	monoclinic	monoclinic
Space group	P2 ₁ /n	P2 ₁ /c
a/Å	12.4966(4)	19.968(4)
b/Å	21.3798(7)	12.863(3)
c/Å	17.4791(6)	19.229(4)
α/°	90	90
β/°	99.826(3)	105.75(3)
γ/°	90	90
Volume/Å ³	4601.5(3)	4753.6(18)
Z	4	4
ρ _{calc} /cm ³	1.459	1.4320
μ/mm ⁻¹	0.609	0.591
F(000)	2088.0	2118.2
Crystal size/mm ³	0.336 × 0.209 × 0.114	0.43 × 0.425 × 0.278
Radiation	MoKα (λ = 0.71073)	Mo Kα (λ = 0.71073)
2θ range for data collection/°	3.036 to 49.998	3.86 to 55
Index ranges	-14 ≤ h ≤ 14, -25 ≤ k ≤ 24, -20 ≤ l ≤ 20	-25 ≤ h ≤ 25, -16 ≤ k ≤ 16, -24 ≤ l ≤ 24
Reflections collected	25509	61939
Independent reflections	8070 [R _{int} = 0.0789, R _{sigma} = 0.0869]	10887 [R _{int} = 0.0304, R _{sigma} = 0.0208]
Data/restraints/parameters	8070/188/609	10887/56/609
Goodness-of-fit on F ²	1.031	1.040
Final R indexes [I ≥ 2σ (I)]	R ₁ = 0.0544, wR ₂ = 0.1124	R ₁ = 0.0356, wR ₂ = 0.0844
Final R indexes [all data]	R ₁ = 0.0840, wR ₂ = 0.1271	R ₁ = 0.0363, wR ₂ = 0.0851
Largest diff. peak/hole / e Å ⁻³	0.67/-0.41	0.84/-0.74

The single-crystal X-ray diffraction study of **Ru2** and **Ru3** was conducted on a Rigaku Sealed Tube CCD (Saturn 724+) diffractometer with graphite-monochromated Mo-Kα radiation (λ = 0.71073 Å) at 173(2) K and the cell parameters were obtained by global refinement of the positions of all collected reflections. Intensities were corrected for Lorentz and polarization effects

and empirical absorption. The structures were solved by direct methods and refined by full-matrix least-squares on F^2 . All non-hydrogen atoms were refined anisotropically and all hydrogen atoms were placed in calculated positions. Structure solution and refinement were performed by using the SHELXT (Sheldrick, 2015).⁵ The disorder displayed by the ClO_4 anion was also processed by the SHELXL-2015 software. Details of the crystal data and structure refinements for **Ru2** and **Ru3** are summarized in Table S5.

8. References

1. K. Mashima, K. Kusano, N. Sate, Y. Matsumura, K. Nozaki, H. Kumobayashi, N. Sayo, Y. Hori, T. Ishizaki, S. Akutagawa, H. Takaya, *J. Org. Chem.* **1994**, 59, 3064-3076.
2. T. Saito, T. Yokozawa, T. Ishizaki, T. Moroi, N. Sayo, T. Miura, H. Kumobayashi, *Adv Synth Catal*, **2001**, 343, 264-267.
3. (a) S. Wesselbaum, V. Moha, M. Meuresch, S. Brosinski, K. M. Thenert, J. Kothe, T. v. Stein, U. Englert, M. Hçlscher, J. Klankermayer, W. Leitner, *Chem. Sci.* **2015**, 6, 693-704; (b) I. Mellone, M. Peruzzini, L. Rosi, D. Mellmann, H. Junge, M. Beller and L. Gonsalvi, *Dalton Trans.*, **2013**, 42, 2495–2501.
4. (a) F. Novio, D. Monahan, Y. Coppel, G. Antorrena, P. Lecante, K. Philippot, B. Chaudret, *Chem. Eur. J.* **2014**, 20, 1287 – 1297; (b) F. Novio, K. Philippot, B. Chaudret, *Catal Lett* **2010**, 140, 1–7
5. (a) G. M. Sheldrick, *Acta Cryst.* **2015**, A71, 3–8; (b) G. M. Sheldrick, *Acta Cryst.* **2015**, C71, 3–8.